UNIVERSITÀ DEGLI STUDI DI PADOVA

Sede Amministrativa: Università degli Studi di Padova

Dipartimento di Scienze Chimiche

Facoltà di Scienze Matematiche, Fisiche e Naturali.

DOTTORATO DI RICERCA IN SCIENZE MOLECOLARI

INDIRIZZO SCIENZE CHIMICHE

XXII CICLO

Synthesis, characterization and anticancer activity of Gold(III) complexes with peptido ligands

Coordinatore: Ch.mo Prof. Maurizio Casarin

Supervisore: Prof. Fernando Formaggio

Dottorando: Dr. Morelle Negom Kouodom

À ma défunte maman qui nous a aimés
mes frères et moi d'un amour spécial.

.

À mon défunt papa.

À Karol, Mariane et Philbert.

À mes frères Diane, Magnote, Romuald et Yves.

Moi, je t'ai choisi, je ne t'ai pas rejeté, répondit le Seigneur Ne crains pas, je suis avec toi! Ne regardes pas autour, car je suis Ton Dieu! Je prends ta main droite et je te dis: Ne crains pas, je t'aide!

Isaïe 41, 9-10

INDEX

Abstract

The selective delivery of pharmacologically active compounds into the tumor cell represents a major issue in cancer research. The therapeutic use of cisplatin is associated with some serious clinical problems, such as severe normal tissue toxicity and resistance to the treatment. To overcome these problems, the anticancer activity of Au(III)-dithiocarbamato derivatives has been recently investigated.. Those complexes turned out to be extremely promising in terms of greater *in vitro* and *in vivo* antitumor activity, lack of cross-resistance, and reduced toxic and nephrotoxic side-effects compared to cisplatin, accounting for a different mechanism of action. In fact, further biological studies identified proteasome as a major target and showed that the inhibition of the proteasomal activity is associated with both apoptotic and non-apoptotic pathways.

On the other hand, two plasma membrane proteins, PEPT1 and PEPT2, have been recently identified. They are present predominantly in epithelial cells of the small intestine, mammary gland, lung, choroid plexus, kidney and in other cell types. These proteins are able to transport across membranes all possible di- and tripeptides containing L-amino acid residues.

To obtain compounds with superior chemotherapeutic index in terms of increased bioavailability, higher cytotoxicity, and lower side-effects than cisplatin, we extended our research to Au(III)-dithiocarbamato complexes functionalized with peptides, to exploit peptide transporters PEPT1 and PEPT2. These complexes should be able to maintain the properties of the previously reported gold(III) analogues together with an enhanced bioavailability through the peptide-mediated cellular internalization.

We report in this work on a series of Au(III)-dithiocarbamato complexes, covalently bound to oligopeptides (from di- to penta-), of different amino acids sequences (chiral and achiral, hydrophobic and hydrophilic, aliphatic and aromatic), bearing different C-terminal protecting/blocking groups.

All the peptides have been synthesized, purified and characterized by mass spectrometry, mono or/and bidimensional NMR and FT-IR spectroscopy. In addition the conformation of rigid peptides (based on the 3_{10} helix promoting C^{α}-tetrasubstituted residue Aib) have been studied.

The corresponding Au(III)dithiocarbamato derivatives were synthesized, purified and characterised by elemental analysis, mono or/and bidimensional NMR and FT-IR spectroscopy

and thermogravimetric analysis. Moreover, the conformation of two chiral compexes was investigated.

In order to clarify their interaction with biological active molecules, in particular the glutathione, the study of the reaction between the gold(III)-dibromo(sarcosylglycyl*tert*butyl-ester)dithiocarbamato complex with L-NAC has been performed.

Some of the complexes have been tested for their *in vitro* cytotoxic activity. Among all, the Gly- and Aib-*tert*butyl-ester-containing-dipeptides Au(III) derivatives, have notably shown, to a high degree, to be more cytotoxic than cisplatin and the previously synthesized Au(III) analogues.

Preliminary *in vivo* antitumour activity studies have also been performed, showing prominent results in term of higher *in vivo* effectiveness compared to the previously synthesized Au(III) analogues.

Riassunto

Una delle sfide maggiori a cui deve dare risposta l'attuale ricerca sul cancro è quella di riuscire a indirizzare i farmaci in modo selettivo verso la cellula tumorale. Tra i chemioterapici maggiormente utilizzati in terapia ci sono i composti a base di platino, tra cui il cisplatino, ma la loro notevole attività antitumorale è accompagnata da una elevata tossicità Infatti presentano numerosi inconvenienti che ne precludono l'utilizzo per lunghi periodi di tempo: sono altamente neuro- e nefrotossici, inducono pesanti effetti collaterali (alopecia, diminuzione dell'udito, ecc) ed in molti casi, dopo un iniziale successo terapeutico, causano l'insorgenza di resistenza da parte delle cellule cancerose.

Per superare tali limiti, è stata recentemente studiata l'attività antitumorale di derivati ditiocarbammici di Au(III). Questi composti hanno dimostrato di avere un'attività più elevata delcisplatino, sia *in vitro* che *in vivo*, e una tossicità sistemica inferiore. Inoltre, poichè non presentano resistenza crociata col chemioterapico di riferimento, agiscono probabilmente secondo un meccanismo diverso. Infatti, vari studi hanno evidenziato che il proteasoma è uno dei bersagli dei complessi di Au(III) e che l'inibizione dell'attività proteasomica è associata ai meccanismi apoptotici e non apoptotici.

In letteratura è stato recentemente riportato che due proteine di membrane, PEPT1 e PEPT2, localizzate principalmente nelle cellule epiteliali dell'intestino, delle ghiandole mammarie, del plesso coroideo polmonare e dei reni, sono in grado di trasportare attraverso la membrana cellulare tutti i di- e tripeptidi costituiti da L-amminoacidi.Abbiamo pertanto sintetizzato complessi ditiocarbammici di Au(III) funzionalizzati con leganti peptidici, che, grazie ai sistemi cooperativi con le proteine di trasporto, potrebbero avere un indice terapeutico superiore ai composti di platino in termini di migliore biodisponibilità, maggiore citossicità e minori effetti collaterali.

In questo lavoro di tesi, si riportano la sintesi, la purificazione e la caratterizzazione di una serie di complessi ditiocarbammici di Au(III), covalentemente legati ad oligopeptidi (dal di- al penta), con sequenze amminoacidiche diverse (achirali e chirali, idrofobiche e idrofiliche, alifatiche e aromatiche), recanti diversi tipi di gruppi protettori/bloccanti C-terminali.

I peptidi sono stati sintetizzati, purificati e caratterizzati tramite spettrometria di massa, spettroscopia NMR mono e bidimensionale e FT-IR. Inoltre, studi conformazionali sono stati effettuati su peptidi rigidi (contenenti l'aminoacido C^{α}-tetrasostituito Aib, che favorisce l'assunzione di strutture elicoidali 3_{10})

I corrispondenti complessi ditiocarbammici di Au(III) sono stati sintetizzati, purificati e caratterizzati tramite analisi elementari, spettroscopie FT-IR e NMR mono e bidimensionale,

termogravimetria. Oltre a ciò, è stato eseguito uno studio conformazionale di due complessi con peptidi chirali.

Per chiarire i meccanismi d'interazione con le molecole di interesse biologico come il glutathione, è stata inoltre studiata la reazione fra L-NAC e il complesso di bromo(sarcosilglicil*tert*butil-estere)dithiocarbamato di Au(III).

Sono stati eseguiti studi preliminari *in vitro* di citotossicità su alcuni complessi presi come riferimento. Fra questi, i derivati Au(III) dei dipeptidi contenti Gly- e Aib-O*t*Bu hanno dimostrato di avere una citotossicità molto maggiore rispetto a quella del cisplatino.

Dati molto incoraggianti sono stati, infine, messi in evidenza dai test *in vivo*, eseguiti recentemente su un tumore xenografico della mammella.

ABBREVIATIONS

AcOEt = ethyl acetate

Aib = α-amino*iso*butyric acid

AIDS = acquired immune deficiency syndrome

AuD_2 = gold(III)-dibromo-(sarcosylglycylmethylester)dithiocarbamato

AuD_3 = gold(III)-dibromo-(sarcosyl-α-amino*iso*butyrylmethylester)dithiocarbamato

AuD_6 = gold(III)-dibromo-(sarcosylglycyl*tert*-butylester)dithiocarbamato

AuD_7 = gold(III)-dichloro-(sarcosylglycyl*tert*-butylester)dithiocarbamato

AuD_8 = gold(III)-dibromo-(sarcosyl-α-amino*iso*butyryl*tert*-butylester)dithiocarbamato

AuD_9 = gold(III)-dichloro-(sarcosyl-α-amino*iso*butyryl*tert*-butylester)dithiocarbamato

AuD_{10} = gold(III)-dibromo-(sarcosylphenylalanyl*tert*-butylester)dithiocarbamato

AuD_{11} = gold(III)-dichloro-(sarcosylphenylalanyl*tert*-butylester)dithiocarbamato

AuD_{12} = gold(III)-dibromo-[sarcosyl-tri-(α-amino*iso*butyryl)glycylethylester]dithiocarbamato

AuD_{13} = gold(III)-dibromo-[sarcosyl-di-(α-amino*iso*butyryl)*tert*-butylester]dithiocarbamato

AuD_{14} = gold(III)-dichloro-[sarcosyl-di-(α-amino*iso*butyryl)*tert*-butylester]dithiocarbamato

AuD_{15} = gold(III)-dichloro-[sarcosyl-tri-(α-amino*iso*butyryl)glycylethylester]dithiocarbamato

AuD_{16} = gold(III)-dibromo-[sarcosyl-(C^{β}-O-*tert*-butyl)seryl*tert*-butylester]dithiocarbamato

AuD_{17} = gold(III)-dichloro-[sarcosyl-(C^{β}-O-*tert*-butyl)seryl*tert*-butylester]dithiocarbamato

AuD_{18} = gold(III)-dibromo-[sarcosyl-tri-(α-amino*iso*butyryl)*tert*-butylester]dithiocarbamato

AuD_{19} = gold(III)-dichloro-[sarcosyl-tri-(α-amino*iso*butyryl)*tert*-butylester]dithiocarbamato

AuD_{20} = gold(III)-dibromo-[prolyl-di-(α-amino*iso*butyryl)*tert*-butylester]dithiocarbamato

AuD_{21} = gold(III)-dichloro-[prolyl-di-(α-amino*iso*butyryl)*tert*-butylester]dithiocarbamato

AuD_{21} = gold(III)-dichloro-(prolyl-α-amino*iso*butyryl*tert*-butylester)dithiocarbamato

Bzl = benzyl

Boc = *tert*-butyldicarbonate

C = concentration

CD = circular dichroism

COSY = correlation spectroscopy

CTR1 = copper transporter 1

DNA = deoxyribonucleic acid

DMAP = 4-(dimethylamino)pyridine

DMSO = dimethylsulphoxide

EDC = 1-ethyl-3-[3-(dimethylamino)propyl]carbodiimide
Et = ethyl
EtOH = ethanol
FDA = food and drug administration
FBS = fetal vovine serum
FITC = fluorescein-5(6)*iso*thiocyanate
Fmoc = fluorenylmethyloxycarbonyl
FT = fourier transform
Gly = glycine
HIV = human immunodeficiency virus
HMBC = heteronuclear multiple bond coherence
HOAt = 7-aza-1-hydroxy-benzotriaxzol
HOAt = 1-hydroxy-benzotriaxzol
IR = infrared absorption
M = molarity
M = molecular mass
Me = methyl
Mp = melting point
NCI = national cancer institute
NER = nucleotide excision repair
NMM = *N*-methylmorpholine
NMR = nuclear magnetic resonance
OCT = organic cation transporter
Phe = phenylalanine
Pro = proline
Rf = retention coefficient
RNA = ribonucleic acid
ROESY = rotational frame nuclear overhauser spectroscopy
Sar = sarcosine
Ser = serine
*t*Bu = *tert*butyl
TEA = triethylamine
TFA = trifluoracetic acid
THF = tetrahydrofuran

TLC = tin layer chromatography

UV-Vis = ultraviolet-visible

Z-OSu = N^{α}-(benzyloxycarbonyloxy)succinimide

Z = benzyloxycarbonyl

α, [α] = optical rotation, specific optical rotation

δ = chemical shift

Θ, Θ_T = ellipticity, molar ellipticity

ν = frequency

ν = wavenumber

CHAPTER I

INTRODUCTION AND AIM OF THE THESIS

1.1 INTRODUCTION

1.1.1 What about cancer?

The term cancer refers to any disease characterised by an accumulation of cells. It can result from either increased proliferation or failure of cells to undergo apoptosis in response to appropriate stimuli.[1] There is a variety of malignancies but the most common types are cancers of lung, breast, colon and rectum, stomach, prostate, liver, cervix and oesophagus. In a 2002 report from the GLOBOCAN database, cancer resulted to be second among the three leading causes of death in the developing countries. In the year 2002, it killed 6.7 million people around the world, more than the deaths caused by HIV/AIDS, tuberculosis, and malaria put together.[2] The strategies adopted to avoid this disease are prevention, early detection/screening, healthy diet, active lifestyle, appropriate and effective treatment. Several treatment methods are used to treat cancer: surgery, radiotherapy, hormonal therapy, biotherapy and chemotherapy. The surgery is the oldest and the most preferred method that is used in the treatment of cancer: the afflicted part is removed from the body. For most cases of solid tumours, it plays a leading role in the early treatment. The radiotherapy is the simplest approach: it consists in the exposure of the cancer cells to an emission of radiations that will alter the composition of the genetic information of these dangerous cell. The radiotherapy is used after a surgery and in combination with other methods of treatment. The hormonotherapy exploits the hormones to suppress the hormonal activity that keep up the proliferation of some neoplasias. The employment of natural resources that have been modified, reinforced or diverted from their usual role is the basis of biotherapy. Chemotherapy is the use of synthetic chemical substances or drugs extracted from plants: these compounds are toxic against cancer cells (cytotoxic), inhibiting their reproduction and division.

1.1.2 Cisplatin

1.1.2.1 Historical survey

Cisplatin was synthesised for the first time by an Italian researcher, Michele Peyrone, who first graduated as a medical doctor in Turin in 1835, but soon afterwards (1939) abandoned medicine for chemistry and spent several years in different laboratories in France, Germany,

Netherlands, Belgium and Great Britain.[3] In the Liebig's laboratory, in Giessen, he synthesised in 1845 a new platinum compound[4] containing two amines and two chlorines, like the Reyset's salt,[5] but having different physico-chemical properties. There is no way to justify the obtainment of two different compounds assuming a tetrahedral geometry, in those days retained usual for tetravalent compounds. 50 years later, Alfred Werner proposed for these compounds a square planar geometry which can accommodate a *cis* and a *trans* isomer, the Peyrone's and Reyset's compounds respectively (**Scheme 1.1**).[6]

(a) **(b)**

Scheme 1.1 Isomers of diaminodichloroplatinum(II): *cis*-DDP (cisplatin) **(a)** and *trans*-DDP **(b)**.

It was by accident that Barnett Rosenberg, a microbiologist, while investigating the effect of an electric field on cell division in *Escherichia coli*, generated electrochemically the Peyrone's compound by reaction of the platinum electrodes and the various components present in the cell culture medium.[7-9] In 1968, following further tests against various bacteria, *cis*-diaminodichloroplatinum(II) (cisplatin) was successfully administrated to mice bearing the standard murine transplantable tumour sarcoma-180, causing tumour regression.[10] With confirmatory in vivo tests performed at the Chester Beatty Institute in London, cisplatin was taken on by the US national Cancer Institute (NCI) for clinical testing. The first patients were treated in 1971, a remarkably short time, in modern terms, from the original discovery.[11] Approval by the US Food and Drug Administration (FDA) was granted in 1978.[12] Since then, cisplatin has become one of the most used anticancer drugs in the world. It is an effective cure for testicular cancer, one of the most useful against melanoma and non-small-cell-lung carcinoma, and in combination therapy, it is considerably active against ovarian cancer.[13]

1.1.2.2 Molecular and cellular pharmacology

1.1.2.2.1 *Chemistry and mechanism of action*

Cisplatin is administrated to cancer patients by intravenous injection as a sterile saline solution, that is, containing salt, specifically sodium chloride. Once the drug is in the blood stream and in the extra-cellular fluids, it remains intact due to the high concentration of chloride

ions (about 100 mM). The neutral compound enters the cell by passive diffusion across the lipid bilayer, or by active uptake mediated by carrier import proteins, like organic cation transporters (OCT)[14-17] or copper transporter 1 (CTR1),[18-20] or by an as-yet unidentified sodium-dependent system.[21-26] Because of the low Cl^- concentration inside a cell (4-20 mM), the neutral cisplatin is activated through aquation to monoaquo species in which one of the two chlorine atoms is replaced by water, thus generating positively charged species (**Scheme 1.2**).[27,28] This partially hydrolysed cisplatin does react with DNA; in fact, it has been proved that the formation of Pt(II)-DNA adducts and the first cisplatin hydrolysis reaction occur with similar rates, thus suggesting that the mono-aqua species $[(NH_3)PtCl(H_2O)]^+$ is predominant in the cytoplasm.[28]

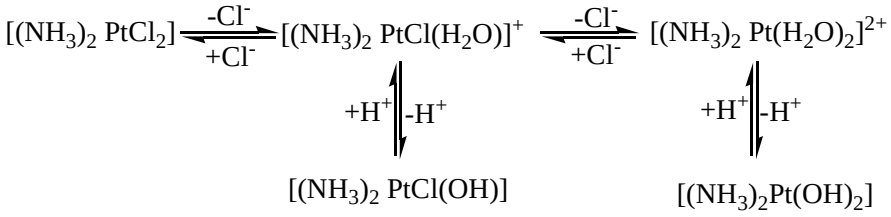

Scheme 1.2: Hydrolysis reactions of diaminodichloroplatinum(II).

Once inside the cell, cisplatin has a number of possible targets: DNA, RNA, sulphur-containing species (such as metallothionein and glutathione) and mitochondria. The effect of cisplatin on mitochondria is not well understood, but it is possible it damages the mitochondrial DNA thus contributing to cell death. The interaction of cisplatin with sulphur-containing species is better understood and is believed to be involved in promoting cell resistance toward cisplatin. The effects of cisplatin on RNA and DNA have been studied extensively. Although cisplatin can coordinate to RNA, this interaction is not believed to play an important role in cisplatin's physiological mechanism of action. First, a single damaged RNA molecule can be replaced by newly synthesised material; studies have revealed that cisplatin does not affect RNA synthesis. Second, when cisplatin was administrated *in vitro* at its lethal dose to a strain of cancer cells, only a small fraction (1 to 10%) of RNA molecules were damaged.[29] On the contrary, there is a strong evidence that cellular DNA is the target of the drug. In fact, cisplatin is a well known DNA-damaging agent and the specific adducts produced in DNA have been well characterized.[30] The reaction between cisplatin and DNA results in formation of different kinds of adducts (**Fig. 1.1**).[31]

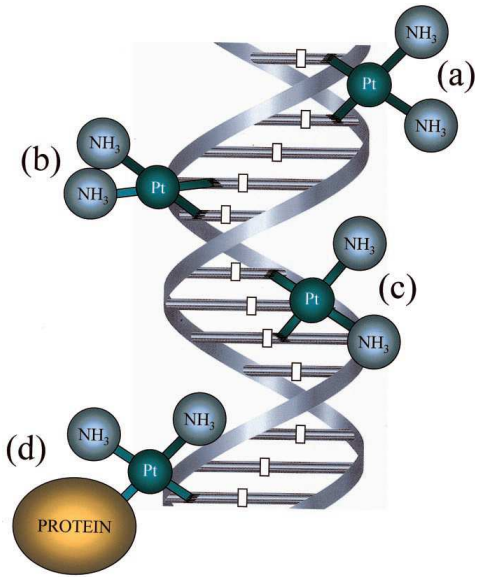

Figure 1.1: Main adducts formed in the interaction of cisplatin with DNA: (a) interstrand cross-link; (b) 1,2-intrastrand cross-link; (c) 1,3-intrastrand cross-link; (d) protein-DNA cross-link.

Enzymatic studies of DNA platinated by cisplatin[32-35] revealed a strong preference for binding to sequences containing two or more adjacent guanosine nucleosides. The quantification of these and other, less common, adducts was achieved by first degrading platinated DNA *in vitro*[36-38] or *in vivo*[39] to a mixture of oligo-nucleotides and then separating them by immunochemical techniques.

The major site of platination in double-stranded DNA (65%) derives from intrastrand cross-links between two neighbouring deoxyguanosines, d(GpG). About 20% of the DNA platination derives from intrastrand cross-links at a d(ApG) sequence, but no adducts were detected when these two nucleosides, adenosine and guanosine, were in opposite order *i.e*, d(GpA). Another 9% of the platination derives from cross-links between two deoxyguanosines separated by a third nucleoside [d(GpNpG), were N is any nucleoside]. All of these modifications occur through the N(7) position on the purine ring because it does not form hydrogen bonds with any other DNA base; these nitrogen atoms are located in the DNA major groove, so they are more exposed to platination(**Scheme 1.3**).[40]

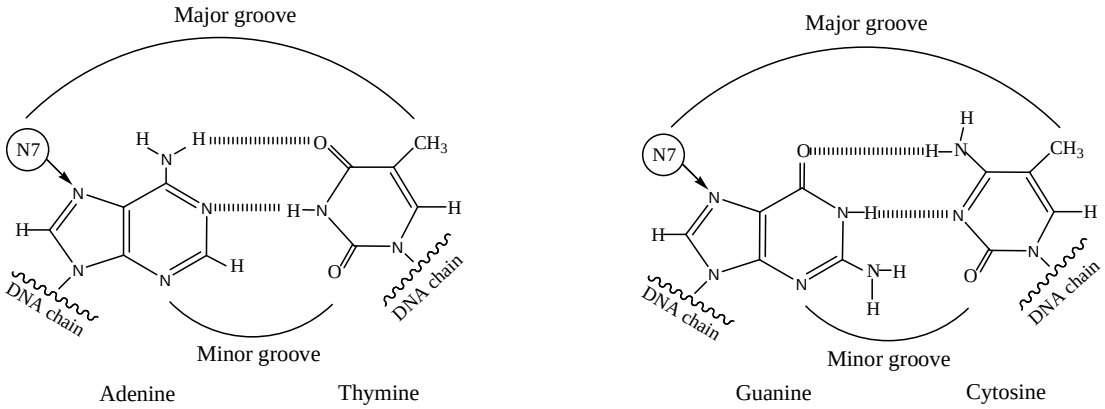

Scheme 1.3 The base pairs; cisplatin coordinates to the N(7) atoms of the guanine and adenine purine rings.

Following DNA platination for few minutes, over 40% of the platinated DNA is in the form of monofunctional modification of deoxyguanosine; however, after a few hours, there is no evidence for monofunctional platination of DNA, these adducts rearranging rapidly to the various bifunctional adducts.[41] Monofunctional adducts, rapidly produced by cis- and trans-diamminodichloroplatinum(II), are not believed to have any biological activity, as they are labile, determine only slight structural modifications on DNA and do not inhibit DNA synthesis. [42-44]

DNA interstrand cross-links have been also found to be formed between two deoxyguanosines, but this requires a major contortion of the DNA structure and may occur when an alternate purine is not in close proximity on the same strand.[45] This observation presumably explains why interstrand cross-links occur at less than 1% of the total platination of DNA.

One other adduct that was shown to be formed was a cross-link between deoxyguanosine and a protein or a glutathione molecule; this adduct can be produced when DNA is first platinated for a short time to give monofunctional adducts, and then protein or glutathione is added.[46]

Hence it has been proved that the formation of the monofunctional platinum(II)-DNA adduct is the first step involved in the platination of DNA, followed by the solvolysis of the second chloride atom and the subsequent rearrangement to a bifunctional adduct, mainly identified as a d(GpG) intrastrand cross-link. In this second phase, it is determinant the *cis* or *trans* geometry of the platinum (II) complex, as reactions with DNA occur with retention of stereogeometry.[47] Due to its geometry, *trans*-DDP cannot form d(GpG) intrastrand adducts with DNA; since *trans*-DDP is inactive in killing cancer cells, it is believed that these intrastrand adducts formed between cisplatin and DNA are important for the anticancer activity of cisplatin itself. [32-35]

When cisplatin binds to DNA forming adducts, it promotes superhelical unwinding and shortens the double helix;[48,49] the distortions induced in the DNA double helix by inter- and intrastrand cross-links have been characterised by several techniques. For example, in the interstrand d(GpG) cross-links the platinum residue is localised in the minor groove, and the axis of the double helix is bent of about 45-47° towards the minor groove, with a large unwinding of about 70-79°.[50] On the other hand, the formation of intrastrand d(GpG) cross-links causes purines to be destacked and the DNA helix to become kinked **(Fig. 1.2)** with a bending of 26-35° towards the major groove and a shorter unwinding of the double helix (~13°).[13]

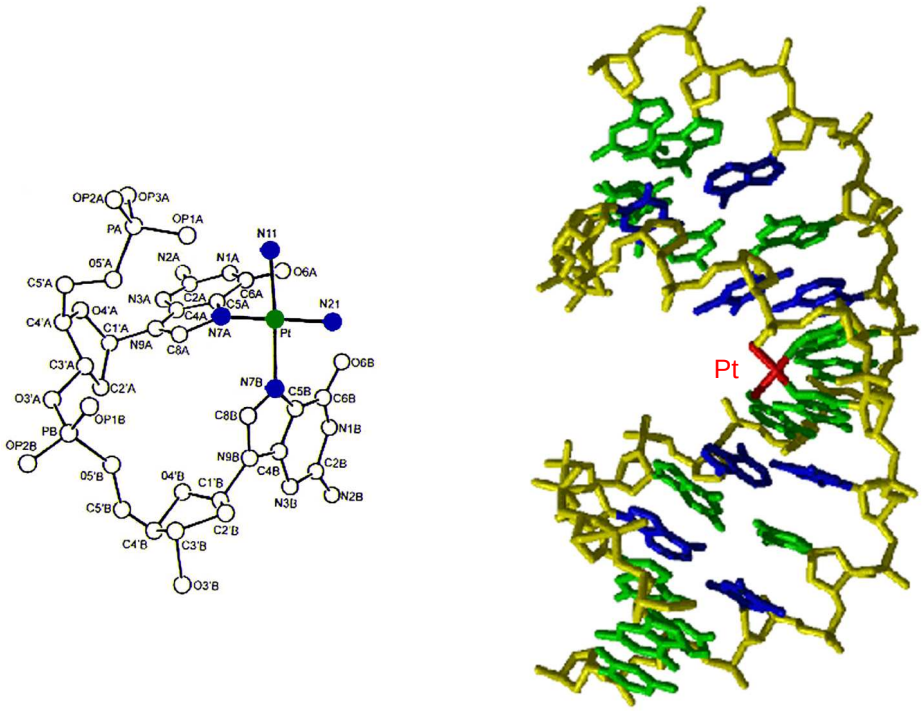

Figure 1.2: On the left, the structure of cisplatin (with platinum shown in green and nitrogen ligands shown in blue) coordinated with a dinucleotide containing two guanines. Notice the destacking of guanine bases, wich would normally be parallel to one another. On the right, the structure of cisplatin coordinated to two guanines in a DNA duplex.

1.1.2.2.2 *Proteins that recognize cisplatin-induced DNA damage*

The efficacy of cisplatin against cancer cells could be related not only to the inhibition of DNA synthesis, but also to the saturation of the cellular capacity to repair the platinum-DNA adducts.[51] To limit genetic mutations and prevent the ensuing of malignant transformations that might arise from exposure to such agents, there are a variety of cellular defence mechanisms, such as many types of proteins, which interact with or respond to damaged DNA, and may be

able to remove lesions from DNA and correct any unwanted change. Several types of proteins can interact with cisplatin-damaged DNA: NER (nucleotide excision repair), TFs (transcription factors), MMR (mismatch repair), the p53 tumour suppressor gene, *i.e.* a nuclear protein that exerts its effects through transcriptional regulation maintaining the genomic stability, and HMG (high mobility group) proteins (**Fig. 1.3**).[52]

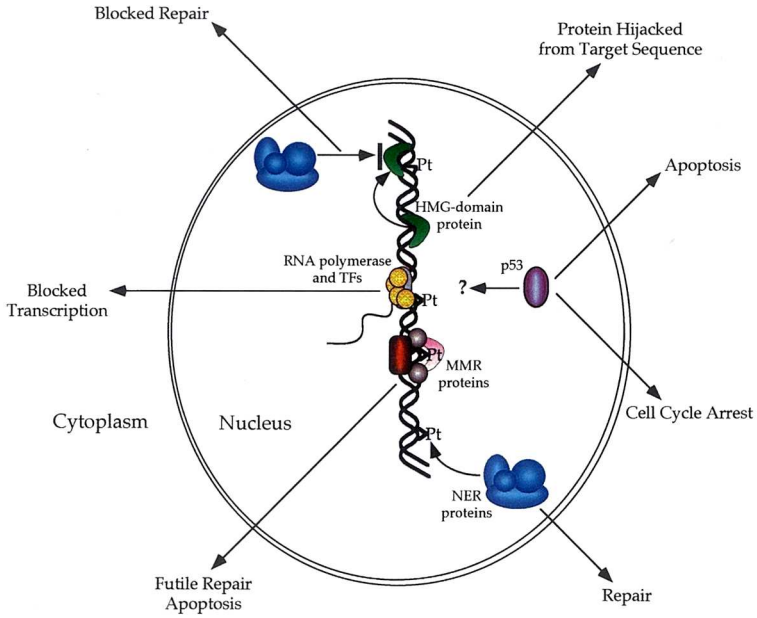

Figure 1.3: Effects of cisplatin-DNA adducts on some of the proteins in the nucleus that interact with the lesions.

Nucleotide excision repair (NER) is the major cellular defence mechanism against the toxic effects of cisplatin. Some studies on free and nucleosomal DNA extracted from a mammalian cell have revealed that nucleosome significantly inhibits NER.[53] Interestingly, post-translational modification of histones can modulate NER from damaged chromatin. Phosphorylation and acetylation of histones causes nucleosomal structural changes, increasing accessibility of other proteins. These events facilitate the binding of the remodelling complex and repair proteins to the nucleosome, thereby stimulating DNA repair[53-55] and helping cells to survive cisplatin-induced stress. Elsewhere, researchers have conducted studies to address the possibility that cisplatin's cytoxicity activity may result from failure of the excision repair system. In this repair system, before the damaged portion of DNA is even excised from the rest of the strand, it must be recognized by the cell. The cell detects DNA damage by the action of damage recognition proteins. Therefore, as a first step in studying the excision repair system, researchers looked for evidence of proteins attached to cisplatin- DNA adducts. Several types of essays can differentiate between platinated DNA that is bound to a protein and the free one; by these essays a number of

proteins called HMG-domain proteins have been isolated. They contain a common portion, similar or with identical amino acids sequences, called High Mobility Group.

The HMG-domain proteins are the largest extensively characterized group of non-histone chromosomal proteins. They can bind to specific structures in DNA or in chromatin with little or no specificity for target DNA sequence.[56] Two families of HMG have been reported. The first consists of proteins containing two or more HMG domains; it includes HMG1 and HMG2 proteins, the nucleosomal RNA polymerase I transcription factor UBF (upstream binding factor) and the mitochondrial transcription factor mtTF. In the second family there are proteins containing a single HMG domain, such as tissue-specific transcription factors. Several types of HMG proteins, including HMG1, HMG2 and UBF bind to cisplatin-DNA adducts with high affinity and specificity.[57,58] These proteins recognize 1,2-intrastrand cross-links that comprise the majority of adducts formed by cisplatin in vivo. Domain A of the structure-specific HMG protein HMG1 was reported to bind the widened minor groove of a 16-base-pair DNA duplex containing a site-specific cis-$(NH_3)_2$Pt-d(GpG) adduct.[59] DNA was strongly kinked at the hydrophobic notch created at the DNA-platinum cross-link and the protein binding was extended exclusively at the 3' side of the platinated strand.

1.1.2.2.3 *From platinum-induced DNA damage to apoptosis*

One important mechanism of translation of cisplatin-DNA damage to cell death is apoptosis. Considerable evidence indicates that cisplatin kills cells through the induction of apoptosis.[40] Apoptosis or 'programmed cell death' is a generally regulated mechanism of cell turnover that occurs during embryonic development, normal cellular homeostasis, and spontaneous and drug-induced tumour cell death.[60] Apoptosis is characterized by unique morphological and biochemical features. These features include cell shrinkage, blebbling of the cell surface, loss of cell-cell contact, chromatin condensation with activation of endogeneous endonucleases, recognition by phagocytic cells, and dependence on the energy supplied by ATP as well as on active protein synthesis.[61] To understand the apoptosis it is necessary to consider three different stages (**Fig. 1.4**). The first is an initiation phase, in which a stimulus is received followed by engagement of anyone of several possible pathways that respond to the stimulus. The second one is an effector phase, in which all the possible initiating signals are integrated and a decision to live or to die is made. The last one is a common irreversible execution phase, in which some proteins autodigest and DNA is cleaved.[40] *Bcl-2* is an oncogene that seems to be at the convergence of many apoptotic pathways. The ratio of *Bcl-2* to *Bax* protein[62] might be the final determinant of whether a cell enters the execution phase. *Bax* is a gene that encodes a dominant

inhibitor of *Bcl-2*.[63] A conserved feature of the execution phase of apoptosis is the specific degradation of a series of proteins by the cysteine-aspartic-specific proteases, or caspases. Caspases are activated when an apoptotic stimulus induces the release of cytochrome c from mitochondria.[64]

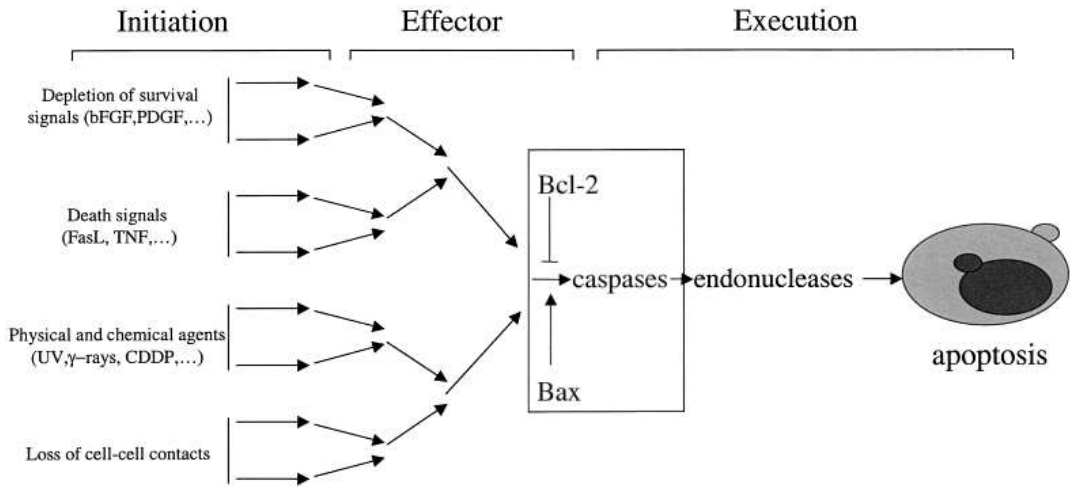

Figure 1.4 Scheme of the converging pathways leading to apoptosis in mammalian cells.

The specific mechanism(s) that trigger apoptosis in response to cisplatin insult have not yet been defined. In principle, such mechanism(s) must include ways to detect DNA damage and determine if it is strong to be lethal. Among the mechanisms that have been proposed for how proteins that bind to cisplatin-DNA adducts might modulate the sensitivity of cells to the drug, two seem to be the most feasible.[65] In the 'hijacking model', HMG proteins, binding to cisplatin-DNA adducts, could modulate cell cycle events after DNA damage and trigger apoptosis. In the 'repair shielding model', HMG proteins could protect cisplatin-DNA adducts from recognition by DNA repair enzymes. These mechanisms of cisplatin-induced cytotoxicity are not necessarily exclusive and could work in concert.

The HMG box proteins bind with high affinity to cisplatin-DNA adducts but not to *trans*-DDP, UV-induced or other DNA lesions. In contrast, a repair protein (RP) possessing DNA binding affinity flexible enough to recognize different lesions would have a much lower affinity for cisplatin-DNA adducts than for *trans*-DDP or UV-induced lesions. Consequently, DNA repair would proceed slowly because the repair protein would displace HMG box proteins from the cisplatin-DNA adducts very slowly. Alternatively, the binding of HMG box or other proteins to the cisplatin-DNA adduct might lead to the cell cycle arrest and the induction of apoptosis. Therefore, in a particular cell line, cisplatin cytotoxicity might be determined by a 'dynamic contest' between proteins that repair DNA and proteins that interfere with DNA repair and trigger apoptosis.

Several factors may influence the ability of cisplatin to induce apoptosis: a defective apoptotic program, pro-apoptotic and anti-proapoptotic proteins, caspases, apoptotic endonucleases and divalent cations, oncogenes and tumor suppressor genes, growth factors and cytokines, and viral proteins.[66]

The caspase cascade is activated in response to cisplatin insult; this activation leads to an irreversible commitment to apoptotic cell death. Caspases are usually classified in two groups:[40] initiators (caspase-2, caspase-8, and caspase-9) and effectors (caspase-3, caspase-6, caspase-7, and caspase-14). Initiator caspases interact with signaling adaptor molecules through motifs in the prodomains called caspase recruitment domains.[67] Two regulatory pathways of the caspases cascade have been reported. The first pathway begins with the assembly of death-inducing signalling complex (DISC) at the Fas receptor.[68] Activation of Fas receptor by its natural Fas Ligand (FasL) induces the formation of a DISC consisting of the adaptor molecule Fas-associated death domain and caspase-8. Activated caspase-8 in the Fas/FasL initiated DISC activates effector caspase-3, and the activated caspase-3 can directly initiate certain caspase-activated deoxynucleases.[69] This first pathway may be activated in tumour cells in response to cisplatin.[70] The second pathway begins with the release of cytochrome c from the mitochondria, which subsequently causes apoptosis by activation of caspase-9 and caspase-3.[71] In the presence of ATP and cytochrome c, the apoptotic protease-activating factor-1 (Apaf-1) binds through its recruitment domain region to the corresponding motif in caspase-9, causing the activation of this caspase that in turn activates caspase-3.[72] Cisplatin may cause mitochondrial release of cytochrome c and caspase-3 activation.[73] In addition, in human osteosarcoma cells, cisplatin induces apoptosis through a sequential activation of caspase-8, caspase-3, and caspase-6.[74] It has been also reported that cisplatin-induced apoptosis may also proceed via a caspase-3 independent pathway.[75] This lack of caspase-3 activation after cispatin treatment is consistent with inefficient formation of DNA ladders and altered apoptotic morphology. In fact, caspase-3 has been specifically implicated as the effector caspase responsible of the cleavage of the human DNA factor that subsequently activates the DNA endonuclease (DFF40) required for the formation of apoptotic DNA ladders.[76]

Tumour suppressor genes also influence cisplatin-induced apoptosis. *p53* is considered a 'guardian of the genome' and facilitates DNA repair before DNA replication. Cisplatin DNA damage may lead to expression of the p53 protein that subsequently induces both expression of downstream p21WAF protein and G_1 phase cycle arrest.[77] In the event of irreparable DNA damage, the p53 protein induces apoptosis.[62] The *p53* gene also directly affects expression of other downstream genes that regulate sensitivity to apoptosis, activating transcription of proapoptotic Bax and repressing transcription of antiapoptotic Bcl-2 proteins.[40] On the other

hand, although cisplatin may initiate apoptosis through pathways modulated by *p53*, this tumour suppressor gene is not always required for apoptosis. Thus, cisplatin induces apoptosis in cells expressing either wild type or mutant p53 protein or even in cells lacking p53.[78]

1.1.2.3 Cisplatin toxicity and its modulation

Since cancer is a disease in which tumour cells divide rapidly, many chemotherapeutic agents used to treat cancer target rapidly dividing cells. Unfortunately, most of them are non-selective and attack other types of rapidly dividing cells in the body. Such cells can be found in the gastrointestinal tract, in hair follicles and in bone marrow. For this reason, some of the common adverse side effects of drugs used in cancer chemotherapy are nausea, alopecia (hair loss) and myelosuppression (decreased bone-marrow function that results in lower numbers of red blood cells, white blood cells and platelets).

Indeed, nearly all people who are treated with cisplatin experience gastrointestinal problems, specifically intense nausea and vomiting. Nausea and vomiting usually begin within 1-4 hours after treatment and can last up to 24 hours.[79] However, in the case of cisplatin it is believed that the nausea and vomiting result from an effect on the central nervous system rather than from gastrointestinal damage.[7]

Some people who are given cisplatin treatments also experience alopecia. Furthermore, myelosuppression occurs in 25 to 30 percent of people who undergo treatments with cisplatin. The levels of platelets and white blood cells (leukocytes) associated with myelosuppression are generally lower about 3 weeks after treatment and returns to normal levels a little more than 2 weeks after that. The loss of platelets (called thrombocytopenia) and the loss of leukocytes (called leucopenia) are more pronounced when higher doses of cisplatin are used. In addition to a loss of platelets and white blood cells, the use of cisplatin can also cause a decrease in the number of red blood cells (anemia). Anemia occurs with the same frequency and with the same timing as thrombocytopenia and leucopenia.[80] Some people receiving cisplatin treatments also experience hearing difficulties (ototoxicity). Ototoxicity has been observed in up to a third of people treated with cisplatin and can be manifested in the form of tinnitus (a buzzing, ringing or whistling in the ears) or hearing loss in the high frequency range, and, in a few cases, total deafness. This hearing loss results from damage to the sound detecting hair cells in the inner ear.[7]

Several other negative side effects are sometimes associated with the use of cisplatin: serum electrolytes disturbances, particularly those involving low levels of magnesium, calcium,

sodium, potassium and phosphates, have been reported and are probably related to renal tubular damage. Hyperuricemia (increase in uric acid) has been also reported. In addition, neurotoxicity (abnormalities in the nervous system) can be a complication; symptoms include muscle cramps, seizures and loss of taste. Cases of ocular toxicity, including inflammation of the optic nerve and cerebral blindness, have been reported in rare cases even when cisplatin is administrated in the recommended doses. Anaphylactic-like reactions have been occasionally reported in conjunction with the use of cisplatin and can controlled by injection of epinephrine with corticosteroids and/or antihistamines. Finally, hepatotoxicity, in which liver enzymes are elevated, has also been reported.[80]

In addition to the adverse side effects listed above, use of cisplatin has been linked also to nephrotoxicity (kidney toxicity); indeed, renal insufficiency is the major and the most severe form of toxicity associated with the use of cisplatin as chemotherapeutic agent. Renal toxicity can result from doses that are higher than recommended and from an accumulation of cisplatin in the body.[80] It has been hypothesized that cisplatin nephrotoxicity may be a consequence of platinum binding and inactivation of thiol-containing enzymes.[81] On the basis of these considerations, a large number of thiol-based or sulphur-containing nucleophiles have been tested as chemoprotectors to modulated cisplatin nephrotoxicity.[82]

Chemoprotectors are molecules of different pharmacological classes, that can interact by specific inhibition of a chemotherapy in normal cells. By this, they reduce the toxicity endured by normal cells and ameliorate the tolerance.[83] Two concepts for the development of chemoprotectors are required: selective protection of non-tumour normal tissues and the addition of a little, if any, toxicity. For this reason, most of the potential modulators of cisplatin toxicity have been based on the endogenous defense system for electrophiles, the tripeptide glutathione.[84] Studies in platinum resistance clearly indicate an up-regulation of either glutathione,[85] or, more specially one of the family members of glutathione-*S*-tranferase enzymes.[86] These ubiquitous cytosolic enzyme systems are responsible of conjugating toxic electrophiles to the sulphur moiety in glutathione to yield a non-toxic thioether. This conjugated species can be further metabolized and excreted in the urine or the bile. Most of the platinum modulators are believed to act similarly, as alternative sulphur-based nucleophiles are capable to bind activated electrophilic and ligand-exposed platinum species.[87] Although few of those species have been isolated, it is presumed that the direct mechanism may explain most of the activity of the thiol-based modulators, even if there are some evidences that other mechanisms, such as growth factor stimulation, may be operant.[82] Pre-clinical studies have shown that glutathione reduces cisplatin-induced nephrotoxicity without reducing the antitumour activity of the drug.[88,89]

Many other chemoprotectors such as L-SBO (L-buthionine sulfoximine),[90] disulfiram (or antabuse, tetraethylthiuram disulfide),[91] NAC (*N*-acetylcysteine),[92] mesna (mercaptoethane sulfonate sodium salt),[93] sodium thiosulfate[94] and ORG-2766 (amelanocortin-derived peptide),[95] have been tested to modulate cisplatin toxicity. Many of them appear to be effective against platinum-induced nephrotoxicity and, possibly, for the peculiar cumulative-dose limiting neuropathy.

A treatment with diethyldithiocarbamate (DEDT, $[NaS_2CN(C_2H_5)_2]$) reduces the nephrotoxicity of cisplatin chemotherapy.[96] The capability of DEDT to inhibit *cis*-DDP toxicity results from its ability to remove platinum from protein thiol groups.[81] Even if a number of sulphur nucleophiles have been studied as inhibitors of cisplatin-induced nephrotoxicity, as previously reported, a selective protection of normal tissue without inhibition of antitumour activity has been difficult to achieve. On the contrary, DEDT has shown to provide protection against renal, gastrointestinal and bone-marrow toxicity induced by cisplatin without concomitant loss of its antitumour effect.[97] This finding suggests that DEDT selectively reverses platinum-thiol complexes without reversal of platinum-DNA cross-links. 1,2-intrastrand cross-links were decreased by ~50% when cells were treated with DEDT, soon after cisplatin administration, while no change in platinum-DNA intrastrand cross-links was observed when DEDT administration occurred 3 hours after cisplatin. This behaviour is due to the fact that the reaction of cisplatin with DEDT is 40,000-fold faster than with water (hydrolysis), so when DEDT is administered immediately after cisplatin, it first reacts with cisplatin itself by direct substitution rather than by initial rate-limiting hydrolysis, inactivating the drug. If DEDT is administrated a long time after *cis*-DDP treatment, it is not able to react with cisplatin complexes, in which chlorides have been replaced by guanine residues, but removes platinum from a variety of the other sulphur-containing molecules.[50]

However, the overall nephroprotective benefits of DEDT against platinum-containing agents is significantly constrained by its acute toxicity profile; in fact, potential human health hazards associated with free dithiocarbamates include genotoxicity and possible carcinogenicity.[98] Furthermore, DEDT does not extend the ability to deliver dose-intensive chemotherapy and there is a little evidence that it significantly reduces non-renal toxicities, particularly the cumulative neuropathies associated with cisplatin.[82] Thus, a continuous effort is still made by researchers in order to reduce cisplatin-induced toxicity.

1.1.2.4 Cisplatin resistance

Resistance mechanisms can be acquired in some tumour cells or intrinsic in others.[51] Studies on cell lines have demonstrated that cisplatin resistance might be mediated through two broad mechanisms: first, a failure of a sufficient amount to reach the target DNA (i.e drug pharmacokinetics, cell uptake, drug reaction with other molecule than DNA), and, second, a failure to achieve cell death after platinum-DNA adducts formation (DNA repair, modification of gene expression and cell death).[13,51]

Until recently, the underlying complex molecular mechanism by which cisplatin enters cells remained poorly defined. Cisplatin is highly polar and enters cells relatively slowly in comparison to other classes of small-molecule cancer drugs. The uptake of cisplatin is influenced by factors such as sodium and potassium ion concentrations, pH and the presence of reducing agents. A role for transporters or gated channels has also been postulated in addition to passive diffusion.[99] In the past few years, the major plasma-membrane transporter involved in copper homeostasis, copper transporter-1 (CTR1), has also been shown to have a substantial role in cisplatin influx.[20,100] Cisplatin uptake by CTR1 requires micropinocytosis; probably, cisplatin binds to the extracellular domain of CTR1 and is rapidly internalized into endosomes.[101] CTR1 is also a major determinant of responsiveness to cisplatin both *in vitro* and *in vivo*.[102]

In contrast to the mechanism of multidrug resistance (MDR) to mainly natural product-based drugs, which is caused by overexpression of ATP-dependent efflux pumps (such as P-glycoprotein), it is generally a decreased uptake rather than an increased efflux that predominates in platinum-drug resistance.[99] There were early reports of a partial role for efflux proteins such as MDR1 (also known as ATP-binding cassette, subfamily B ABCB1), multidrug resistance protein-1 (MRP1 or ABCC1), MRP 2 (ABCC2 or CMOAT), MRP3 (ABCC3) and MRP (ABCC5) in platinum-drug efflux. However, in recent years, efflux proteins that are involved in copper transport (the ATPases ATP7A and ATP7B) have been shown to modulate cisplatin export.[103]

There is an extensive body of evidence implicating increased levels of cytoplasmic thiol-containing species as causative of resistance to cisplatin. These species, such as the tripeptide glutathione and the metallothioneins, are rich in the sulphur-containing amino acid cysteine and methionine, and lead to detoxification because platinum binds avidly to sulphur. For example, early studies using a panel of eight human ovarian carcinoma cell lines showed a significant correlation between sensitivity to cisplatin and levels of glutathione.[104] The conjugation of cisplatin with glutathione is catalysed by glutathione-S-transferases (GSTs), which makes the compound more anionic and more rapidly exported from cells by the ATP-dependent

glutathione-S-conjugate export (GS-X) pump (that is MRP1 or MRP2).[105] In addition, some translational studies support a role for the glutathione metabolic pathway in acquired and inherited resistance to platinum drugs. Increased levels of other low-molecular-weight thiol-containing proteins that are involved in heavy-metal binding and detoxification, the metallothioneins, have also shown to lead to resistance to cisplatin.

After platinum-DNA have been formed, cellular survival (and therefore tumour drug resistance) can occur either by DNA repair or removal of these adducts, or by tolerance mechanism. There is good evidence to indicate that the hypersensitivity of testicular cancer to cisplatin results from DNA-repair deficiency. Among the four major DNA-repair pathways that have been identified [nucleotide-excision repair (NER), base-excision repair (BER), mismatch repair (MMR), and double-strand-break repair], NER is the major pathway known to remove cisplatin lesions from DNA. The NER endonuclease protein ERCC1 (excision repair cross-complementing-1) forms a heterodimer with XPF [xeroderma pigmentosum (XP), complementation group F] and acts to make a 5' incision into the DNA strand, relative to the site of platinated DNA. Increased NER in cisplatin-resistant ovarian cancer cells was associated with increased expression of ERCC1and XPF (predominantly ERCC1),[106] and knockdown of ERCC1 by small interfering RNAs enhanced cellular sensitivity to cisplatin and decreased NER of cisplatin-induced DNA lesions.[107] Moreover, clinical studies in ovarian cancer patients have correlated increased ERCC1 and mRNA levels with platinum-based chemotherapy.[108]

Increased tolerance to platinum-induced DNA damage can also occur through loss of function of the MMR pathway. Loss of this repair pathway leads to low-level resistance to cisplatin.[109] During MMR, cisplatin-induced DNA adducts are recognized by the MMR proteins MSH2, MSH3 and MSH6 (homologues of the bacterial protein MutS).[110] It is postulated that cells then undergo several unsuccessful repair cycles, finally triggering an apoptotic response; loss of MMR with respect to cisplatin-DNA adducts therefore results in reduced apoptosis and, consequently, drug resistance. Some studies indicate a possible role in acquired drug resistance,[111] whereas other data show no correlation with intrinsic resistance.[112] Another tolerance mechanism involves enhanced replicative bypass, whereby certain DNA polymerases such as β and η can bypass cisplatin-DNA adducts by translesion synthesis;[113] polymerase η has been shown to have a role in cellular tolerance of cisplatin.[114] Finally, tolerance might occur to platinum, and other cancer drugs, through decreased expression or loss of apoptotic signalling pathways (either the mitochondrial or the death-receptor pathways) as mediated through various proteins such as p53, anti-apoptotic or pro-apoptotic members of the BCL2 family and JNK.[115]

1.1.2.5 Circumvention of clinical cisplatin resistance

Armed with the acquired information described above, concerning mechanisms of action and tumour resistance, four major strategies can now be proposed to circumvent platinum-resistance in cancer patients: new improved drugs (discussed further down), improved delivery of platinum to tumours, co-administration of platinum drugs with pharmacological modulators of resistance mechanisms, combining platinum drugs with new molecularly target drugs.

The strategy of using delivery vehicles to selectively transport higher amounts of tumour-killing agents to tumours is attractive and has now been clinically validated with the cytotoxics doxorubicin and paclitaxel.[116,117] Liposomal preparations of cisplatin-like molecules have also been produced, but they have not achieved the good release and activation needed. In addition, it has been evaluated the possibility of linking a platinum-based to a water-soluble, biocompatible co-polymer, such as hydroxypropylmethacrylamide (HPMA), in order to exploit the enhanced permeability and retention (EPR) effect of macromolecules in tumours. In particular situations, such as patients with ovarian cancer, localized platinum-drug administration through intraperitoneal injection might be applied.[13]

As described above, much is now known about how tumours are or become resistant to cisplatin. This, in turn, has provided clinical opportunities to specifically target these resistance mechanisms, either alone or in combination with other platinum drug. For example, the glutathione-mediated detoxification pathway is an important determinant of platinum-drug sensitivity and resistance, and phase I clinical trials were performed using an inhibitor of glutathione synthesis, buthionine sulfoximine. Moreover, another approach exploits loss of the DNA MMR pathway through hypermethylation of the MutL homologue (MLH1) gene, which has been shown to lead to resistance to cisplatin, and predicts for poor survival of patients with ovarian cancer.[111] This has led to the concept of using a DNA demethylating agent such as 2'-deoxy-5-azacytidine in combination with cisplatin to reverse this resistance mechanism.[13]

Most contemporary cancer discovery and development involves the targeting of specific molecular abnormalities that are characteristic of cancer, described in terms of various phenotypic 'hallmarks'.[118] An emerging clinical theme is that, in some cases, these agents might not possess spectacular activity as monotherapy, but they perform optimally in combination with existing cytotoxics.[13]

1.1.3 New, improved platinum drugs

Cisplatin is a very effective cancer drug and has had a major clinical impact, particularly for patients with testicular or ovarian cancers. But, it is notoriously toxic to the kidneys and gastrointestinal tract. Since its efficacy was established in the 1970s, the research for new platinum derivatives was greatly stimulated. Around 3000 platinum compounds have been synthesised.[51] Three of them are currently in clinical use: carboplatin, oxaliplatin and nedaplatin (**Scheme 1.4**). Like cisplatin, all of them have a square-planar geometry with two amino ligands in *cis* position.

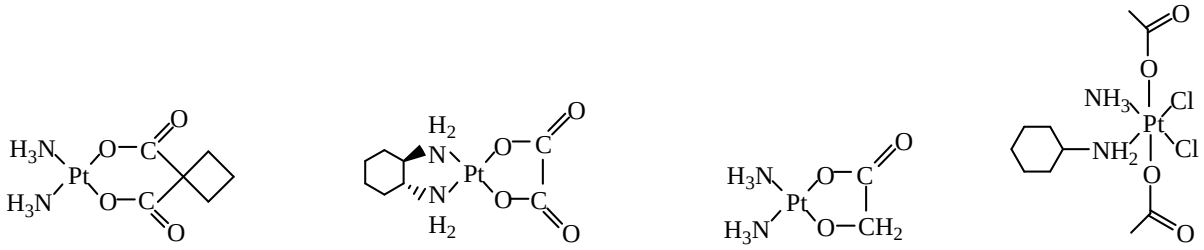

(a) **(b)** **(c)** **(d)**

Scheme 1.4 The anticancer platinum drugs carboplatin **(a)**, oxaliplatin **(b)**, nedaplatin **(c)** and satraplatin **(d)**.

The first wave of drug-development activity aimed at discovering a less toxic analogue that retained anticancer activity. In the mid-1980s, carboplatin (cis-diammine-[1,1-cyclobutanedicarboxylato]platinum(II)) was introduced in the clinic.[119] Carboplatin was based on the hypothesis that a more stable leaving group than chloride might lower toxicity without affecting antitumour efficacy. It turned out to be correct: compared to cisplatin, carboplatin is essentially devoid of nephrotoxicity, and is less toxic to the gastrointestinal tract and less neurotoxic; by contrast, myelosuppression, principally thrombocytopenia, is dose-limiting for carboplatin. Interestingly, the adducts formed by carboplatin on DNA are essentially the same as those formed by cisplatin, but 20-40-fold higher concentrations of carboplatin are required and the rate of adduct formation is around 10-fold slower.[120] Numerous randomized clinical trials have demonstrated essentially equivalent survival rates for carboplatin and cisplatin in patients with ovarian cancer,[121] and in most countries, a carboplatin-based regimen is the standard to cure the ovarian cancer. In fact FDA approval was granted in 1989 for this indication.[13]

Oxaliplatin [1R,2R-diaminocyclohexane oxalatoplatinum(II)] is based on the 1,2-diaminohexane carrier ligand and was originally described in the late 1970s.[122] It is a more water-soluble derivative of the failed drug tetraplatin (**Scheme 1.5**). Interestingly, oxaliplatin showed a differing pattern of sensitivity to that of cisplatin in the NCI 60-cell human tumour panel.[123] In addition, in contrast to cisplatin and carboplatin, the accumulation of oxaliplatin

seems to be less dependent on the copper transporter CTR1;[124] MMR recognition proteins do not recognize oxaliplatin-induced DNA adducts;[109] some differences exist in the structure of oxaliplatin-induced 1,2-intrastrand DNA cross-links;[125] and oxaliplatin retains activity against some cancer cells with acquired resistance to cisplatin.[126] In 2002, it became the third platinum to be approved by the US FDA.[13]

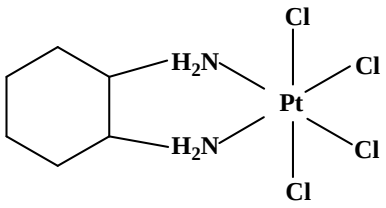

Scheme 1.5 Structure of tetraplatin

Nedaplatin has a glycolate moety as leaving group. It is available only in Japan.[51] It was selected because it produced better results than cisplatin in preclinical studies. Unfortunately, nedaplatin is cross-resistant with cisplatin. It main toxicity in humans is myelosuppression, with a delayed nadir and recovery. The official indications in Japan are head and neck, testicular, lung (non-small-cells and small-cells lung cancer), oesophagal, ovarian and cervical cancer. Compared to cisplatin (both in combination with vindesine), nedaplatin showed no advantage over cisplatin in objective response and overall survival, but nedaplatin was less toxic. More thrombocypenia was observed, but less leucopenia, nephrotoxicity and gastrointestinal toxicity.[127-129]

In addition to carboplatin and other second-generation cisplatin analogs, several third-generation drugs have been synthesized and tested. As more attention is paid to quality-of-life of the patient nowadays, orally formulated chemotherapy has been investigated for many years. One orally available platinum complex, satraplatin [bisacetoamminedichlorocyclohexyl-amineplatinum(IV), **Scheme 1.4**] is currently under clinical trial. It was originally developed to be an orally active version of carboplatin (that is, to possess a carboplatin rather than a cisplatin-like toxicity profile). Preclinical studies showed that the drug possessed good antitumour activity by the oral route, at least comparable to intravenously administrated cisplatin or carboplatin, in mice with human ovarian cancer xenografts,[130] especially when administered over a 5-consecutive-day schedule.[131] It also retained activity in human cells with acquired cisplatin-resistance, in which resistance was due to reduced platinum transport.[132] In vivo satraplatin is transformed to around six products, the major one being JM118 [cis-amminedichlorocyclohexylamineplatinum(II)].[133] JM118 retained activity in cells that had lost the copper-influx transporter CTR1,[134] and has been shown to bind DNA in a very similar

manner to that described for cisplatin[135] and to be repaired by the NER pathway with similar kinetics.[136]

The wide success of platinum drugs has been promoting the development of both platinum- and other metal-based compounds.[137] Owing to the intrinsic nature of metal centers, characteristic coordination modes and kinetic properties, metallodrugs function through mechanisms that cannot be mimicked by organic agents, *i.e.* they affect cellular processes such as cell division and carcinogenic reactions in different ways. The latest approaches focus on complexes with tumour-targeting properties, thereby maximizing the impact on cancer cells and minimizing the occurrence of adverse side-effects, and on complexes with biological ligands.[138] Among the non-platinum antitumour agents, gold complexes have recently gained increasing attention.

1.1.4 Gold in medicine

1.1.4.1 History

Medical properties of gold have been explored throughout the history of civilization. Gold has been exploited for various medicinal preparations even in India and Egypt. The earliest therapeutic application of gold can be tracked back to 2500 B.C in China, where gold was used to treat smallpox, skin, ulcers and measles.[139] Moreover, 'medicinal gold' was developed as elixirs.[140] Although gold and gold complexes have historically been used for the treatment of a wide range of aliments, the rational use of gold in medicine began in the early 1920s when gold was clinically tested for its *in vitro* bacteriostatic effect. The first gold complex used for that purpose was gold cyanide $K[AuCN_2]$, employed by Robert Koch to kill mycobacteria, the causative agent of tuberculosis.[141] Because of the toxicity observed when used to treat pulmonary tuberculosis, the treatment was switched to the less toxic gold(I) thiolate complexes. In the early 1930s, Jacques Forestier introduced the same thiolate complexes for the treatment of rheumatoid arthritis, which he believed was related to tuberculosis. These compounds were considered for many decades the drug of choice for the treatment of rheumatoid arthritis. The application of gold complexes in medicine has been called 'chrysotherapy' and aims at reducing inflammation and disease progression in patients with rheumatoid arthritis. The structures of the four clinically used compounds are reported in **Scheme 1.6** (compounds **a**-**d**). However, the toxic side effects (*e.g*: nephrotoxicity at high concentration) observed with these complexes, prompted the search for new, less toxic therapeutic gold complexes with capacity for oral

administration[142] in low doses. As a result of intense work on synthesis and evaluation of many new gold complexes, auranofin [(tetra-O-acetyl-β-D-glucopyranosyl)-thio](triethylphosphine)-gold(I) was developed as new drug for rheumatoid arthritis treatment.

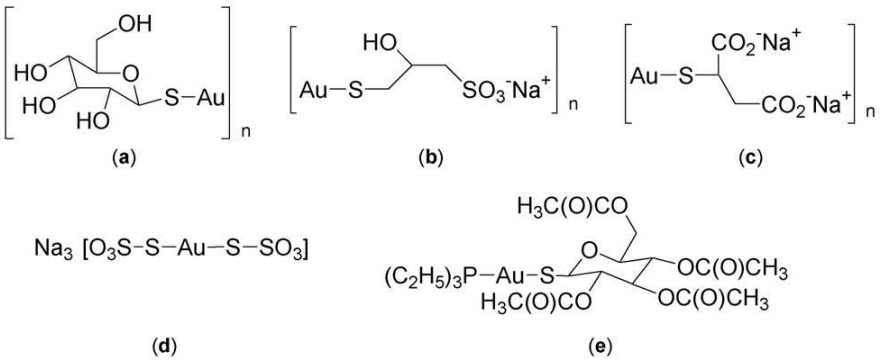

Scheme 1.6 Some gold(I) thiolates used in the treatment of rheumatoid arthritis: solganol (a), allocrysin (b), myocrysin (c), sanocrysin (d) and auranofin (e).

Unfortunately, not all patients benefit from gold treatment and for those who do respond, most suffer from deleterious side effects of varying extents (dermatis, diarrhea, …). For these reasons, gold(I) drugs are currently used mainly as last-resort treatment for severe cases of rheumatoid arthritis.[143]

The known immunodepressive and anti-inflammatory actions of anticancer drugs such as 6-mercaptopurine and cyclophosphamide have established, at least in principle, a connection between antiarthritic and anticancer therapies. Importantly, one long-term study suggested that rheumatoid arthritis patients treated with gold-based drugs have lower malignancy rate.[144] Subsequently, experimental research on auranofin revealed that it presented an *in vitro* activity similar to or even greater than cisplatin.[145,146]

In the last few decades, the properties of some gold compounds have been evaluated against immunodeficiency virus (HIV) for the treatment of AIDS.[147,148] Gold complexes have also been explored for effectiveness against acute forms of asthma and pemphigus (an immune corticosteroid-dependent asthma). Additionally, current research has described promising results using complexes to treat malaria,[149] Chagas disease[150] and cancer.[151]

1.1.4.2 Gold(I) complexes

Starting from the gold(I) species used in chrysotherapy for the treatment of rheumatoid arthritis, the research on gold complexes has so far focused mainly on complexes with gold in the oxidation state +1. Auranofin and a number of its analogs showed potent cytotoxic activity

against melanoma and leukaemia *in vitro* and antitumour activity against leukaemia *in vivo*. However, these compounds were completely inactive against solid tumours. Based on that, a series of digold phosphine complexes (**Scheme 1.7**), such as gold(I) 1,2-bis(diphenylphosphine)ethane (DPPE), was synthesized and found to confer *in vitro* cytotoxic activity especially in some cisplatin-resistant cell lines.[152] Surprisingly, mechanistic studies suggested that, in contrast to cisplatin, DNA was not the primary target for these gold(I) complexes and that their cytoxicity was mediated by their ability to alter the mitochondrial functions and inhibit the protein synthesis by interfering with DNA-protein interactions.[153] This could be explained by higher affinity of gold(I) toward the so-called soft ligands with sulphur (*e.g.* thiolates) and phosphorous (*e.g.* phosphines), and the lower affinity for nitrogen and oxygen-containing ligands. Although these gold(I) complexes had marked cytotoxic antitumour activity against P388 leukaemia, they had limited antitumour activity against solid tumour models. These complexes never entered clinical trials, due to problems associated with cardiotoxicity highlighted during preclinical toxicology studies.[154]

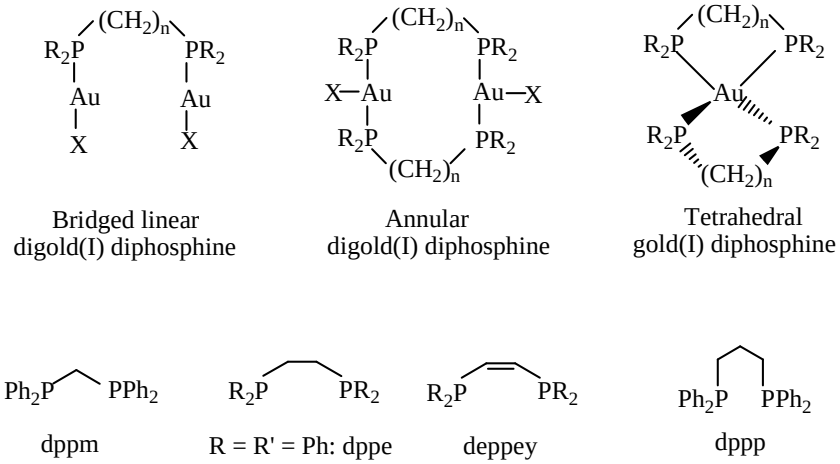

Scheme 1.7 General structure of some *in vitro* cytotoxic diphosphine gold(I) complexes.

Investigations on the cytotoxic scores of gold(I) dithiocarbamato compounds and derivatives have been recently reported. Mono- and digold- dithiocarbamato esters (**Scheme 1.8**) showed no or comparable cytotoxicity to that displayed by cisplatin in the investigated cell lines.[155]

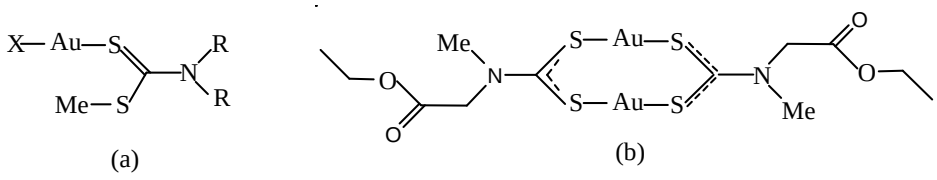

Scheme 1.8 Gold(I) dithiocarbamate complexes (X = Cl or Br).

1.1.4.3 Gold(III) complexes

1.1.4.3.1 *Compounds of biological interest*

The promising results of platinum(II) complexes stimulated the interests in the area of metal-based antitumour agents. As gold(III) is isoelectronic and isostructural with Pt(II), square-planar gold complexes appeared to be suitable candidates for biological testing. But, in comparison with Pt(II) compounds, gold(III) analogues turned out to be relatively unstable and light-sensitive and to undergo easy reduction to metallic gold, under physiological conditions. As a consequence of these difficulties, that heavily hindered their pharmaceutical applications, gold(III) compounds were rapidly abandoned and then neglected for several years.[156] However during the early 90's, there was a revival of interest for gold(III)-based anticancer compounds, as a few novel compounds displayed improved stability and encouraging pharmacological properties. For instance, a series of organogold(III) DAMP (o-$C_6H_4CH_2NMe_2$) complexes, [Au(DAMP)X_2] (**Scheme 1.9**, (g)), were prepared and screened for antitumour activity with positive results. Recently, *in vitro* activities of a series of gold(III) complexes (**Scheme 1.9**), [Au(en)$_2$]Cl_2 (a), [Au(dien)Cl]Cl_2 (b), [Au(cyclam)](ClO_4)Cl_2 (c), [Au(terpy)Cl]Cl_2 (d) and [Au(phen)Cl_2]Cl (e), against the A2780 ovarian cancer cell lines and a cisplatin-resistant variant were described. The relative order of cytotoxicity was: Au(terpy)>>Au(phen)>Au(en), Au(dien)>>Au(cyclam). Interestingly, the three most active complexes retained activity against the cisplatin-resistant cell lines.[157,158] In the same years, the cytotoxic properties of chloro-glycylhistidinate gold(III) (**Scheme 1.9**, (f)), a complex with promising chemical and biological activities was reported.[159-160] Notably, this gold(III) peptide complex manifested a far higher cytotoxic activity towards the established A2780 ovarian cancer cell line compared to zinc(II), palladium(II), platinum(II) and cobalt(II) analogues, proving that the gold(III) centre has a crucial role in determining the pharmacological effects.[160]

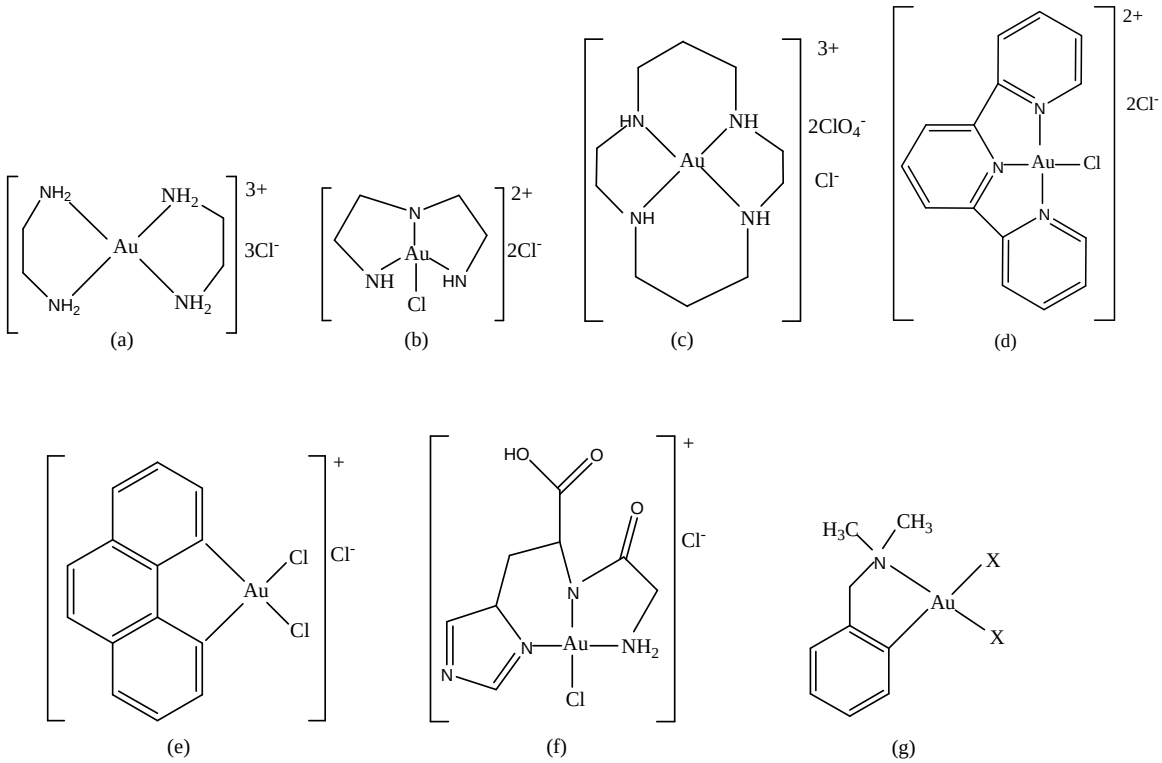

Scheme 1.9 Structures of $[Au(en)_2]Cl_2$ (a), $[Au(dien)Cl]Cl_2$ (b), $[Au(cyclam)](ClO_4)Cl_2$ (c), $[Au(terpy)Cl]Cl_2$ (d), $[Au(phen)Cl_2]Cl$ (e), GHAu (f) and $[Au(DAMP)X_2]$ (g).

1.1.4.3.2 *Gold(III)-dithiocarbamato complexes*

In these few past years, a number of gold(III)-dithiocarbamato derivatives of general formula $[Au^{III}X_2(dtc)]$ (X= CL, Br, dtc = various dithiocarbamato ligands) have been synthesized by Fregona and coworkers. These compounds have been designed to reproduce very closely the main features of cisplatin (**Scheme 1.10**)[155] and to obtain drugs with a better therapeutic index, in terms of high anticancer activity and reduced toxicity, compared to cisplatin.

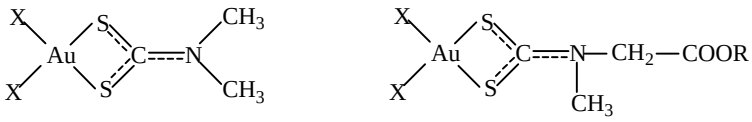

(a) $Au(DMDT)X_2$ **(b)** $Au(SSC\text{-}Sar\text{-}OR)X_2$

Scheme 1.10 Gold(III)-dithiocarbamato complexes; X = Cl, Br; R = CH_3, CH_2CH_3, $(CH_3)_3C$.

The choice of the dithiocarbamato ligands was not accidental. In fact, being sulphur donor ligands, they can effectively chelate the metal centre, preventing by this the reaction with proteins sulfide sites when crossing the renal tubules. Moreover, as previously discussed in the

case of platinum-based drugs, the therapeutic effectiveness is highly limited with resistance onset during treatment. This phenomenon is due to drug inactivation resulting from the affinity of the metal for thiol ligands such as glutathione and metallothioneins. Although Au(III) is a metal centre quietly hard that prefers coordination with nitrogen ligands, Au(III) complexes can present, in analogy with platinum, a high affinity for thiol ligands. The Au(III) reaction with sulfide moieties could lead to the breaking of coordinative bonds and a successive reduction of Au(III) to Au(I) and Au(0).

- *In vitro* and *in vivo* cytotoxicity studies

From comparative *in vitro* studies on various cell lines, the Au(III)-MSDT (MSDT= methylsarcosinedithiocarbamato) derivatives (**Scheme 1.10**, R = CH_3) resulted to be more active than the reference drug. Moreover, after a short exposure, they induced strong and rapid apoptosis by down-regulating the anti apoptotic molecule Bcl-2 and upregulating the proapoptotic molecule Bax, whereas cisplatin did not. Finally, after long exposure, they were proved to induce only modest cell cycle perturbations but high DNA fragmentation, whereas classical platinum(II) complexes are known to promote characteristic cell cycle alterations resulting in increased G_2M cell fraction.[40] Therefore, [$Au^{III}X_2$(MSDT)]-type complexes are able to promote early apoptosis and membrane damage to a much greater extent than cisplatin, suggesting a different mechanism of action. [161]

The other Au(III)-dithiocarbamato derivatives, namely [$Au^{III}X_2$(DMDT)] and [$Au^{III}X_2$(ESDT)] DMDT being dimethyldithiocarbamato and ESDT ethylsarcosine-dithicarbamato) (**Scheme 1.10**, R = CH_2CH_3) were proved to be much more cytotoxic *in vitro* than cisplatin even toward human tumour cell lines intrinsically resistant to cisplatin itself. In addition, they appeared to be extremely more active also on cisplatin-resistant cell lines, with activity levels comparable to those recorded on the corresponding cisplatin-sensitive parent cell lines, ruling out the occurrence of cross-resistance phenomena.[155]

In vivo antitumour activity of [$Au^{III}Br_2$(ESDT)] has been evaluated on Ehrlich solid-tumour-bearing mice, resulting in significant tumour mass reduction compared to cisplatin-treated animal. Moreover, tumours taken up from [$Au^{III}X_2$(ESDT)]-treated mice after 11-day treatment showed 74% inhibition of tumour growth compared to untreated animals. This Au(III)-dithiocarbamato derivative resulted to have *in vivo* low nephrotoxicity, compared to cisplatin, and a good tolerance during chemotherapy. [162]

More recently, a group of thirteen Au(III) complexes, including [$Au^{III}Br_2$(ESDT)], has been tested at Oncotest GmbH according to a specific comparative *in vitro* strategy for the development of new anticancer agents. Among all, [$Au^{III}Br_2$(ESDT)] turned out to be the second

best performer with IC_{50} values in the low micromolar range on all the screened 36 human tumour cell lines, in particular against ovary and brain cancers, and an excellent degree of selectivity.[163]

Given the strict structural and chemical analogy of these Au(III) complexes with cisplatin, their cytotoxicity was expected to rise from a direct interaction with intracellular DNA. Experimental results established their high affinity towards some biologically-relevant isolated macromolecules, resulting in a dramatic inhibition of both DNA and RNA synthesis in a non-dose-dependent way, whereas, as expected, cisplatin promoted a strong dose-dependent inhibition of DNA without significantly affecting RNA synthesis. In addition, these compounds showed extremely fast rates of DNA-binding, achieving 100% binding to calf thymus DNA after less than 3 hours, compared to 51% reached by cisplatin under the same experimental conditions after 24 hours. They were also shown to form interstrand cross-links with a faster kinetics than cisplatin, whereas they were unable to induce DNA-proteins cross-links.[164]

- Mechanistic studies

Altogether, the experimental results suggests that the mechanism of action of these Au(III)-dithiocarbamato derivatives differs from that of the classical platinum(II)-based anticancer drugs. Their binding to DNA to a greater extent than cisplatin is more likely a consequence of their higher reactivity towards isolated biologically-relevant macromolecules rather than of a preference for DNA as their ultimate target.

In this regard, recent reports have identified the enzyme thioredoxin reductase (TrxR) as a reliable target for anticancer gold compounds. [165] The thioredoxin (Trx) system plays a key role in regulating the overall intracellular redox balance. TrxR is a large homodimeric selenoenzyme controlling the redox state of Trx. TrxR was proved to be inhibited by a number of gold derivatives, thus triggering alterations of the mitochondrial functions and induce severe oxidative stress, eventually leading to cell apoptosis. In order to get insights into the mechanism of action, the previous four Au(III) complexes have been studied in-depth as inhibitors of the thioredoxin system. All the tested compounds induce cancer cell death through both apoptotic and non-apoptotic mechanisms, and inhibit TrxR activity.[166]

Based on these results, a working model suggesting that deregulation of TrxR/Trx system is a major mechanism involved in their anticancer activity was proposed. These compounds trigger cell death, favour generation of reactive oxygen species (ROS), modify some mitochondrial functions (*i.e* membrane potential, thus promoting mitochondrial swelling, but not respiratory chain), and inactivate both cytosolic and mitochondrial thioredoxin reductase. Thioredoxin protects the cell from a variety of oxidative stresses by regulating the redox state and activity of

some cellular proteins that control cell growth. All the tested complexes inhibit TrxR by irreversibly binding to the catalytic site, thus hampering the function of TrxR that acts as a mediator of electron flow of nicotinamide adenine dinucleotide phosphate (NADPH) to peroxiredoxins through Trx, leading to the accumulation of ROS (especially hydrogen peroxide). Moreover, the inhibition of TrxR/Trx redox system promotes the dissociation of the Trx-AS-1 (apoptosis signal-regulating kinase-1) and the subsequent activation of the MAPK (mitogen-activated protein kinase) system. Both the increase level of the ROS and the activation of MAPK system induce elevated long-lasting levels of phosphorylated extracellular signal-regulated kinases-1 (phosphor-ERK-1) and -2 (phosphor-ERK-2) that may lead to cell death. Intriguingly, ERK phosphorylation, and the consequent cell death, were inhibited by the oxidant NAC (itself preventing the dissociation of the complex Trx-ASK-1 by keeping Trx in the reduced state), whereas the peroxyl scavenger trolox (6-hydroxy-2,5,7,8-tetramethylchroman-2-carboxylic acid) was only slightly efficient. Thus, it was hypothesized that a persistent ERK-1/2 activation, triggered by accumulation of hydrogen peroxide first and then by ASK-1 pathway deregulation, might be responsible for cell death through both apoptotic and non–apoptotic routes. Cisplatin leads to cell death only through an apoptotic pathway (as determined by the poly-(ADP-ribose)-polymerase (PARP) cleavage).[167]

Recently, the proteasome has been investigated as a major *in vitro* and *in vivo* target for these Au(III)-dithiocarbamato complexes.[168] The ubiquitin-proteasome pathway (**Fig. 1.5**) plays a major role in the degradation of oxidatively damaged and mutated proteins as well as proteins involved in the cell cycle.

The proteasome is a large multisubunit protease complex localized in the nucleus and cytosol that identifies and degrades the proteins tagged by a chain of ubiquitin molecules. The 20S proteasome, the proteolytic core of a 26S complex, contains multiple peptidase activities (chymotrypsin-, trypsin- and caspase-like) and acts as a catalytic machine. Ubiquitinated proteins are escorted to the 26S proteasome where they undergo final degradation, while the ubiquitin is released and recycled. Aberrant proteasome-dependent proteolysis seems to be associated with pathophysiology of some malignancies, including cancer, in which some regulatory proteins are either stabilized, due to decreased degradation, or lost, due to accelerated degradation. Therefore, the ubiquitin-proteasome pathway has become an attractive target for the development of new anticancer agents, the validation of which arise from the approval of the proteasome-inhibiting chemotherapeutic agent bortezomib, used in the treatment of multiple myeloma.[169]

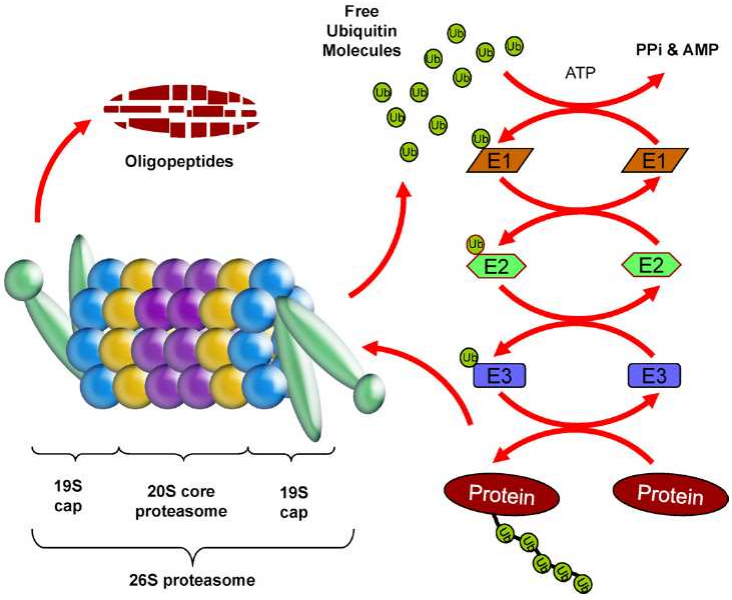

Figure 1.5 The ubiquitin-proteasome pathway

The proteasome-inhibiting properties of $[Au^{III}X_2(DMDT)]$ have been investigated.[161] First, it was shown to inhibit cell proliferation on several breast cancer cell lines. In particular, it exhibited *in vitro* cytotoxic activity greater than cisplatin towards the highly metastatic and invasive, estrogen receptor, α-negative MDA-MB-231, breast cancer cell line (85% *vs.* about 20% inhibition, respectively, both at 5μM concentration). $[Au^{III}X_2(DMDT)]$ strongly inhibit also the chymotrypsin-like activity in MDA-MB-231 whole-cell extract in a dose-dependent way. This evidence is particularly important since inhibition of chymotrypsin-like activity is associated with growth arrest and/or apoptosis induction in cancer cells.[170] Inhibition of all three activities was observed also on a purified rabbit 20S proteasome. Proteasome inhibition was further detected in intact MDA-MB-231 cells, confirmed by decreased proteasomal activity and increased levels of ubiquitinated proteins and the target protein p27.

Induction of apoptosis by $[Au^{III}X_2(DMDT)]$ *in vitro* has been confirmed by multiple assays identifying cellular and biochemical hallmarks, such as morphological changes, the presence of apoptotic nuclei, and apoptosis-specific PARP cleavage. Finally, treatment of MDA-MB-231 breast tumour-bearing nude mice with this complex resulted in significant inhibition of tumour growth (*ca.* 50% inhibition after a daily treatment with 1.0 $mg.kg^{-1}$ for 29-days). No toxicity was observed, and mice did not display signs of weight loss, decreased activity or anorexia.[161]

Similar results have been obtained with the complex $[Au^{III}X_2(ESDT)]$, which was even more effective than $[Au^{III}X_2(DMDT)]$ as both *in vitro* and *in vivo* proteasome inhibitor.[171] In addition, in this case, a more in-depth investigation has been performed to better elucidate the involved mechanism of action, and generation of ROS was detected.

These results clearly identify the proteasome as a primary target of the investigated Au(III) complexes. Anyway, it is worth pointing out that this hypothesis is not in contrast with the previously discussed model related to the Trx/Trx system as potential target. In fact, it has been recently reported that the proteasome inhibitor bortezomib induces apoptosis through generation of ROS.[172] Since ROS are produced also in these cases,[171] the observed proteasome inhibition can favour the long-lasting persistence of phosphorylated ERK-1/2.

1.1.5 Peptides transporters as drug delivery systems

The main problem of the therapeutic efficiency lies in the crossing of the cellular membranes. Therefore, attention is being directed towards different systems that could improve the overcoming of the cellular membrane barrier. Recently, two plasma membrane proteins, PEPT1 and PEPT2, have been individuated. They are present predominantly in epithelial cells of the small intestine, mammary gland, lung, choroids plexus, kidney and in other cell types. These proteins couple the movement of substrate across the membrane with that of protons, according to electrochemical proton gradient. The peptide transport allowed by PEPT1 and PEPT2 results to be against the concentration gradient. PEPT1 is a low affinity/high capacity and PEPT2 is a high affinity/low capacity transporter. A unique feature is their ability to transport inside the cells all possible di- and tripeptides, including different charged species. These transporters are stereoselective for peptides that contain L- enantiomers of α-amino acids.[173]

With this Thesis work we planned to exploit the peculiarities of PEPT1 and PEPT2 to favor the uptake by a tumor cell of Au(III)-dithiocarbamato drugs. To this aim, we synthesised, characterised and tested a series of Au(III)-dithiocarbamato complexes containing di- and tripeptides as ligands. We extensively used the α-aminoisobutyric acid (Aib), a natural, but non coded, α-amino acid. The reason for this choice comes from the observation that Aib is abundant in a class of natural peptides (the antibiotic peptaibols), that are characterized by a relevant ability to cross or perturbate the cell membranes. In these natural peptides the role of Aib is crucial, as it bias the peptide backbone to fold into helical arrangements.

Therefore, in the following section the main conformational features of Aib-containing peptides will be summarised.

1.1.6 Aib-containing peptides

1.1.6.1 Biological activity

Peptides antibiotics are used as the first defensive barrier of the organism against microbial infection. They possess a broad spectrum of antimicrobial activity against Gram-positive and Gram-negative bacteria, fungi and protozoa.[174-176] It has been shown that some of these peptides exhibit antiviral and anticancer activity.[177-182] $C^{\alpha,\alpha}$-dialkyl amino acids are also found in peptide antibiotics. Aib, the simplest $C^{\alpha,\alpha}$-dialkyl amino acid, is particularly abundant in the peptaibol family of peptide antibiotics. The peptaibols, produced by many classes of fungi, are characterized by a high proportion of Aib residues, an acylated N-terminus and an amino alcohol at their C-terminus.[183] Their length spans from 5 to about 20 residues. Recently, it was proved that the presence of Aib residues is useful in the design of effective peptide antibiotics with increased protease resistance without decreasing the antimicrobial activity.[184]

1.1.6.2 Stereochemistry

Understanding the tridimensional structure of a protein or a peptide is fundamental to obtain detailed information on molecular recognition, and on peptide biological functions in general. Peptide structure can be described at different size scales and levels of complexity: the *primary* structure of a peptide is the sequence of amino acid residues along its backbone, the *secondary* structure refers to ordered conformations of the peptide backbone, whereas the *tertiary* structure refers to its the global shape considering also the side-chains. The secondary structure is deeply influenced by the nature of the amino acids in the sequence and by the hydrogen bonding pattern between backbone amide protons and carbonyl oxygens. Its univocal description relies on the specification of the *dihedral*, or torsion, angles of the three backbone bonds of each residue (Fig.1.12), called ϕ, ψ, ω by the convention recommended by the IUPAC-IUB Commission on Biochemical Nomenclature.[185]

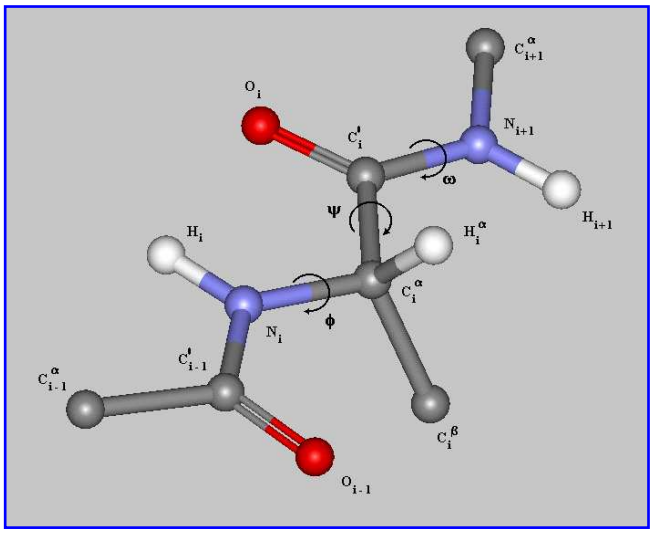

Figure 1.6. Representation of a polypeptide chain (two peptide units). Recommended notations for the torsion angles are represented in the central residue. The chain is represented in the fully extended conformation ($\phi_i = \psi_i = \omega_i = 180°$) and the central residue is in L (S) configuration.

The most important and widespread peptide secondary structures are[186] the α-helix, the β-structures, the β-turns and the 3_{10}-helix; the most common organized secondary structures are helical. Various helical structures differ in the dihedral angles ϕ and ψ of each residue, in the number of residues per turn, in the pitch and in the number of atoms involved in the pseudocycles formed by intramolecular hydrogen bonds C=O···H-N.[187]

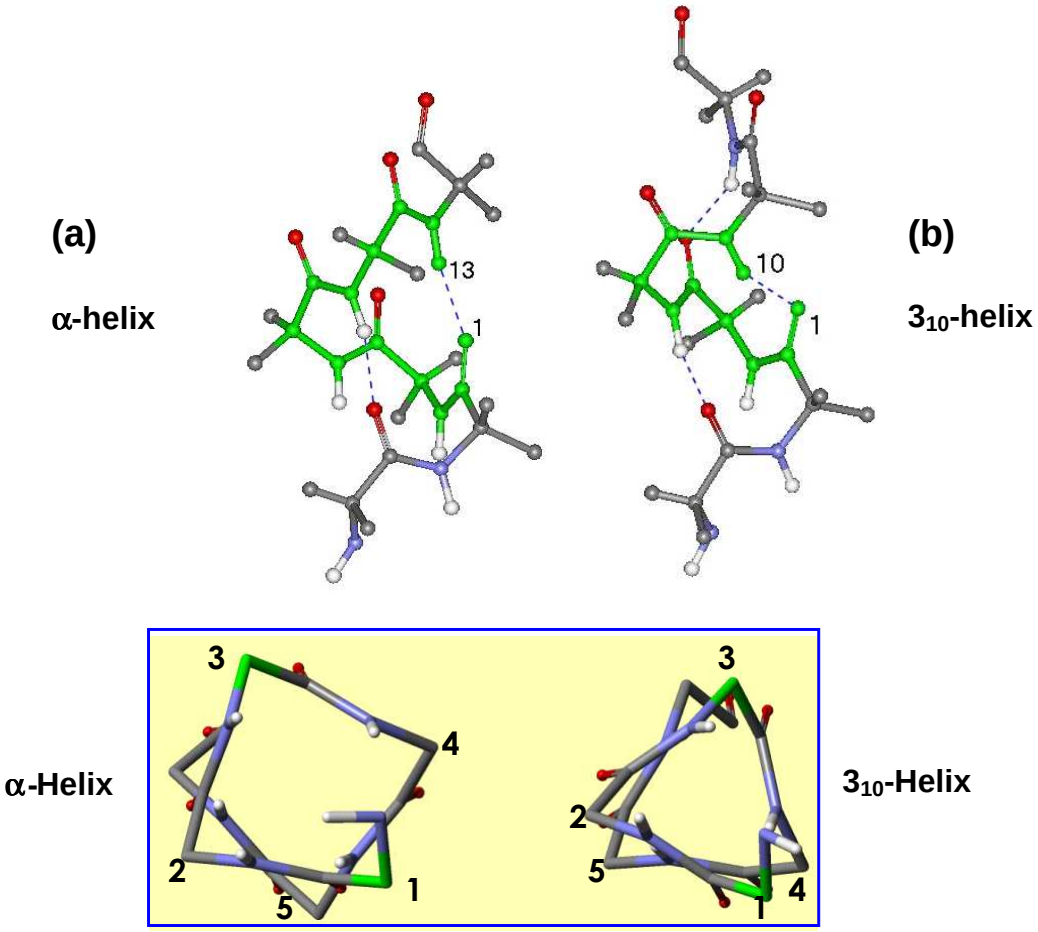

Figure 1.7 Top: side view of right-handed α-helix **(a)** and 3_{10}-helix **(b)**; bottom: projections of the α-helix and of the 3_{10}-helix along the helical axis.

As mentioned above, the α-helix and the 3_{10}-helix are the most common helical structures. The α-helix (**Fig. 1.7a**) is characterized by 3.63 residues per turn and it is stabilized by intramolecular hydrogen bonds between the C=O group of residues in position *i* and the N-H group of residues in position *i*+4 (*i* ← *i*+4 H-bonds), thus forming 13-atoms pseudocycles (α-turns or C_{13} structures). The 3_{10}-helix (**Fig. 1.7b**) has 3.24 residues per turn and it is stabilized by intramolecular hydrogen bonds between the C=O group of residues in position *i* and the N-H groups of residues in position *i*+3 (*i* ← *i*+3 H-bonds), thus forming 10-atoms pseudocycles (β-turns or C_{10} structures).[186] Hydrogen bonding patterns of both helices are compared in **Fig. 1.8**.

Even if the difference in the torsion angle values of the two helices is not large, the 3_{10}-helix is significantly thinner (refer to **Fig. 1.7**, bottom) and more elongated than the α-helix (the pitch is 6.3 Å for the first one and 5.7 Å for the second one). Characteristic structural parameters of the two helices are reported in **Table 1.1**.[188]

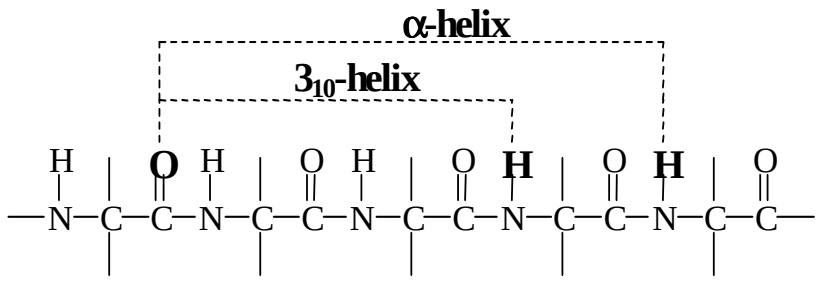

Figure 1.8 Intramolecular hydrogen bonds in α- and 3_{10}-helices.

Parameter	**3_{10}-helix**	**α-helix**
ϕ	-57°	-63°
ψ	-30°	-42°
H-bonding angle N···O=C	128°	156°
Rotation per residue	111°	99°
Rise (axial translation per residue)	1.94 Å	1.56 Å
Residues per turn	3.24	3.63
Helical pitch	6.29 Å	5.67 Å

Table 1.1. Structural parameters for right-handed 3_{10}- and α-helices.

A 3_{10}-helix formed by C^{α}-trisubstituted (protein) α-amino acids is less stable than an α-helix, due to the larger distortion of the H-bonds and some unfavorable Van der Waals interactions.[189-191] Although the 3_{10}-helical structure is thus less widespread than the α-counterpart, nevertheless it is not rare. The recent improvements in analytical techniques allowed to identify the 3_{10}-helical patterns in numerous natural proteins.[192-194] A statistical analysis of the X-ray diffraction structures of 57 globular proteins revealed the presence of 71 3_{10}-helical motifs of different length. Interestingly, in most cases such structures were found at the N- and C-termini of α-helices.

The main β-turn patterns were classified by Venkatachalam.[195] Six pairs of β-turn types (each one made of a right- and a left-handed turn) were described, depending on the values of the torsion angles of the 'internal' *i*+1 and *i*+2 residues. **Table 1.2** gives ϕ, ψ torsion angle values for the right-handed β-turns with central peptide bond in trans conformation (types I, II, and III, **Fig. 1.9**).

β-Turn	$\phi(i+1)$	$\psi(i+1)$	$\phi(i+2)$	$\psi(i+2)$
Type I	-60°	-30°	-90°	0°
Type II	-60°	+120°	+80°	0°
Type III	-60°	-30°	-60°	-30°

Table 1.2. Dihedral angle values for the three most common types of right-handed β-turns. Left-handed β-turns have opposite dihedral angle values.

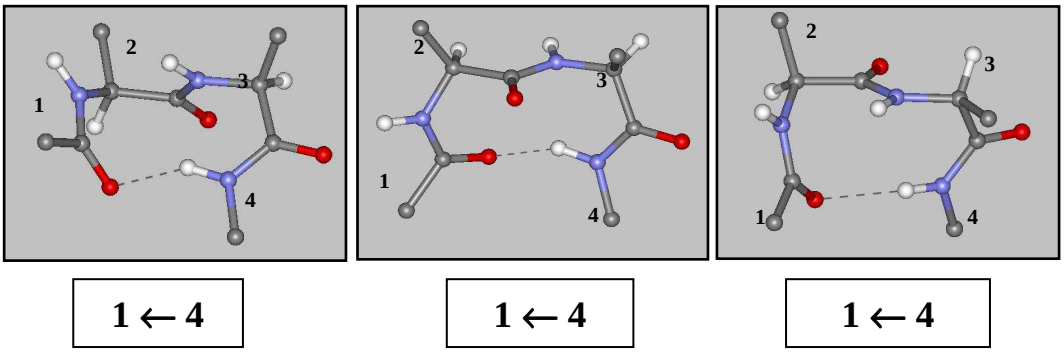

Figure 1.9 Representation of the three ideal β-turns (I, II, III, from left to right) with *transoid* central peptide bond (ω_2= 180°).

Repeating type III β-turns lead to the formation of right-handed 3_{10}-helical structures, while type II β-turns are not helix forming and type I β-turns can be accommodated in helical structures, although with some distortions.

As regards the conformational properties, the increased sterical hindrance induced by the substituent at the C^{α} atom drastically limits the N-C^{α} and C^{α}-C' bond rotations (ϕ and ψ torsion angles, respectively),[196] thus favouring the assumption of stable structures in C^{α}-tetrasubstituted residue based peptides already in very short sequences (starting from three amide groups).[184]

In the case of Aib, conformational energy calculations[197,198] highlighted that the presence of two methyl groups on the C^{α}-atom significantly restricts the conformational space accessible, which is essentially limited to the region of α- and 3_{10}-helical conformations. It is also worth recalling a recent theoretical study, from which it appears that Aib homopolymers would prefer the 3_{10}-helical structure,[199] since the α-helical structure would result very perturbed by unfavourable interchain interactions. Because the Aib residue is achiral, right- and left-handed helices of its homo-polymers are isoenergetic and the probability of each helical handedness is the same.

The extreme facility with which Aib containing peptides form single crystals allowed the X-ray diffraction analysis of the complete series of Aib homo-oligopeptides up to the

undecamer.[200-211] The N-protected homo-tripeptides form a C_{10} structure; all longer peptides of the series invariably form the maximum number of consecutive C_{10} structures compatible with the length of the backbone, thus generating 3_{10}-helices. As an example the structure of the decapeptide *p*BrBz-$(Aib)_{10}$-O*t*Bu[208,209] is represented in **Fig. 1.10**.

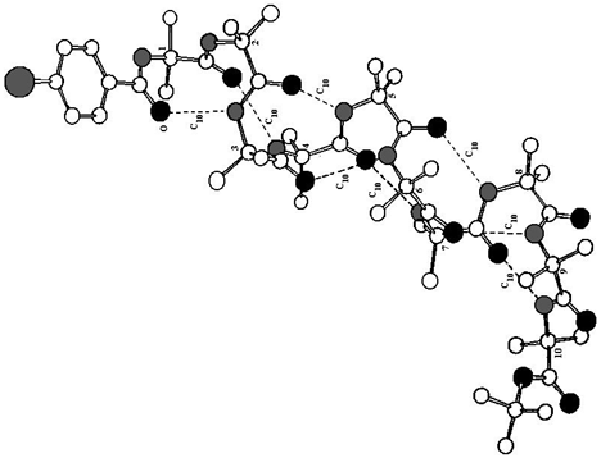

Figure 1.10 X-ray diffraction structure of *p*BrBz-$(Aib)_{10}$-O*t*Bu, the second longest Aib homopeptide whose structure has been solved.

Conformational analyses in solution (by IR absorption and ^{1}H-NMR spectrometry) showed that this conformation prevails strongly also in solvents of reduced polarity as deuterated chloroform.[201,212]

In the case of peptides containing Aib residues and C^{α}-trisubstituted residues, in the solid state only helical structure are observed. Such helices can be of 3_{10} type, of α type, or 'mixed' (an α-helical segment preceded or followed by some C_{10} structures). More than 40 structures obtained by X-ray diffraction of peptides made of Aib and protein amino acids with length between 4 and 16 residues were reported in the literature until 1990. From their analysis it was found that chain length, Aib content and peptide sequence are among the most important factors directing the conformation towards one of the two helical structures.[213,214] In particular, the α-helix tends to be favoured as the chain length increases and as the content of Aib decreases, even if there are several exceptions and evaluation of the role played by peptide sequence is difficult. On the other side, very short peptides (six residues or less) display an overwhelming preference for the 3_{10}-helix. In summary, the vast amount of structural data on Aib containing peptides highlights the remarkable capability of this non proteogenic residue of promoting and stabilizing β-turns as well as helical conformations, particularly 3_{10}-helices.

1.2. AIM OF THE PRESENT WORK

The selective delivery of pharmacologically active compounds into the tumour cell represents a major issue in cancer research. Recently, Fregona and co-workers synthesized Au(III)-dithiocarbamato derivatives lacking cross-resistance and endowed with greater *in vitro* and *in vivo* antitumor activity and reduced toxic and nephrotoxic side-effects as compared to cisplatin (the first and the most used metal-based chemotherapeutic drug).[51] These encouraging results prompted us to move one step forward. As PEPT1 and PEPT2 can transport across membranes all possible di- and tripeptides containing L-amino acid residues, we designed and synthesisized Au(III)-dithiocarbamato complexes of formula $[AuX_2(pdtc)]$ (X = Cl, Br; pdtc = di- to pentapeptidedithiocarbamato). Because of the peptide-mediated cellular internalization, these molecules are expected to have a superior chemotherapeutic index, in terms of increased bioavailability, higher cytotoxicity, and lower side-effects.

We report here on the synthesis, purification and characterization of a series of Au(III)-dithiocarbamato complexes, covalently bound to oligopeptides (from di- to penta-), focusing on issues related to the design of the oligopeptide chain. We selected amino acids with different features (chiral and achiral, hydrophobic and hydrophilic, aliphatic and aromatic) in order to evaluate the influence of various factors on the biological activity of the corresponding metal-dithiocarbamato complexes. A full physico-chemical characterization has been performed by means of elemental analysis, mono- and bidimensional NMR, FT-IR and thermogravimetric analysis.

The biological behaviour of the synthesized complexes has been examinated by means of:

- ✓ in vitro cytotoxic properties towards some human tumour cell lines;
- ✓ preliminary mechanistic studies of the active compounds;
- ✓ in vivo anticancer activity of the active compounds on nude mice.

Morever, we studied by means of NMR spectroscopy the interaction of one of the active complexes with L-NAC to stimulate possible reactions that could arise in physiological surroundings between these new Au(III) complexes and the glutathione reductive agent. We also compared these results with those obtained with the previous Au(III)-dithiocarbamato derivatives.

This Ph.D project is a fruit of the collaboration between Prof. Fernando Formaggio, who supervised the synthesis and characterization of the oligopeptides, and Prof. Dolores Fregona, who did supervise synthesis, characterization and biological tests of the gold(III) complexes. The preliminary *in vitro* tests were done by Dr. D. Aldinucci of the *Centro di Riferimento Oncologico*

di Aviano whereas, the *in vivo* preliminary studies were done by Dr. Q. P. Dou of the Wayne State University of Detroit.

CHAPTER II. EXPERIMENTAL SECTION

2.1. Materials and methods

2.1.1 Reagents and solvents

Acros-Janssen (Geel, Belgium):

1-hydroxy-*1H*-benzotriazole, phosphoric anhydride.

Alfa Aesar (Germany):

Potassium tetrabromo- and tetracloroaurate(III).

Bachem (Bubendorf, Switzerland):

N-benzyloxycarbonyl-O-tert-butylserine, L-NACy.

Biocrom KG (Berlin, Germany)

L-glutamine, Iscove's-modified Dulbecco's medium.

Cambrex Bio Science (Milan, Italy):

L-glutamine, Iscove's-modified Dulbecco's medium, Roswell Park Memorial Institute medium, penicillin, streptomycin.

Carlo Erba (Milan, Italy):

Acetic acid, 1-butanol, calcium chloride anhydrous, chloroform, dichloromethane, diethyl ether, ethanol, ethyl acetate, hydrochloric acid (37% aqueous solution), methanol, petroleum ether (boiling range 40-60°C), potassium hydrogenocarbonate, potassium hydrogenosulphate, 2-propanol, sodium carbonate dodecahydrate, sodium hydroxyde, sodium hypochlorite, sodium sulphate anhydrous, sulphuric acid (98% aqueous solution), toluene, triethylamine.

Euriso Top (France):

Deuterochloroform, hexadeuterated dimethylsulphoxide.

Fluka (Buchs, Switzerland):

Acetonitrile, ethanol, methanol, *N*-methylmorpholine, ninhydrin, palladium catalyst (10% on activated charcoal), phenylalanine, sarcosine, tetrahydrofurane, *N*-tert-butyloxycarbonyl-O-benzylserine.

German Collection of Microorganisms and cells cultures (Braunschweig, Germany):

PC3, DU145, L540 cells.

Gibco (Braunschweig, Germany):

Fetal bovine serum.

Iris Biotech (Marktredwitz, Germany):

N-ethyl-*N*'-(3-dimethylamino)propyl-carbodiimide chlorohydrate, *N*-benzyloxycarbonyl-oxysuccinimide.

Laboratory (University of Padua, Italy) *:*

N^{α}-Benzyloxycarbonylglycyltert-butyl ester, N^{α}-benzyloxycarbonyl-α-aminoisobutyric acid, N^{α}-benzyloxycarbonylproline, glycyltert-butyl ester hydrochloride, glycylmethyl ester hydrochloride, α-aminoisobutyryl methyl ester hydrochloride and phenylalanylmethyl ester hydrochloride.

Lancaster (England):

Isochloroformiate.

Pharmingen (California, United States of America):

AnnexinV-fluorescein isocyanate.

Roche Diagnotics (Boehringer-Mannheim, Germany):

Bromo-2'-deoxyuridine Cell Proliferation ELISA kit.

Siad (Bergamo, Italy):

*Iso*butene.

Sigma-Aldrich (Milwaukee, USA):

Hexadeuterated acetone, fetal calf serum, deuterated methanol, hexadeuterated dimethylsulphoxide, trifluoroacetic acid.

Taconic Animal Services (Hudson, U.S.A):

Athymic nude mice.

2.1.2. Instruments and methods

Melting point determination

Melting points were measured on a Stuart apparatus model SMP10 and are uncorrected.

Thin layer chromatography

Silica gel 60 F_{254} (Merck) or Alugram® Sil G UV 254 (Macherey-Nagel) on aluminium foil was used to follow the reactions.

Silica gel 60 F_{254} (Merck) on glass was used for TLC characterization. Retention factors (R_f) have been measured using three different solvent mixtures as eluents.

Rf_1: $CHCl_3$/EtOH 9:1; **Rf_2**: BuOH/AcOH/H_2O 3:1:1; **Rf_3**: PhMe/EtOH 7:1.

Products were detected either by UV lamp irradiation or with exposition to I_2 vapours or by warming with a heat gun and spraying firstly with a 1.5 % NaClO solution and then with a ninhydrin-TDM solution.[215]

Flash chromatography

For FC purifications silica gel 60 Merck (40-63 μm diameter, mesh 230-400) was used. For the various purifications, one of the following loading methods was used:

1) direct loading on top of the column of the crude mixture dissolved in a small amount of the eluent used for the purification;
2) direct loading on top of the column of the crude mixture dissolved in the minimum amount of a different solvent mixture;
3) loading on top of the column of the crude mixture adsorbed on silica gel ('dry-loading').

Polarimetric measurements

Optical rotations were measured on a a Perkin-Elmer model 241 polarimeter with an Haake model D8 thermostat at the mercury line wavelength, using a cell with an optical pathlength of 10 cm. Concentrations are expressed in g/100 mL. $[\alpha]$ are calculated using the formula $[\alpha]= \alpha/(c \cdot l)$, where c is the concentration (in g/mL) and l is the optical path (in dm). Spectrophotometric grade MeOH was used as a solvent.

Circular dichroism

CD spectra were recorded either on a Jasco dichrograph model J-715 provided with a Haake model F3 thermostat using Hellma quartz cells (pathlenght 0.1 cm). Instrumental parameters were as follow: response 2 sec, standard sensitivity, scan speed 100 nm/min, data pitch 0.5 nm.

Experimental values are expressed in molar ellipticity $[\Theta]_T$ (degrees·cm^2·dmol^{-1}) and were calculated, using the relation $[\Theta]_T = \Theta/(l \cdot c)$, where Θ is the observed ellipticity (in degrees), l is the optical path (in dm) and c is the peptide concentration (in mol/L).

UV spectroscopy

UV-Vis spectra were recorded on a Shimadzu UV 2501PC spectrophotometer or on a Cary 5000 spectrophotometer using Hellma 1.0 cm optical path quartz cell.

Mass spectrometry (MS)

ESI-TOF mass spectra were collected on a Mariner ESI-TOF mass spectrometer (Perseptive Biosystems). Prior to injection, samples were dissolved in a 1:1 mixture of water-MeOH containing 0.1 % formic acid. The positive ions were accelerated at 10, 15, 20 or 30 keV.

IR absorption spectroscopy

IR absorption measurements on KBr pellets were performed on a Perkin-Elmer model 580 B spectrophotometer, equipped with a Perkin-Elmer 3600 IR data station, or at room temperature on a Nicolet 55XC spectrophotometer (1000 scans, resolution: 2 cm^{-1}) for the range (4000-400) cm^{-1} and in solid on a Nicolet Nexus 870 (32 scans, resolution: 2 cm^{-1}) for the range (600-50) cm^{-1}. IR absorption measurements in deuterated chloroform solution were performed on a Perkin-Elmer model 1720 X FT-IR spectrophotometer, equipped with a sample-shuttle device, at 2 cm^{-1} nominal resolution, averaging 100 scans, nitrogen flushed, connected with a IBM PS/2 model 50 Z personal computer. Solvent (baseline) spectra were obtained under the same conditions. Cells with pathlengths of 0.1, 1 and 10 mm (with CaF_2 windows) were used. Absorption maxima, shoulder and partially overlapping bands were detected with the inverse second derivative method. Spectral elaborations (solvent subtraction and derivatization) were performed using the program SpectraCalc by Galactic (Salem, MA, USA).

NMR spectroscopy

^{1}H-NMR and 2D-NMR spectra were recorded on Bruker AC 200, Bruker AC 250, Bruker AC 300, Bruker advance DRX 300 or DRX 400 spectrometers. ^{13}C-NMR spectra were recorded on a Bruker AC 300 spectrometer. 2D-NMR spectra were recorded on DRX 400 Bruker or DMX 600 spectrometers. Chemical shifts (δ) are expressed in parts per million with regard to tetramethylsilane signal. Solvent residual peaks ($CHCl_3$, δ 7.26 ppm, or d_6-DMSO, δ 2.50 ppm, for ^{1}H-NMR, $H_3{}^{13}\boldsymbol{C}S(O)CH_3$, δ 39.52 ppm for ^{13}C-NMR) were used to calibrate the spectra. Peak multiplicity is described as follows: s (singlet), br s (broad singlet), d (doublet), m (multiplet).

For the elaboration of the spectra the programs XwinNMR, MestRe-C2.3 and MestreNova 5.2.5 (MestreLab Res. S. L.) were applied.

Thermogravimetry

Thermogravimetric (TG) and differential scanning calorimetry (DSC) curves were recorded with a TA Instruments thermobalance with a DSC 2929 calorimeter; the measurements were carried out in the range (100-1200 °C) in alumina crucibles under air (flux rate 30 $cm^3 \cdot min^{-1}$) and at a heating rate of 5 $°C \cdot min^{-1}$.

Cell cultures:

PC3 cells are androgen-independent prostatic carcinoma line of high metastatic potential *i.e.* they grow rapidly *in vitro* and form multiple site metastases when inoculated into athymic nude mice.[216,217] This cell line (established from bone marrow metastasis and unresponsive to androgen treatment) was cultured in IMDM (Iscove's-modified Dulbecco's medium) supplemented with 10 % heat-inactivated fetal bovine serum (FBS), penicillin (2 $mg \cdot ml^{-1}$), streptomycin (2 $mg \cdot ml^{-1}$), L-glutamine (0.1 % W/V) at 37 °C in 5 % CO_2 and moisture-enriched atmosphere.

Du145 are human prostate cancer cell line of moderate metastatic potential compared to PC3[218] and they were cultured as above reported for PC3 cells.

L540 cells are Hodgkin's lymphoma derived line. This cell line was maintained in Iscove's modified Dulbecco's medium (IMDM) supplemented with 10 % heat inactivated fetal calf serum, 0.2 mg/ml penicillin/streptomycin and 0.1 % (w/v) L-glutamine at 37°C in a 5% CO2 fully humidified atmosphere.

MDA-MB-231 are high invasive estrogen receptor α-negative human breast cancer cells and they were grown in RPMI 1640 medium supplemented with 10 % heat-inactivated

fetal bovine serum, penicillin (100 units·ml^{-1}), streptomycin (100 µg·ml^{-1}), L-glutamine (0.1 % W/V) at 37 °C in 5 % CO_2 and moisture-enriched atmosphere.

In vitro cytotoxic activity assay

Before use, gold(III) complexes and cisplatin were dissolved in dimethyl sulfoxide (DMSO) just before the experiments. Calculated amounts of drug solutions were then added to the proper medium to a final concentration of 0.5 % (v/v) DMSO which had no discernable effect on cell death. All the tested complexes were proved by ^{1}H NMR studies, to be stable in DMSO in 48h.

For this assay, PC3 and DU145 cells (2.5x10^3 cells·ml^{-1}) were seeded in 96-well flat-bottomed microplates in IMDM supplemented with 10 % heat-inactivated FBS and incubed at 37 °C in a 5 % CO_2 atmosphere. The medium was then removed and replaced with fresh one containing the compounds to be studied (previously dissolved in DMSO) at increasing concentrations (0.05-10 µM), thus exposing cells to the investigated compounds for 72 h. Triplicate cultures were established for each treatment. Cell viability was determined by a Cell Proliferation ELISA bromo-2'-deoxyuridine colorimetric kit, according to the manufacturer's protocol. The percent of cell viability was calculated by dividing the average absorbance of the cells treated with the tested compounds by that of the control, and plotted against drug concentration (logarithmic scale) to determine the IC_{50} (drug concentration required to cause 50 % of cells growth inhibition relative to the control), the standard deviation being estimated from the average of three trials. For comparison purpose, the cytotoxicity of cisplatin was evaluated in the same conditions.

L540 cells (2x10^5/ml) were incubated with in 24 well flat bottomed plates in the presence of drugs (CONC). After 72 hours, viable cells were counted, recovered and protein content and apoptosis analyzed.

Ability to induce apoptosis test (in vitro)

PC3 and DU145 cells in exponential growth phase were incubated in IMDM supplemented with 10 % heat-inactivated FBS either in presence or without the investigated compounds (5 µM) for 24 h. Cells were then harvested and resuspended in 100 µl of binding buffer (10 µM Hepes/NaOH pH 7.4, 140 mM, 2.5 mM $CaCl_2$), incubated with 5 µl of Annexin V-fluorescein isothiocyanate, and 10 µl of propydium iodide (10 µg/ml in binding buffer) in the dark for 15 min, and assayed after the addition of 0.3 µl of binding buffer to each sample. Viable, Annexin V labelled cells were

identified by flow cytometry according to their forward and right-angle scattering, electronically gated analyzed on a FACScan flow cytometer.

In vitro growth inhibitory effect

MDA-MB-231 cells were seeded in 96-well microplates in RPMI 1640 medium and grown to 70 % to 80 % confluency followed by addition of the compounds to be studied (previously dissolved in DMSO) at increasing concentrations (1-50 μM) and incubated at 37 °C in a 5 % CO_2 atmosphere, thus exposing cells to the investigated compounds for 22 h. Triplicate cultures were established for each treatment. Cell respiration, as an indicator of cell viability, was determined by the mitochondrial-dependent reduction of 3-(4,5-dimethylthiazol-2-yl)-2,5-diphenyltetrazolium bromide) to formazan as previously described.[219] Cell viability was calculated by dividing the average absorbance of the cells treated with the tested compounds by that of the control, the standard deviation being estimated from the average of the three trials.

Inhibition of proteasomal chymotrypsin-like activity (in vitro)

Purified rabbit 20S proteasome (35 ng) or MDA-MB-231 whole extract (10 μg) were incubated with 20 μM of the substrate (for proteasomal chymotryptic (CT) activity) in 100 μl assay buffer (20 $mmol \cdot l^{-1}$ Tris·HCl (pH 7.5) in the presence of the compounds to be studied (previously dissolved in DMSO) at increasing concentrations (0.1-25 μM) or equivalent volume of neat DMSO as control. After 2 h incubation at 37 °C, inhibition of each proteasomal chymotryptic activity was measured as previously described.[5]

In vivo experiments

Five week-old female athymic nude mice were purchased and housed according to protocols approved by the Institutional Laboratory Animal Care and Use Committee of Wayne State University. MDA-MB-231 cells ($5.0x10^6$ $cells \cdot ml^{-1}$ suspended in 1.0 ml of serum-free RPMI 1640 medium) were inoculated subcutaneously (*s.c.*) in right flank of each mouse (four mice per group). When tumours reached the size of *ca.* 120 mm^3, mice were randomly grouped and treated daily with injection of either 1.0 $mg \cdot kg^{-1}$ of tested compound, or vehicle [10 % DMSO, 20 % Cremophore/ethanol (3:1) and 70 % PBS]. Tumour size was measured every other day using callipers and their volumes were calculated according to the formula $width^2$ x length / 2. Mice have being treated for 13 days. Initial tumour growth inhibition was analyzed.

2.2. SYNTHESIS AND CHARACTERIZATION OF PEPTIDES

2.2.1 Synthesis of amino acid derivatives

All chiral amino acids are of "L" configuration.

Boc-Sar-OH[220]

H-Sar-OH (4.45 g, 10 mmol) was dissolved in a mixture of dioxan-water 2:1 (150 ml) and 1 N NaOH (50 ml). Di-*t*-butyldicarbonate (Boc_2O, 11 mmol) was added, and the reaction mixture was stirred at room temperature for 3h. Dioxan was evaporated and the solution was cooled in an ice bath. The excess of Boc_2O was extracted with cooled ethyl acetate (AcOEt). The stirred acqueous solution was acidified to pH 3, at 0 ºC, with citric acid. The product was extracted with AcOEt. The organic layer was washed with water, dried over Na_2SO_4 concentrated and precipitated with petroleum ether.

Yield: 83 %.

M.p.: 85-87 °C (AcOEt-petroleum ether).

Rf_1: 0.50; Rf_2: 0.95; Rf_3 : 0.20.

IR (KBr): 1746, 1646 cm^{-1}.

^1H NMR ($CDCl_3$, 200 MHz), δ/ppm: 10.15 [br s, 1H, OH], 3.94 [s, 2H, Sar α-CH_2], 2.90 [s, 3H, NCH_3], 1.40 [s, 9H, Boc $(CH_3)_3$].

MS, $[M]^+$ calculated (found): 189.22 (189.11).

Z-Sar-OH[221,222]

To a solution of H-Sar-OH (20 g, 0.19 mol) in water and TEA (27.04 ml, 0.19 mol) a solution of Z-OSu (48.35 g, 0.19 mol) in CH_3CN was added. The pH was adjusted to 8 by addition of TEA, and the solution was stirred at room temperature for 4 days. CH_3CN was evaporated under reduced pressure. The solution was diluted with 5% $NaHCO_3$ and the unreacted Z-OSu was extracted with diethyl ether (Et_2O). The aqueous layer was acidified to pH 2 with $KHSO_4$ and extracted with AcOEt. The organic layer was washed several times with water, dried over Na_2SO_4, and concentrated. Yield: 90 %.

Rf_1: 0.55; Rf_2: 0.85; Rf_3 : 0.30.

IR (KBr): 1706, 1692 cm^{-1}.

^1H NMR ($CDCl_3$, 300 MHz), δ/ppm: 7.34 [m, 5H, Z phenyl CH] , 5.12 [m, 2H, Z CH_2], 4.08 [s, 2H, Sar CH_2], 3.02 [s, 3H, NCH_3].

MS, $[M]^+$ calculated (found): 224.23 (224.08).

Z-Phe-OH[221,222]

To a solution of H-Phe-OH (10 g, 0.06 mol) in water and TEA (13.94 ml, 0.06 mol) a solution of Z-OSu (15.09 g, 0.06 mol) in CH_3CN was added. The pH was adjusted to 8 by addition of TEA, and the solution was stirred at room temperature for 4 days. CH_3CN was evaporated under reduced pressure. The solution was diluted with 5% $NaHCO_3$ and the unreacted Z-OSu was extracted with diethyl ether (Et_2O). The aqueous layer was acidified to pH 2 with $KHSO_4$ and extracted with AcOEt. The organic layer was washed several times with water, dried over Na_2SO_4, and concentrated. The solid product was precipitated with petroleum ether.

Yield: 86%.

M.p.: 83-84 °C (AcOEt-petroleum ether).

Rf_1: 0.40; Rf_2: 0.95; Rf_3 : 0.20.

IR (KBr): 3327, 1691, 1538 cm^{-1}.

^1H NMR (200 MHz, $CDCl_3$), δ/ppm: 7.37-7.13 [m, 10H; 5H Z phenyl CH; 5H Phe phenyl CH], 5.17 [d, 1H, NH], 5.12 [m, 2H, Z CH_2], 4.75 [m, 1H, α-CH], 3.17 [m, 2H, β-CH_2].

MS, $[M+H]^+$ calculated (found): 300.24 (300.12).

Z-Phe-O*t*Bu[222]

A solution of Z-Phe-OH (15 g, 0.05 mol) in CH_2Cl_2 (150.33 ml) was placed in a pression-proof container and cooled to -70 °C in an acetone-dry ice bath. *Iso*butene (57.19 ml) was bubbled, and concentrated H_2SO_4 (0.50 ml) was added dropwise. The container was plugged and left for 7 days at room temperature. Then, the container was cooled to -60 °C and the solution poured into a cold 5% $NaHCO_3$ solution (150 ml). From this mixture CH_2Cl_2 was removed under reduced pressure and the remaining aqueous layer extracted with AcOEt. The organic phase was washed with 10 % $KHSO_4$, H_2O, 5% $NaHCO_3$, H_2O, dried over Na_2SO_4 and evaporated to dryness.

Yield: 90 %.

M.p: 78-80 °C

Rf_1: 0.95; Rf_2: 0.95; Rf_3: 0.70.

IR(KBr): 3395, 1740, 1698, 1512 cm^{-1}.

^1H NMR ($CDCl_3$, 400 MHz), δ/ppm: 7.27 [m, 5H, Z phenyl CH; 5H, Phe phenyl CH], 5.12 [m, 2H, Z CH_2], 4.53 [m, 1H, α-CH], 3.08 [m, 2H, β-CH_2], 1.39 [s, 9H, $C(CH_3)_3$].

Z-Aib-O*t*Bu[222]

This derivative was prepared as previously described for Z-Phe-O*t*Bu, dissolving Z-Aib-OH (10 g, 0.04 mol) in CH_2Cl_2 (126.44 ml) in a pression-proof container and cooled to -70 °C in an acetone-dry ice bath. *Iso*butene (48.10 ml, 0.51 mol) was bubbled, and concentrated H_2SO_4 (0.42 ml) was added dropwise. The container was plugged and left for 7 days at room temperature.

Yield: 80 %.

M.p: 63-64 °C (from AcOEt-petroleum ether).

Rf_1: 0.95; Rf_2: 0.95; Rf_3 :0.40.

IR (KBr): 3370, 1712, 1519 cm^{-1}.

^1H NMR ($CDCl_3$, 200 MHz), δ/ppm: 7.33 [5H, Z phenyl], 5.45 [s, 1H, NH], 5.08 [s, 2H, Z CH_2], 1.51 [s, 6H, β-CH_3], 1.43 [s, 9H, $C(CH_3)_3$].

Boc-Ser(Bzl)-OMe[223]

To a solution of Boc-Ser(Bzl)-OH (2 g, 6.77 mmol), DMAP (0.41g, 3.33 mmol) and MeOH (0.31 ml, 7.69 mmol) in CH_2Cl_2 (25 ml), cooled to 0 °C, EDC·HCl (1.41 g, 7.38 mmol) was added. The reaction mixture was stirred at 0 °C for 2h and at room temperature overnight. The solvents were evaporated under reduced pressure and the residue taken up in AcOEt and water. The organic layer was separated, washed with saturated $NaHCO_3$ and H_2O, dried over Na_2SO_4 and evaporated to dryness.

Yield: 90 %.

Rf_1: 0.95; Rf_2: 0.95, Rf_3 : 0.85.

[α] = + 0.8 ° (c = 0.5, MeOH).

IR (KBr): 3444, 3374, 1751, 1716 cm^{-1}.

^1H NMR (DMSO, 200 MHz), δ/ppm: 8.51 [d, 1H, NH], 7.28 [m, 5H, Bzl phenyl], 4.47 [s, 2H, Bzl CH_2], 4.28 [m, 1H, Ser α-CH], 3.65-3,63 [m, 5H, OMe, Ser β-CH_2], 1.38 [s, 9H, Boc $(CH_3)_3$].

TFA·H-Ser(Bzl)-OMe

To a solution of Boc-Ser(Bzl)-OMe (2.64 g, 8.54 mmol) in CH_2Cl_2 (10 ml), an equivalent volume of TFA was added. After stirring for 90 min at room temperature, TFA was evaporated using nitrogen flow and the residue was taken up and evaporated several times from CH_2Cl_2 and Et_2O.

Yield: 93 %.

Rf_1: 0.60; Rf_2: 0.70; Rf_3 : 0.30.

[α] = + 7.0 ° (c = 0.5, MeOH).

IR (KBr): 3033, 2960, 2879, 1754, 1673 cm^{-1}.

^1H NMR ($CDCl_3$, 250 MHz), δ/ppm: 7.31 [m, 5H, Bzl phenyl], 5.64-5.59 [m, 3H, Ser NH_3^+], 4.52 [m, 2H, Bzl CH_2], 4.20 [m, 1H, Ser α-CH], 3.87 [m, 2H, Ser β-CH_2], 3.74 [s, 3H, OMe].

MS, $[M+H]^+$ calculated (found): 210.26 (210.11).

Z-Ser(*t*Bu)-OMe[223]

To a solution of Z-Ser(*t*Bu)-OH (5.25 g, 17.78 mmol), DMAP (1.09 g, 8.89 mmol) and MeOH (0.82 ml, 20.19 mmol) in CH_2Cl_2 (65 ml), cooled to 0 °C, EDC·HCl (3.71 g, 19.40 mmol) was added. The reaction mixture was stirred at 0 °C for 2h and at room temperature overnight. The solvents were evaporated under reduced pressure and the residue taken up in AcOEt and water. The organic layer was separated, washed with saturated $NaHCO_3$ and H_2O, dried over Na_2SO_4 and concentrated. The product was purified by column "flash chromatography" (silica gel), by eluting with a 3:2 mixture of petroleum ether-AcOEt.

Yield: 89 %.

M.p: 43-44 °C (AcOEt- petroleum ether).

Rf_1: 0.95; Rf_2: 0.95; Rf_3 : 0.45.

[α] = +6.5° (c = 0.5, MeOH).

IR (KBr): 3429, 3370, 1732, 1718, 1519 cm^{-1}.

^1H NMR ($CDCl_3$, 400 MHz), δ/ppm: 7.35 [m, 5H, Z phenyl], 5.61 [d, 1H, NH], 5.13 [s, 2H, Z CH_2], 4.46 [m, 1H,Ser α-CH], 3.82-3.56 [m, 2H, Ser β-CH_2], 3.75 [s, 3H, OMe], 1.12 [s, 9H, *t*Bu $(CH_3)_3$].

MS, $[M+H]^+$ calculated (found): 310.38 (310.16).

Z-Ser(*t*Bu)-O*t*Bu[223]

To a solution of Z-Ser(*t*Bu)-OH (5.35 g, 18.10 mmol), DMAP (1.11 g, 9.07 mmol) and *t*BuOH (1.94 ml, 20.60 mmol) in CH_2Cl_2 (66 ml), cooled to 0 °C, EDC·HCl (3.78 g, 19.80 mmol) was added. The reaction mixture was stirred at 0 °C for 2h and at room temperature overnight. The solvents were evaporated under reduced pressure and the residue taken up in AcOEt and water. The organic layer was separated, washed with saturated $NaHCO_3$ and H_2O, dried over Na_2SO_4 and concentrated. The product was purified by column "flash chromatography" (silica gel), by eluting with a 9:1 mixture of petroleum ether-acetone.

Yield: 75 %.

Rf_1: 0.95; Rf_2: 0.90; Rf_3 : 0.85.

IR (KBr): 3446, 3338, 1728, 1503 cm^{-1}

^{1}H NMR ($CDCl_3$, 250 MHz), δ/ppm: 7.35 [m, 5H, Z phenyl], 5.61 [d, 1H, NH], 5.17 [s, 2H, Z CH_2], 4.34 [m, 1H, Ser α-CH], 3.53 [m, 2H, Ser β-CH_2], 1.31 [s, 9H, O*t*Bu $(CH_3)_3$], 1.31 [s, 9H, *t*Bu $(CH_3)_3$].

MS, $[M+H]^+$ calculated (found): 352.46 (352.21).

Fmoc-Ser(Bzl)-O*t*Bu[222]

This derivative was prepared as described above for Z-Phe-O*t*Bu, dissolving Fmoc-Ser(Bzl)-OH (3 g, 7.19 mmol) in CH_2Cl_2 (21.56 ml) in a pression-proof container and cooled to -70 °C in an acetone-dry ice bath. *Iso*butene (8.20 ml, 0.86 mol) was bubbled, and concentrated H_2SO_4 (0.07 ml) was added dropwise. The container was plugged and left for 7 days at room temperature. It took 4 days for Fmoc-Ser(Bzl)-OH to be completely dissolved.

Yield: 86 %.

Rf_1: 0.95; Rf_2: 0.95; Rf_3 : 0.85.

IR (KBr): 3436, 3336, 1724, 1504 cm^{-1}.

^{1}H NMR ($CDCl_3$, 250 MHz), δ/ppm: 7.76 [d, 2H, Fmoc fluorenylic CH], 7.63 [d, 2H, Fmoc fluorenylic CH], 7.43-7.29 [m, 4H, Fmoc fluorenylic CH; 5H, Bzl phenyl], 5.69 [m, 1H, Ser NH], 4.54 [m, 2H, Bzl CH_2], 4.43-4.35 [m, 2H, Fmoc CH_2; 1H, Fmoc CH], 4.25 [m, 1H, Ser α-CH], 3.92-3.66 [m, 2H, Ser β-CH_2], 1.47 [s, 9H, $C(CH_3)_3$].

MS, $[M+H]^+$ calculated (found): 474.69 (210.19).

$(Z\text{-}Aib)_2O$[221,222]

EDC (4.04 g, 0.02 mol) was added to a cooled solution of Z-Aib-OH (10 g, 0.04 mol) in CH_2Cl_2 (25 ml) and the reaction stirred at room temperature for 4 hours. The solvent was evaporated, the residue was taken up with AcOEt, washed with 10% $KHSO_4$, H_2O, 5% $NaHCO_3$, H_2O, and dried over Na_2SO_4. The organic layer was concentrated, triturated with petroleum ether and filtered.

yield: 80 %.

M.p: 101-102 °C (AcOEt-petroleum ether).

Rf_1: 0.95; Rf_2: 0.95; Rf_3 :0.60.

IR (KBr): 3288, 1815, 1740, 1697, 1681, 1538 cm^{-1}.

^{1}H NMR ($CDCl_3$, 200 MHz), δ/ppm: 7.33 [5H, Z phenyl], 5.07 [s, 2H, Z CH_2], 5.00 [s, 1H, NH], 1.44 [s, 6H, β-CH_3].

2.2.2 Synthesis of oligopeptides

Boc-Sar-Gly-OMe

To a solution of Boc-Sar-OH (0.97 g, 5.12 mmol) and NMM (0.56 ml, 5.12 mmol) in THF (15ml), cooled to -15 °C, isobutylchloroformiate (0.70 g, 5.12 mmol) was added.[224] After 10 min, a cooled suspension of HCl·H-Gly-OMe (0.96 g, 7.68 mmol) and NMM (0.85 ml, 7.68 mmol) in $CHCl_3$ (12 ml) was added. The pH was adjusted and kept to 8 by addition of NMM. After stirring at room temperature overnight, the reaction mixture was concentrated under reduced pressure. The residue was taken up with AcOEt, washed with 10% $KHSO_4$, H_2O, 5% $NaHCO_3$, H_2O, and dried over Na_2SO_4. The organic layer was concentrated and the product precipitated by addition of petroleum ether.

Yield: 70 %.

M.p.: 85-90 °C (AcOEt-petroleum ether).

Rf_1: 0.90; Rf_2: 0.90; Rf_3 : 0.40.

IR (KBr): 3321, 2976, 1755, 1700, 1537 cm^{-1}.

^1H NMR ($CDCl_3$, 200 MHz), δ/ppm: 6.60 [br s, 1H, Gly NH], 4.07 [d, 2H, Gly α-CH_2], 3.93 [s, 2H, Sar α-CH_2], 3.77 [s, 3H, OMe], 2.97 [s, 3H, NCH_3], 1.49 [s, 9H, Boc $C(CH_3)_3$].

MS, $[M+H]^+$ calculated (found): 261.31 (261.14).

HCl·H-Sar-Gly-OMe

A saturated solution of HCl in diethyl ether was added to a solution of Boc-Sar-Gly-OMe (0.95 g, 3.65 mmol) in Et_2O and stirred. At the end of the reaction (about 30 min, checked by TLC), the mixture was evaporated to dryness. The residue was taken up with Et_2O, triturated with petroleum ether and filtered.

Yield: 85 %.

M.p.: 85-90 °C (MeOH- Et_2O).

Rf_1: 0.05; Rf_2: 0.35; Rf_3 : 0.00.

IR: 3068, 2956, 3231, 3419, 1684, 1558 cm^{-1}.

^1H NMR (DMSO, 200 MHz), δ/ppm: 8.84 [br s, 2H, Sar NH_2Cl], 8.94 [d, 1H, Gly NH], 3.64 [s, 3H, OCH_3], 3.92 [d, 2H, Gly α-CH_2], 3.75 [m, 2H, Sar α-CH_2], 2.54 [s, 3H, NCH_3].

$C_6H_{13}ClN_2O_3$ (PM 196.63) Elemental analysis %: (calculated) found, C (36.65) 35.54, H (6.66) 6.86, N (14.24) 13.71.

MS, $[M]^+$ calculated (found): 161.20 (161.08).

Boc-Sar-Aib-OMe

To a solution of Boc-Sar-OH (1.5 g, 7.93 mmol) and NMM (0.87 ml, 7.93 mmol) in THF (20 ml), cooled to -15 °C, isobutylchloroformiate (1.08 g, 7.93 mmol) was added.[224] After 10 min, a cooled suspension of HCl·H-Aib-OMe (1.83 g, 11.89 mmol) and NMM (1.20 ml, 11.89 mmol) in $CHCl_3$ (15 ml) was added. The pH was adjusted and kept to 8 by addition of NMM. After stirring at room temperature overnight, the reaction mixture was concentrated under reduced pressure. The residue was taken up with AcOEt, washed with 10% $KHSO_4$, H_2O, 5% $NaHCO_3$, H_2O, and dried over Na_2SO_4. The organic layer was concentrated and the product precipitated by addition of petroleum ether.

Yield: 60 %.

M.p.: 101-102 °C (AcOEt-petroleum ether).

Rf_1: 0.95; Rf_2: 0.95; Rf_3 : 0.45.

IR (KBr): 3314, 2968, 1742, 1695, 1654, 1540 cm^{-1}.

^1H NMR (CDCl3, 200 MHz), δ/ppm: 6.51 [s, 1H, NH], 3.78 [s, 2H, Sar α-CH_2], 3.71 [s, 3H, OCH_3], 2.92 [s, 3H, NCH_3], 1.53 [s, 6H, Aib β-CH_3], 1.47 [s, 9H, Boc $(CH_3)_3$].

MS, $[M+H]^+$ calculated (found): 289.34 (289.18).

HCl·H-Sar-Aib-OMe

This dipeptide was obtained as described above for HCl·H-Sar-Gly-OMe, using Boc-Sar-Aib-OMe (0.81 g, 2.81 mmol) as starting material.

Yield: 96 %.

M.p.: 165-170 °C (MeOH- Et_2O).

Rf_1:0.05; Rf_2: 0.45; Rf_3 : 0.00.

IR (KBr): 3314, 1740, 1679, 1555 cm^{-1}.

^1H NMR (DMSO, 200 MHz), δ/ppm: 8.91 [s, 1H, Aib NH], 8.81 [br s, 2H, Sar NH_2Cl], 3.68 [m, 2H, Sar α-CH_2], 3.59 [s, 3H, OMe], 2.52 [s, 3H, NCH_3], 1.40 [s, 6H, β-CH_3].

$C_8H_{17}ClN_2O_3$ (PM 224.69) Elemental analysis %: (calculated) found, C (42.76) 44.28, H (7.63) 7.96, N (12.47) 12.00. Color: white.

MS, $[M+H]^+$ calculated (found): 189.24 (189.11).

Boc-Sar-Phe-OMe

To a solution of Boc-Sar-OH (0.72 g, 3.81 mmol) and NMM (0.42 ml, 3.81 mmol) in THF (15 ml), cooled to -15 °C, isobutylchloroformiate (0.52 g, 3.81 mmol) was added.[224] After 10 min, a cooled suspension of HCl·H-Phe-OMe (1.23 g, 5.71 mmol) and NMM (0.63 ml, 5.71 mmol) in $CHCl_3$ (12 ml) was added. The pH was adjusted and kept to 8 by addition of NMM. After

stirring at room temperature overnight, the reaction mixture was concentrated under reduced pressure. The residue was taken up with AcOEt, washed with 10% $KHSO_4$, H_2O, 5% $NaHCO_3$, H_2O, and dried over Na_2SO_4. The organic layer was concentrated to dryness.

Yield: 85 %.

Rf_1: 0.95; Rf_2: 0.95; Rf_3 : 0.65.

$[\alpha]^{20}_D$: + 5.8 ° (c = 0.5, MeOH).

IR (KBr): 3313, 2975, 1746, 1702, 1454 cm^{-1}.

^1H NMR (CDCl3, 200 MHz), δ/ppm: 7.28-7.08 [m, 5H, Phe phenyl], 4.91-4.88 [m, 1H, α-CH], 3.85 [s, 2H, Sar α-CH_2], 3.73 [s, 3H, OMe], 3.13 [m, 2H, β-CH_2], 2.83 [s, 3H, NCH_3], 1.43 [s, 9H, Boc $(CH_3)_3$].

MS, $[M+H]^+$ calculated (found): 351.42 (351.19).

HCl·H-Sar-Phe-OMe

This dipeptide was obtained as described above for HCl.H-Sar-Gly-OMe, using Boc-Sar-Phe-OMe (0.96 g, 2.75 mmol).

Yield: 83 %.

M.p.: 169-170 °C (MeOH- Et_2O).

Rf_1: 0.20; Rf_2: 0.55; Rf_3 : 0.05.

$[\alpha]^{20}_D$: + 6.6 ° (c = 1.7, MeOH).

IR (KBr): 3473, 3427, 2979, 2612, 3117, 1718 , 1666, 1556 cm^{-1}.

^1H NMR (DMSO, 300 MHz), δ/ppm: 8.98 [d, 1H, Phe NH], 7.25 [m, 5H, Phe phenyl], 4.60-4.55 [m, 1H, α-CH], 3.67 [m, 2H, Sar α-CH_2], 3.63 [s, 3H, OMe], 3.31 [s, 3H, NCH_3], 3.04 [m, 2H, β-CH_2].

$C_{13}H_{19}ClN_2O_3$ (PM. 286.76) Elemental analysis %: (calculated) found, C(54.45) 51.18, H (6.68) 6.67, N (9.77) 9.29.

MS, $[M]^+$ calculated (found): 251.31 (251.12).

Z-Sar-Gly-O*t*Bu

To a solution of Z-Sar-OH (1.43 g, 6.37 mmol) and NMM (0.70 ml, 6.37 mmol) in THF (20 ml), cooled to -15 °C, isobutylchloroformiate (0.87 g, 6.37 mmol) was added.[224] After 10 min, a cooled suspension of (1.25 g, 9.56 mmol) of H-Gly-O*t*Bu (obtained by catalytic hydrogenation in CH_2Cl_2 of the corresponding Z-protected derivative) and NMM (1.05 ml, 9.56 mmol) in $CHCl_3$ (12 ml) was added. The pH was adjusted and kept to 8 by addition of NMM. After stirring at room temperature overnight, the reaction mixture was concentrated under reduced pressure. The residue was taken up with AcOEt, washed with 10% $KHSO_4$, H_2O, 5% $NaHCO_3$,

H_2O, and dried over Na_2SO_4. The organic layer was concentrated to dryness. The product was purified by "flash chromatography" (silica gel column), using a petroleum ether-AcOEt 1:1 mixture as eluant.

Yield: 66 %.

Rf_1: 0.95; Rf_2: 0.95; Rf_3 : 0.50.

IR (KBr): 3324, 1743, 1706, 1536 cm^{-1}.

^1H NMR (DMSO, 400 MHz), δ/ppm: 8.28 [m, 1H, NH], 7.37, 7.31 [2m, 5H, phenyl CH isomers], 5.05 [2s, 2H, Z CH_2 isomers], 3.91 [d, 2H, Gly α-CH_2], 3.73 [2s, 2H, Sar α-CH_2 isomers], 2.88, 2.86 [s, 3H, NCH_3 isomers], 1.39 [s, 9H, $C(CH_3)_3$].

MS, $[M+H]^+$ calculated (found): 337.41 (337.16).

HCl·H-Sar-Gly-O*t*Bu

To a solution of (0.75 g, 3.63 mmol) of H-Sar-Gly-O*t*Bu (obtained by catalytic hydrogenation in MeOH of the corresponding Z-protected derivative) in Et_2O, a diluted solution of HCl 2.3 M (1.58 ml) in Et_2O was dropwise added under stirring. The solvent was evaporated to dryness, the residue taken up with Et_2O and filtered.

Yield: 78 %.

M.p: 129-130 °C (MeOH- Et_2O).

Rf_1: 0.05; Rf_2: 0.50; Rf_3 : 0.05.

IR (KBr): 3416, 3307, 1745, 1729, 1669, 1576, 1538 cm^{-1}.

^1H NMR (DMSO, 300.13 MHz), δ/ppm: 8.99 [m, 1H, NH_2Cl], 8.91 [t, 1H, Gly NH], 3.82 [d, 2H, Gly α-CH_2], 3.72 [m, 2H, Sar α-CH_2], 2.53 [s, 3H, NCH_3], 1.41 [s, 9H, $C(CH_3)_3$].

^{13}C NMR (DMSO, 75.48 MHz), δ/ppm: 168.42 [Gly carbonylic C], 165.61 [Sar carbonylic C], 80.75 [OtBu quaternary C], 48.59 [Sar secondary C], 41.13 [Gly secondary C], 39.51 [NCH_3 C], 27.46 [$(CH_3)_3$ C].

$C_9H_{19}ClN_2O_3$ (PM. 238.72) Elemental analysis %: (calculated) found, C(45.28) 45.27, H (8.02) 8.18, N (11.74) 11.52.

Z-Sar-Aib-O*t*Bu

To a solution of Z-Sar-OH (1.32 g, 5.87 mmol) and NMM (0.65 ml, 5.87 mmol) in THF (20 ml), cooled to -15 °C, isobutylchloroformiate (0.80 g, 5.87 mmol) was added.[224] After 10 min, a cooled suspension of (1.40 g, 8.81 mmol) of H-Aib-O*t*Bu (obtained by catalytic hydrogenation in CH_2Cl_2 of the corresponding Z-protected derivative) and NMM (0.89 ml, 8.81 mmol) in $CHCl_3$ (15 ml) was added. The pH was adjusted and kept to 8 by addition of NMM. After stirring at room temperature overnight, the reaction mixture was concentrated under reduced

pressure. The residue was taken up with AcOEt, washed with 10% $KHSO_4$, H_2O, 5% $NaHCO_3$, H_2O, and dried over Na_2SO_4. The organic layer was concentrated to dryness. The product was purified by "flash chromatography" (silica gel column), using a petroleum ether-AcOEt 1:1 mixture as eluant.

Yield: 87 %.

M.p: 50-51 °C (AcOEt-petroleum ether).

Rf_1: 0.95; Rf_2: 0.85; Rf_3 : 0.65.

IR (KBr): 3370, 1712, 1519 cm^{-1}.

^1H NMR ($CDCl_3$, 200 MHz), δ/ppm: 8.15 [d, 1H, NH], 7.33 [m, 5H, Z phenyl], 5.05 [d, 2H, Z CH_2 isomers], 3.83 [s, 2H, Sar α-CH_2], 2.83 [d, 3H, NCH_3 isomers], 1.33 [d, 9H, $C(CH_3)_3$ isomers], 1.29 [d, 6H, β-CH_3 isomers].

MS, $[M+H]^+$ calculated (found): 365.46 (335.21).

HCl·H-Sar-Aib-O*t*Bu

To a solution of (1.14 g, 4.94 mmol) of H-Sar-Aib-O*t*Bu (obtained by catalytic hydrogenation in MeOH of the corresponding Z-protected derivative) in Et_2O, a diluted solution of HCl 2.3 M (2.15 ml) in Et_2O was dropwise added under stirring. The solvent was evaporated to dryness, the residue taken up with Et_2O and filtered.

Yield: 84 %.

M.p: 156-157 °C (MeOH- Et_2O).

Rf_1: 0.10; Rf_2: 0.60; Rf_3 : 0.05.

IR (KBr): 3442, 3215, 1735, 1726, 1676, 1557 cm^{-1}.

^1H NMR (DMSO, 300.13 MHz), δ/ppm: 9.05 [m, 1H, NH_2Cl], 8.84 [s, 1H, Aib NH], 3.64 [m, 2H, Sar α-CH_2], 2.52 [s, 3H, NCH_3], 1.37 [s, 9H, $C(CH_3)_3$], 1.35 [s, 6H, β-CH_3].

^{13}C NMR (DMSO, 75.48 MHz), δ/ppm: 172.23 [Aib carbonylic C], 164.24 [Sar carbonylic C], 79.91 [OtBu quaternary C], 55.80 [Aib quaternary C], 48.61 [Sar secondary C], 32.41 [NCH_3 C], 27.32 [$(CH_3)_3$ C], 25.36 [Aib $(CH_3)_2$ C].

$C_{11}H_{23}ClN_2O_3$ (PM. 266.78) Elemental analysis %: (calculated) found, C (49.53) 49.53, H (8.69) 8.47, N (10.50) 10.37.

MS, $[M]^+$ calculated (found): 231.33 (231.16).

Z-Sar-Phe-O*t*Bu

To a solution of Z-Sar-OH (1.95 g, 8.70 mmol) and NMM (0.96 ml, 8.70 mmol) in THF (40 ml), cooled to -15 °C, isobutylchloroformiate (1.19 g, 8.70 mmol) was added.[224] After 10 min, a cooled suspension of (2.89 g, 13.05 mmol) of H-Phe-O*t*Bu (obtained by catalytic hydrogenation

in CH_2Cl_2 of the corresponding Z-protected derivative) and NMM (1.44 ml, 13.05 mmol) in $CHCl_3$ (35 ml) was added. The pH was adjusted and kept to 8 by addition of NMM. After stirring at room temperature overnight, the reaction mixture was concentrated under reduced pressure. The residue was taken up with AcOEt, washed with 10% $KHSO_4$, H_2O, 5% $NaHCO_3$, H_2O, and dried over Na_2SO_4. The organic layer was concentrated to dryness.

Yield: 91 %.

Rf_1: 0.95; Rf_2: 0.95; Rf_3 :0.65.

$[\alpha]$ = + 3.4 ° (c = 0.5, MeOH).

IR (KBr): 3319, 1710, 1529 cm^{-1}.

^{1}H NMR (DMSO, 400 MHz), δ/ppm: 8.35-8.30 [m, 1H, Phe NH], 7.36-7.20 [m, 5H Z phenyl, 5H, Phe phenyl], 5.03 [m, 2H, Z CH_2 isomers], 4.39 [m, 1H, α-CH], 3.86 [m, 2H, Sar α-CH_2 isomers], 2.93 [m, 2H, β-CH_2], 2.78 [m, 3H, NCH_3 isomers], 1.31 [m, 9H, $C(CH_3)_3$ isomers].

MS, $[M+H]^+$ calculated (found): 427.53 (427.21).

HCl·H-Sar-Phe-O*t*Bu

To a solution of (1.73 g, 5.94 mmol) of H-Sar-Phe-O*t*Bu (obtained by catalytic hydrogenation in MeOH of the corresponding Z-protected derivative) in Et_2O, a diluted solution of HCl 2.3 M (2.58 ml) in Et_2O was dropwise added under stirring. The solvent was evaporated to dryness, the residue taken up with Et_2O and filtered.

Yield: 90 %.

M.p: 80-81 °C (MeOH- Et_2O).

Rf_1: 0.20; Rf_2: 0.65; Rf_3 : 0.10.

$[\alpha]$ = + 7.8 ° (c = 0.5, MeOH).

IR (KBr): 3431, 3328, 1736, 1664, 1542 cm^{-1}.

^{1}H NMR (DMSO, 300.13 MHz), δ/ppm: 8.92 [d, 1H, Phe NH], 8.80 [m, 2H, Sar NH_2Cl], 7.26 [m, 5H, Phe phenyl], 4.45 [m, 1H, α-CH], 3.63 [m, 2H, Sar α-CH_2], 3.03-2.89 [m, 2H, β-CH_2], 2.44 [s, 3H, NCH_3], 1.33 [s, 9H, $C(CH_3)_3$].

^{13}C NMR (DMSO, 75.48 MHz), δ/ppm: 170.20 [Phe carbonylic C], 165.81 [Sar carbonylic C], 136.96 [Phe phenylic C_1], 129.30 [Phe phenylic C_2], 128.31[Phe phenylic C_3], 126.63 [Phe phenylic C_4], 81.10 [O*t*Bu quaternary C], 55.80 [Phe α-CH C], 49.20 [Sar secondary C], 36.95 [Phe β-CH_2 C], 32.80 [NCH_3 C].

$C_{16}H_{25}ClN_2O_3$ (PM. 328.85) Elemental analysis %: (calculated) found, C(58.44) 58.81, H (7.66) 8.27, N (8.52) 8.05.

Z-Sar-Ser(Bzl)-OMe

To a solution of Z-Sar-OH (1.01 g, 4.51 mmol) and NMM (0.50 ml, 4.51 mmol) in THF (20 ml), cooled to -15 °C, isobutylchloroformiate (0.616 g, 4.51 mmol) was added.[224] After 10 min, a cooled suspension of TFA·H-Ser(Bzl)-OMe (2.18 g, 6.76 mmol) and NMM (0.75 ml, 6.76 mmol) in $CHCl_3$ (15 ml) was added. The pH was adjusted and kept to 8 by addition of NMM. After stirring at room temperature overnight, the reaction mixture was concentrated under reduced pressure. The residue was taken up with AcOEt, washed with 10% $KHSO_4$, H_2O, 5% $NaHCO_3$, H_2O, and dried over Na_2SO_4. The organic layer was concentrated to dryness. The product was purified by "flash chromatography" (silica gel column), eluting with a petroleum ether-AcOEt 6.5:3.5 mixture.

Yield: 64 %.

M.p: 68-71 °C (AcOEt-petroleum ether).

Rf_1: 0.90; Rf_2: 0.90; Rf_3 : 0.55.

[α] = + 6.6 ° (c = 0.5, MeOH).

IR (KBr): 3297, 1751, 1715, 1649, 1553 cm^{-1}.

^1H NMR (DMSO, 250 MHz), δ/ppm: 8.51 [d, 1H, Ser NH], 7.33 [m, 10H, Z phenyl, Bzl phenyl], 5.05 [s, 2H, Z CH_2], 4.60 [m, 1H, Ser α-CH], 4.48 [s, 2H, Bzl CH_2], 3.97 [s, 2H, Sar α-CH_2], 3.76-3.62 [m, 5H, OMe, Ser β-CH_2], 3.86 [s, 3H, NCH_3].

MS, $[M+H]^+$ calculated (found): 415.48 (415.19).

Boc-Sar-Ser(*t*Bu)-OMe

To a solution of Boc-Sar-OH (1.96 g, 10.34 mmol) and NMM (1.14 ml, 10.34 mmol) in THF (40 ml), cooled to -15 °C, isobutylchloroformiate (1.41 g, 10.34 mmol) was added.[224] After 10 min, a cooled suspension of (2.72 g, 15.51 mmol) of H-Ser(*t*Bu)-OMe (obtained by catalytic hydrogenation in CH_2Cl_2 of the corresponding Z-protected derivative) and NMM (1.71 ml, 15.51 mmol) in $CHCl_3$ (35 ml) was added. The pH was adjusted and kept to 8 by addition of NMM. After stirring at room temperature overnight, the reaction mixture was concentrated under reduced pressure. The residue was taken up with AcOEt, washed with 10% $KHSO_4$, H_2O, 5% $NaHCO_3$, H_2O, and dried over Na_2SO_4. The organic layer was concentrated to dryness. The product was purified by "flash chromatography" (silica gel column), eluting with a petroleum ether-AcOEt 3:2 mixture.

Yield: 76 %.

Rf_1: 0.90; Rf_2: 0.90; Rf_3 :0.50.

[α] = + 11.8 ° (c = 0.5, MeOH).

IR (KBr): 3434, 3324, 1752, 1704, 1692, 1517 cm^{-1}.

^{1}H NMR ($CDCl_3$, 250 MHz), δ/ppm: 6.79 [m, 1H, Ser NH], 4.72 [m, 1H, Ser α-CH], 3.91 [s, 2H, Sar α-CH_2], 3.84-3.54 [m, 2H, Ser β-CH_2], 3.74 [s, 3H, OCH_3], 2.96 [s, 3H, NCH_3], 1.49 [s, 9H, Boc $(CH_3)_3$], 1.13 [s, 9H, Ser(*t*Bu) $C(CH_3)_3$].

MS, $[M+H]^+$ calculated (found): 347.44 (347.21).

HCl·H-Sar-Ser-OMe

Method 1:

To a solution of (0.53 g, 2.76 mmol) of H-Sar-Ser(Bzl)-OMe (obtained by catalytic hydrogenation in MeOH of the corresponding Z-protected derivative) in Et_2O, a diluted solution of HCl 3 M (0.92 ml) in Et_2O was dropwise added under stirring. The solvent was evaporated to dryness, the residue taken up with Et_2O and filtered.

Method 2:

To a solution of Boc-Sar-Ser(*t*Bu)-OMe (2.71 g, 8.28 mmol) in CH_2Cl_2 (5 ml), TFA (15 ml) was added and the reaction was stirred at room temperature. At the end of the reaction (checked by a TLC), TFA was evaporated using nitrogen flow. The solvent was evaporated, the residue taken up and concentrated several times with CH_2Cl_2, Et_2O and finally with a saturated solution of HCl 3 M in Et_2O until the solid formation. The solid was filtered from Et_2O.

Yield: 80 %.

M.p: 105-106 °C (MeOH-Et_2O).

Rf_1: 0.00; Rf_2: 0.30; Rf_3: 0.00.

[α] = - 6.0 ° (c = 0.5, MeOH).

IR (KBr): 3373, 3318, 1743, 1680, 1560 cm^{-1}.

^{1}H NMR (DMSO, 250 MHz), δ/ppm: 9.00 [d, 1H, Ser NH], 8.89 [m, 2H, Sar NH_2Cl], 5.26 [t, 1H, Ser OH], 4.60 [m, 1H, Ser α-CH], 3.77 [s, 2H, Sar α-CH_2], 3.73-3.60 [m, 5H, OMe, Ser β-CH_2], 2.54 [s, 3H, NCH_3].

MS, $[M+H]^+$ calculated (found): 192.23 (192.10).

Color: white.

Z-Sar-Ser(*t*Bu)-O*t*Bu

To a solution of Z-Sar-OH (0.69 g, 3.07 mmol) and NMM (0.34 ml, 3.07 mmol) in THF (15 ml), cooled to -15 °C, isobutylchloroformiate (0.42 g, 3.07 mmol) was added.[224] After 10 min, a cooled suspension of (1.00 g, 4.61 mmol) of H-Ser(*t*Bu)-O*t*Bu (obtained by catalytic hydrogenation in CH_2Cl_2 of the corresponding Z-protected derivative) and NMM (0.51 ml, 4.61 mmol) in $CHCl_3$ (15 ml) was added. The pH was adjusted and kept to 8 by addition of NMM. After stirring at room temperature overnight, the reaction mixture was concentrated under

reduced pressure. The residue was taken up with AcOEt, washed with 10% $KHSO_4$, H_2O, 5% $NaHCO_3$, H_2O, and dried over Na_2SO_4. The organic layer was concentrated to dryness. The product was purified by "flash chromatography" (silica gel column), eluting with a petroleum ether-AcOEt 3:2 mixture.

Yield: 86 %.

Rf_1: 0.95; Rf_2: 0.95; Rf_3 : 0.50.

[α] = + 3.2 ° (c = 0.5, MeOH).

IR (KBr): 3432, 3327, 1738, 1712, 1688, 1519 cm^{-1}.

^1H NMR ($CDCl_3$, 250 MHz), δ/ppm: 7.35 [m, 5H, Z phenyl], 6.67 [d, 1H, Ser NH], 5.17 [s, 2H, Z CH_2], 4.59 [m, 1H, Ser α-CH], 3.99 [s, 2H, Sar α-CH_2], 3.81-3.51 [m, 2H, Ser β-CH_2], 3.04 [s, 3H, NCH_3], 1.46 [s, 9H, O*t*Bu $C(CH_3)_3$], 1.12 [s, 9H, Ser(*t*Bu) $C(CH_3)_3$].

MS, $[M+H]^+$ calculated (found): 423.54 (423.23).

HCl·H-Sar-Ser(*t*Bu)-O*t*Bu

To a solution of (1.09 g, 2.58 mmol) of H-Sar-Ser(*t*Bu)-O*t*Bu (obtained by catalytic hydrogenation in MeOH of the corresponding Z-protected derivative) in Et_2O, a diluted solution of HCl 2 M (1.29 ml) in Et_2O was dropwise added under stirring. The solvent was evaporated to dryness, the residue taken up with Et_2O and filtered.

Yield: 81 %.

M.p: 160-162 °C (MeOH-Et_2O).

Rf_1: 0.35; Rf_2: 0.75; Rf_3 : 0.10.

[α] = + 4.23 ° (c = 0.5, MeOH).

IR (KBr): 3615, 3481, 3299, 1748, 1737, 1668, 1557 cm^{-1}.

^1H NMR (DMSO, 200 MHz), δ/ppm: 8.81 [m, 2H, Sar NH_2Cl], 8.74 [d, 1H, Ser NH], 4.43 [m, 1H, Ser α-CH], 3.89 [m, 2H, Sar α-CH_2], 3.71-3.64 [m, 2H, Ser β-CH_2], 1.42 [s, 9H, O*t*Bu $C(CH_3)_3$], 1.30 [s, 9H, Ser(*t*Bu) $C(CH_3)_3$].

MS, $[M+H]^+$ calculated (found): 290.40 (290.20).

Color: white.

Z-Sar-Ser(Bzl)-O*t*Bu

To a solution of Z-Sar-OH (0.62 g, 2.77 mmol) and NMM (0.31 ml, 2.77 mmol) in THF (15 ml), cooled to -15 °C, isobutylchloroformiate (0.38 g, 2.77 mmol) was added.[224] After 10 min, a cooled suspension of (1.05 g, 4.16 mmol) of H-Ser(*t*Bu)-O*t*Bu (obtained by deprotection in diethylamine:CH_2Cl_2 30% of the corresponding Fmoc-protected derivative, followed by a purification on a "flash column chromatography" with CH_2Cl_2 as eluant) and NMM (0.46 ml,

4.16 mmol) in CH_2Cl_2 (15 ml) was added. The pH was adjusted and kept to 8 by addition of NMM. After stirring at room temperature overnight, the reaction mixture was concentrated under reduced pressure. The residue was taken up with AcOEt, washed with 10% $KHSO_4$, H_2O, 5% $NaHCO_3$, H_2O, and dried over Na_2SO_4. The organic layer was concentrated to dryness.

Yield: 93 %.

Rf_1: 0.95; Rf_2: 0.95; Rf_3 : 0.65.

$[\alpha]$ = - 1.6 ° (c = 0.5, MeOH).

IR (KBr): 3420, 3321, 1737, 1710, 1692, 1520 cm^{-1}.

^1H NMR ($CDCl_3$, 200 MHz), δ/ppm: 8.36 [d, 1H, NH], 7.31 [m, 10H, Z phenyl, Bzl phenyl], 5.05 [s, 2H, Z CH_2], 4.59-4.46 [m, 3H, Ser α-CH, Bzl CH_2], 3.95 [s, 2H, Sar α-CH_2], 3.71-3.55 [m, 2H, Ser β-CH_2], 2.86 [s, 3H, NCH_3], 1.37 [s, 9H, $C(CH_3)_3$].

MS, $[M+H]^+$ calculated (found): 457.56 (457.20).

Z-Pro-Aib-O*t*Bu

To a solution of Z-Pro-OH (1.22 g, 4.90 mmol) and NMM (0.54 ml, 4.90 mmol) in THF (20 ml), cooled to -15 °C, isobutylchloroformiate (0.67 g, 4.90 mmol) was added.[224] After 10 min, a cooled suspension of (0.94 g, 5.89 mmol) of H-Aib-O*t*Bu (obtained by catalytic hydrogenation in CH_2Cl_2 of the corresponding Z-protected derivative) and NMM (0.65 ml, 5.89 mmol) in CH_2Cl_2 (15 ml) was added. The pH was adjusted and kept to 8 by addition of NMM. After stirring at room temperature overnight, the reaction mixture was concentrated under reduced pressure. The residue was taken up with AcOEt, washed with 10% $KHSO_4$, H_2O, 5% $NaHCO_3$, H_2O, and dried over Na_2SO_4. The organic layer was concentrated to dryness. The product was purified by "flash chromatography" (silica gel column), eluting with a petroleum ether-AcOEt 3:2 mixture.

Yield: 90 %.

M.p: 99-100 °C (AcOEt-petroleum ether).

Rf_1: 0.95; Rf_2: 0.95; Rf_3 :0.50.

IR (KBr): 3335, 1732, 1682, 1534 cm^{-1}.

^1H NMR (DMSO, 400 MHz), δ/ppm: 7.36 [m, 5H Z phenyl], 7.20, 6.56 [2s, 1H, NH isomers], 5.13 [m, 2H, Z CH_2 isomers], 4.29-4.25 [m, 1H, Pro α-CH isomers], 3.56-3.44 [m, 2H, Pro δ-CH_2 isomers], 2.33-1.90 [m, 2H, Pro β-CH_2; 2H, Pro γ-CH_2 isomers], 1.43 [m, 6H, Aib β-CH_3 ; 9H, $C(CH_3)_3$].

MS, $[M+H]^+$ calculated (found): 391.48 (391.22).

HCl·Pro-Aib-O*t*Bu

To a solution of (0.75 g, 2.94 mmol) of H-Pro-Aib-O*t*Bu (obtained by catalytic hydrogenation in MeOH of the corresponding Z-protected derivative) in Et_2O, a diluted solution of HCl 2.05 M (1.44 ml) in Et_2O was dropwise added under stirring. The solvent was evaporated to dryness, the residue taken up with Et_2O and filtered.

Rf_1: 0.15 ; Rf_2: 0.65; Rf_3: 0.05.

IR (KBr): 3435, 3205, 1733, 1678, 1551 cm^{-1}.

^1H NMR (DMSO, 400 MHz), δ/ppm: 8.81 [m, 1H, Aib NH], 4.14-4.10 [m, 1H, Pro α-CH], 3.23-3.17 [m, 2H, Pro δ-CH_2 isomers], 2.32-1.83 [m, 2H, Pro β-CH_2; 2H, Pro γ-CH_2 isomers], 1.37-1.34 [m, 6H, Aib β-CH_3 ; 9H, $C(CH_3)_3$].

MS, $[M]^+$ calculated (found): 257.35 (257.18).

Z-(Aib)$_2$-O*t*Bu[222]

$(Z\text{-}Aib)_2O$ (3.54 g, 7.75 mmol) and NMM (0.85 ml, 7.75 mmol) were added to a solution of (1.36 g, 8.52 mmol) of H-Aib-O*t*Bu (obtained by catalytic hydrogenation in CH_2Cl_2 of the corresponding Z-protected derivative). The pH was adjusted and kept to 8 by addition of NMM. The reaction mixture was stirred at room temperature for 2 days. The solvent was evaporated under reduced pressure. The residue was taken up with AcOEt, washed with 10% $KHSO_4$, H_2O, 5% $NaHCO_3$, H_2O, and dried over Na_2SO_4. The organic layer was concentrated to dryness. The product was purified by "flash chromatography" (silica gel column), eluting with a petroleum ether-AcOEt 5:2 mixture.

Yield: 91 %.

P.f: 136-137 °C (AcOEt-petroleum ether).

Rf_1: 0.90; Rf_2: 0.95.

IR (KBr): 3407, 3293, 1719, 1657, 1536, 1516 cm^{-1}.

^1H NMR ($CDCl_3$, 200 MHz), δ/ppm: 7.35 [m, 5H, Z phenyl], 6.91, 5.37 [2s, 2H, NH], 5.10 [s, 2H, Z CH_2], 1.53, 1.50 [s, 12H, β-CH_3], 1.45 [s, 9H, $C(CH_3)_3$].

MS, $[M+H]^+$ calculated (found): 379.49 (379.23).

Z-(Aib)$_3$-O*t*Bu[225]

This derivative was prepared as previously described for Z-$(Aib)_2$-O*t*Bu, using (1.37 g, 3.10 mmol) of $(Z\text{-}Aib)_2O$, (0.33 ml, 3.10 mmol) of NMM and (0.76 g, 3.10 mmol) of H-Aib_2-O*t*Bu (obtained by catalytic hydrogenation in MeOH of the corresponding Z-protected derivative).

Yield: 80 %.

M.p: 162-164 °C (AcOEt-petroleum ether).

Rf_1: 0.75; Rf_2: 0.95; Rf_3 : 0.35.

IR (KBr): 3409, 3329, 1724, 1697, 1668, 1653, 1531 cm^{-1}.

^1H NMR ($CDCl_3$, 200 MHz), δ/ppm: 7.37 [m, 5H, Z phenyl], 7.07, 6.50, 5.14 [3s, 3H, NH], 5.10 [s, 2H, Z CH_2], 1.50, 1.48 [2s, 12H, β-CH_3], 1.44 [m, 6H, β-CH_3; 9H, $C(CH_3)_3$].

MS, $[M+H]^+$ calculated (found): 464.60 (464.27).

Z-$(Aib)_3$-OH[225]

Z-$(Aib)_3$-O*t*Bu (2.48 g, 5.36 mmol) was dissolved in 10 ml of a CH_2Cl_2 distilled-TFA 1:1 mixture and stirred at room temperature for 2h. TFA was evaporated using nitrogen flow and the residue was taken up and evaporated several times from CH_2Cl_2 and Et_2O, until the obtainment of a solid that was filtered.

Yield: 93 %.

M.p: 198-200 °C.

Rf_1: 0.15; Rf_2: 0.90; Rf_3 : 0.05.

IR (KBr): 3420, 3358, 3285, 1736, 1705, 1680, 1646, 1532, 1512 cm^{-1}.

^1H NMR (DMSO, 200 MHz), δ/ppm: 7.36 [m, 5H, Z phenyl], 7.60, 7.20 [2s, 2H, NH], 5.13 [m, 2H, Z CH_2], 1.29 [s, 18H, β-CH_3].

MS, $[M+H]^+$ calculated (found): 408.49 (408.20).

Z-$(Aib)_3$-oxl [5(4*H*)-oxazolone from Z-$(Aib)_3$-OH][225]

To a cooled solution of Z-$(Aib)_3$-OH (2 g, 4.91 mmol) in CH_3CN, EDC (1.41 g, 7.36 mmol) was added. The mixture was stirred for 1h at room temperature. The solvent was evaporated to dryness and the residue taken up with AcOEt, washed with 10% $KHSO_4$, H_2O, 5% $NaHCO_3$, H_2O, and dried over Na_2SO_4. The organic layer was concentrated and the solid product was precipitated by addition of petroleum ether.

Yield: 89 %.

M.p: 122-123 °C (from AcOEt-petroleum ether).

Rf_3 : 0.43.

IR (KBr): 3433, 3404, 1803, 1722, 1681 cm^{-1}.

Z-Sar-$(Aib)_2$-O*t*Bu

To a solution of Z-Sar-OH (0.54 g, 2.40 mmol) and NMM (0.26 ml, 2.40 mmol) in THF (20 ml), cooled to -15 °C, isobutylchloroformiate (0.33 g, 2.40 mmol) was added.[224] After 10 min, a cooled suspension of (0.65 g, 2.64 mmol) of H-$(Aib)_2$-O*t*Bu (obtained by catalytic hydrogenation in MeOH of the corresponding Z-protected derivative) and NMM (0.29 ml, 2.64 mmol) in $CHCl_3$ (15 ml) was added. The pH was adjusted and kept to 8 by addition of NMM. After

stirring at room temperature overnight, the reaction mixture was concentrated under reduced pressure. The residue was taken up with AcOEt, washed with 10% $KHSO_4$, H_2O, 5% $NaHCO_3$, H_2O, and dried over Na_2SO_4. The organic layer was concentrated to dryness.

Yield: 90 %.

Rf_1: 0.90; Rf_2: 0.90; Rf_3 : 0.40.

IR (KBr): 3324, 1685, 1509 cm^{-1}.

^1H NMR ($CDCl_3$, 400 MHz), δ/ppm: 7.36 [m, 5H, Z phenyl], 6.94 [1s, 1H, Aib^1 NH], 6.61 [1s, 1H, Aib^2 NH], 5.17 [d, 2H, Z CH_2], 3.87 [s, 2H, Sar α-CH_2], 3.04 [s, 3H, NCH_3], 1.52 [m, 12H, β-CH_3], 1.45 [s, 9H, $C(CH_3)_3$].

MS, $[M+H]^+$ calculated (found): 450.57 (450.25).

HCl·H-Sar-$(Aib)_2$-O*t*Bu.

To a solution of (0.66 g, 2.09 mmol) of H-Sar-$(Aib)_2$-O*t*Bu (obtained by catalytic hydrogenation in MeOH of the corresponding Z-protected derivative) in Et_2O, a diluted solution of HCl 2 M (1.04 ml) in Et_2O was dropwise added under stirring. The solvent was evaporated to dryness, the residue taken up with Et_2O and filtered.

Yield: 92 %.

M.p: 148-149 °C (MeOH-Et_2O).

Rf_1: 0.10; Rf_2: 0.50; Rf_3: 0.00.

IR (KBr): 3421, 3276, 1727, 1688, 1647, 1545 cm^{-1}.

^1H NMR (DMSO, 300 MHz), δ/ppm: 8.95 [m, 2H, Sar NH_2Cl], 8.49 [1s, 1H, Aib^1 NH], 7.64 [1s, 1H, Aib^2 NH], 3.68 [s, 2H, Sar α-CH_2], 2.51 [s, 3H, NCH_3], 1.39 [s, 6H, Aib^1 β-CH_3], 1.34 [s, 9H, $C(CH_3)_3$], 1.30 [s, 6H, Aib^2 β-CH_3].

^{13}C NMR (DMSO, 75.48 MHz), δ/ppm: 173.47 [Aib^2 carbonylic C], 172.84 [Aib^2 carbonylic C], 164.97 [Sar carbonylic C], 79.61 [O*t*Bu quaternary C], 56.54 [Aib^1 quaternary C], 55.99 [Aib^2 quaternary C], 49.75 [Sar secondary C], 32.95 [NCH_3 C], 27.84 [$(CH_3)_3$ C], 25.22 [Aib^1 $(CH_3)_2$ C], 25.00 [Aib^2 $(CH_3)_2$ C].

$C_{15}H_{30}ClN_3O_4$ (PM. 351.89) Elemental analysis %: (calculated) found C (51.20) 50.24, H (8.59) 8.35, N (11.94) 11.38. Color: white.

Z-Pro-$(Aib)_2$-O*t*Bu

To a solution of Z-Pro-OH (0.98 g, 3.92 mmol) and NMM (0.32 ml, 3.92 mmol) in THF (20 ml), cooled to -15 °C, isobutylchloroformiate (0.54 g, 3.92 mmol) was added.[224] After 10 min, a cooled suspension of (1.05 g, 4.31 mmol) of H-$(Aib)_2$-O*t*Bu (obtained by catalytic hydrogenation in MeOH of the corresponding Z-protected derivative) and NMM (0.48 ml, 4.31 mmol) in

CH_2Cl_2 (10 ml) was added. The pH was adjusted and kept to 8 by addition of NMM. After stirring at room temperature overnight, the reaction mixture was concentrated under reduced pressure. The residue was taken up with AcOEt, washed with 10% $KHSO_4$, H_2O, 5% $NaHCO_3$, H_2O, and dried over Na_2SO_4. The organic layer was concentrated to dryness. The product was purified by "flash chromatography" (silica gel column), eluting with a petroleum ether-AcOEt 2:3 mixture.

Yield: 82 %.

M.p: 176-177 °C (from AcOEt-petroleum ether).

Rf_1 : 0.90; Rf_2 : 0.95; Rf_3 :0.40.

IR (KBr): 3374, 3283, 1738, 1689, 1639, 1549 cm^{-1}.

^1H NMR ($CDCl_3$, 400 MHz), δ/ppm 7.36 [m, 5H Z phenyl], 7.09-6.97 [m, 1H, Aib^1 NH isomers], 6.76-6.53 [m, 1H, Aib^2 NH isomers], 5.17 [m, 2H, Z CH_2 isomers], 4.29-4.25 [m, 1H, Pro α-CH isomers], 3.58-3.49 [m, 2H, Pro δ-CH_2 isomers], 2.22-1,88 [m, 2H, Pro β-CH_2; 2H, Pro γ-CH_2 isomers], 1.58-1.47 [2m, 6H, Aib^1 β-CH_3 isomers; 6H, Aib^2 β-CH_3 isomers], 1.44 [s, 9H, $C(CH_3)_3$].

MS, $[M+H]^+$ calculated (found): 476.59 (476.27).

HCl·H-Pro-$(Aib)_2$-O*t*Bu

To a solution of (0.74 g, 2.18 mmol) of H-Pro-$(Aib)_2$-O*t*Bu (obtained by catalytic hydrogenation in MeOH of the corresponding Z-protected derivative) in Et_2O, a diluted solution of HCl 3 M (0.73 ml) in Et_2O was dropwise added under stirring.

Yield: 90%

M.p: 203-205 °C (MeOH-Et_2O).

Rf_1: 0.20; Rf_2 : 0.75; Rf_3: 0.05.

IR (KBr): 3400, 3284, 1723, 1684, 1650, 1531 cm^{-1}.

^1H NMR (DMSO, 400 MHz), δ/ppm: 8.48, 7.57 [2s, 1H, Aib^1 NH; 1H, Aib^2 NH], 4.21-4.18 [m, 1H, Pro α-CH isomers], 3.21-3.15 [m, 2H, Pro δ-CH_2 isomers], 2.29-1.81 [m, 2H, Pro β-CH_2; 2H, Pro γ-CH_2 isomers], 1.42, 1.40, 1.30, 1.29 [4s, 6H, Aib^1 β-CH_3 isomers; 6H Aib^2 β-CH_3 isomers], 1.35[m, 9H, $C(CH_3)_3$ isomers].

MS, $[M]^+$ calculated (found): 342.46 (342.23).

Z-Sar-$(Aib)_3$-O*t*Bu

HOBt (0.61 g, 4.52 mmol) and EDC (0.87 g, 4.52 mmol) were added to a cooled solution of Z-Sar-OH (1.01 g, 4.52 mmol) in distilled CH_2Cl_2 (10 ml) under stirring. After several minutes, a solution of (1.24 g, 3.77 mmol) of H-$(Aib)_3$-O*t*Bu (obtained by catalytic hydrogenation in MeOH

of the corresponding Z-protected derivative) and NMM (0.42 ml, 3.77 mmol) was added. The reaction mixture was stirred for 4 days. The solvent was evaporated to dryness. . The solvent was evaporated to dryness, the residue taken up with Et_2O and filtered. The residue was taken up with AcOEt, washed with 10% $KHSO_4$, H_2O, 5% $NaHCO_3$, H_2O, and dried over Na_2SO_4. The organic layer was concentrated to dryness. The product was purified by "flash chromatography" (silica gel column), eluting with a CH_2Cl_2-MeOH 30:1 mixture.

Yield: 60 %.

P.f: 145-146 °C (AcOEt-petroleum ether).

Rf_1 : 0.60; Rf_2 : 0.90; Rf_3 : 0.40.

IR (KBr): 3437, 3416, 3310, 1731, 1702, 1679, 1640, 1543 cm^{-1}.

^1H NMR ($CDCl_3$, 250 MHz), δ/ppm: 7.36 [m, 5H, Z phenyl], 7.02, 6.68, 6.28 [3s, 3H, Aib NH], 5.16 [d, 2H, Z CH_2], 3.80 [s, 2H, Sar α-CH_2], 3.09 [s, 3H, NCH_3], 1.49, 1.47, 1.44 [3s, 18H, β-CH_3], 1.43 [s, 9H, $C(CH_3)_3$].

MS, $[M+H]^+$ calculated (found): 535.65 (535.33).

HCl·H-Sar-(Aib)$_3$-O*t*Bu

To a solution of (1.04 g, 2.60 mmol) of H-Sar-(Aib)$_3$-O*t*Bu (obtained by catalytic hydrogenation in MeOH of the corresponding Z-protected derivative) in Et_2O, a diluted solution of HCl 3 M (0.87 ml) in Et_2O was dropwise added under stirring. The solvent was evaporated to dryness, the residue taken up with Et_2O and filtered.

yield: 87 %.

Rf_1: 0.05; Rf_2 : 0.70; Rf_3: 0.00.

IR (KBr): 3435, 1725, 1681, 1540 cm^{-1}.

^1H NMR (DMSO, 400 MHz), δ/ppm: 8.95 [m, 2H, Sar NH_2Cl], 8.82, 7.64, 7.27 [3s, 1H, Aib^1 NH; 1H, Aib^2 NH; 1H, Aib^3 NH], 3.72 [s, 2H, Sar α-CH_2], 2.56 [s, 3H, NCH_3], 1.34 [m, 9H, $C(CH_3)_3$; 6H, Aib β-CH_3], 1.33 [s, 6H, Aib β-CH_3], 1.30 [s, 6H, Aib β-CH_3] .

Z-(Aib)$_3$-Gly-OEt[225]

A solution of Z-(Aib)$_3$-oxl (2.39 g, 6.13 mmol) and H-Gly-OMe (extracted with CH_2Cl_2 from a solution of HCl·H-Gly-OMe in 5% $NaHCO_3$) in THF was refluxed with stirring for 4 days. The solvent was evaporated, the residue diluted in AcOEt, washed with 10 % $KHSO_4$, H_2O, 5% $NaHCO_3$, H_2O, and dried over Na_2SO_4. The organic layer was evaporated to dryness and the product was purified by "flash chromatography" (silica gel column), eluting with CH_2Cl_2.

Yield: 81 %.

M.p: 163-165 °C (from AcOEt-petroleum ether).

Rf_1: 0.80; Rf_2: 0.85; Rf_3 :0.25.

IR (KBr): 3386, 3345, 3285, 1764, 1704, 1708, 1671, 1662, 1531 cm^{-1}.

^1H NMR ($CDCl_3$, 250 MHz), δ/ppm: 7.51 [t, 1H, Gly NH], 7.36 [m, 5H, Z phenyl], 7.19, 6.37 [2s, 2H, NH], 5.11 [s, 2H, Z CH_2], 4.15 [d, 2H, Et CH_2], 4.03 [d, 2H, Gly α-CH_2], 1.55, 1.47, 1.35 [3s, 18H, Aib β-CH_3], 1.24 [s, 3H, Et CH_3].

MS, $[M+H]^+$ calculated (found): 493.60 (493.26).

Z-Sar-$(Aib)_3$-Gly-OEt

HOBt (0.80 g, 5.95 mmol) and EDC (1.14 g, 5.95 mmol) were added to a cooled solution of Z-Sar-OH (1.34 g, 5.95 mmol) in distilled CH_2Cl_2 (15 ml) under stirring. After several minutes, a solution of (1.78 g, 4.96 mmol) of H-$(Aib)_3$-O*t*Bu (obtained by catalytic hydrogenation in EtOH of the corresponding Z-protected derivative) and NMM (0.55 ml, 4.96 mmol) was added. The reaction mixture was stirred for 5 days. The solvent was evaporated to dryness. The solvent was evaporated to dryness, the residue taken up with Et_2O and filtered. The residue was taken up with AcOEt, washed with 10% $KHSO_4$, H_2O, 5% $NaHCO_3$, H_2O, and dried over Na_2SO_4. The organic layer was concentrated to dryness. The product was purified by "flash chromatography" (silica gel column), eluting with a CH_2Cl_2-EtOH 95:5 mixture.

Yield: 67 %.

M.p: 151-153 °C (AcOEt-petroleum ether).

Rf_1: 0.65; Rf_2 : 0.85; Rf_3 : 0.25.

IR (KBr): 3333, 1738, 1729, 1669, 1539 cm^{-1}.

^1H NMR ($CDCl_3$, 400 MHz), δ/ppm: 7.60 [t, 1H, Gly NH], 7.16, 6.91, 6.20, [3s, 3H, NH], 7.37 [m, 5H, Z phenyl], 5.17 [d, 2H, Z CH_2], 4.14 [q, 2H, Et CH_2], 4.02 [d, 2H, Gly α-CH_2], 3.77 [s, 2H, Sar α-CH_2], 2.80 [m, 3H, NCH_3], 1.55, 1.45, 1.41 [m, 18H, Aib β-CH_3], 1.25 [t, 3H, Et CH_3].

MS, $[M+H]^+$ calculated (found): 564.68 (564.28).

HCl·H-Sar-$(Aib)_3$-Gly-OEt

To a solution of (1.38 g, 3.22 mmol) of H-Sar-$(Aib)_3$-Gly-OEt (obtained by catalytic hydrogenation in EtOH of the corresponding Z-protected derivative) in Et_2O, a diluted solution of HCl 3 M (1.07 ml) in Et_2O was dropwise added under stirring. The solvent was evaporated to dryness, the residue taken up with Et_2O and filtered.

Yield: 73 %.

P.f: 243-245 °C (MeOH-Et_2O).

Rf_1: 0.00 ; Rf_2 : 0.50; Rf_3: 0.00.

IR (KBr): 3292, 1750, 1732, 1708, 1661, 1528 cm^{-1}.

^{1}H NMR (DMSO, 300 MHz), δ/ppm: 8.96 [m, 1H, Sar NH_2Cl], 8.88 [s, 1H, Aib^1 NH], 8.04 [s, 1H, Aib^2 NH], 7.90 [t, 1H, Gly NH], 7.26 [s, 1H, Aib^3 NH], 4.05 [q, 2H, Et CH_2], 3.77 [d, 2H, Gly α-CH_2], 3.72 [s, 2H, Sar α-CH_2], 2.57 [s, 3H, NCH_3], 1.39[s, 6H, Aib^3 β-CH_3], 1.35 [m, 6H, Aib^1 β-CH_3], 1.31 [m, 6H, Aib^2 β-CH_3], 1.16 [t, 3H, Et CH_3].

^{13}C NMR (DMSO, 75.48 MHz), δ/ppm: 174.72 [Aib^3 carbonylic C], 173.68 [Aib^1 carbonylic C], 172.98 [Aib^2 carbonylic C], 169.38 [Gly carbonylic C], 165.17 [Sar carbonylic C], 59.84 [OEt secondary C], 55.93 [Aib^2 quaternary C], 55.91 [Aib^1 quaternary C], 55.63 [Aib^3 quaternary C], 48.87 [Sar secondary C], 40.53 [Gly secondary C], 32.41 [NCH_3 C], 24.66 [Aib^3 $(CH_3)_2$ C], 24.43 [Aib^2 $(CH_3)_2$ C], 24.33 [Aib^1 $(CH_3)_2$ C], 13.64 [OEt primary C] .

MS, $[M+H]^+$ calculated (found): 430.55 (430.26).

$C_{19}H_{36}ClN_5O_6$ (PM. 429.539) Elemental analysis %: (calculated) found C (48.97) 49.02, H (7.79) 7.80, N (15.03) 14.92.

2.3. SYNTHESIS OF GOLD(III)-PEPTIDODITHIOCARBAMATO DERIVATIVES

2.3.1 Gold(III)-methyl-ester-containing-dipeptides derivatives

[$Au^{III}Br_2$(dtc-Sar-Gly-OMe)] (AuD_2)

A water solution (3 ml) of HCl·Sar-Gly-OMe (0.10 g, 0.51 mmol) cooled at 0 °C was dropwise treated under continuous stirring with cool CS_2 (0.03 ml, 0.51 mmol) and an aqueous solution (1.5 ml) of NaOH (0.02 g, 0.51 mmol). When the pH turned from 9 to 6 after 3 hours according to proceedings in literature,[155,162(a)] the solution was slowly added under stirring to an aqueous solution (2 ml) of K[$AuBr_4$].$2H_2O$ (0.10 g, 0.25 mmol), leading to the immediate precipitation of a yellowish-green solid that was filtered off, washed with water and dried under pressure with P_2O_5.

Yield: 45 %

M.p.: decomposes at 198.8 °C

IR (KBr): 3409, 1744, 1669, 1558, 961, 560 cm^{-1}.

^{1}H NMR (DMSO, 300 MHz), δ/ppm: 8.89 [s, 1H, Gly NH], 4.56 [s, 2H, Sar α-CH_2], 3.94 [s, 2H, Gly α-CH_2], 3.64 [s, 3H, OCH_3].

$C_7H_{11}AuBr_2N_2O_3S_2$ (MW. 592.08) Elemental analysis %: (calculated) found C (14.20) 13.68, H (1.87) 1.80, N (4.73) 4.66, S (10.83) 10.47. Color: orange.

[$Au^{III}Br_2$(dtc-Sar-Aib-OMe)] (AuD_3)

This complexe was prepared by a similar method to that of the glycyl-methyl-ester-containing derivative. K[$AuBr_4$].2H_2O (0.15 g, 0.25 mmol) reacted with a solution of HCl·Sar-Aib-OMe (0.11 g, 0.51 mmol), CS_2 (0.03 ml, 0.51 mmol) and NaOH (0.02 g, 0.51 mmol).

Yield: 41 %.

M.p.: decomposes at 167.0 °C.

IR (KBr): 3423, 1739, 1685, 1559, 1384, 1364, 995, 583 cm^{-1}.

^{1}H NMR (DMSO, 300 MHz), δ/ppm: 8.82 [2s, 1H, Aib NH isomers], 4.48 [s, 2H, Sar α-CH_2], 3.58 [s, 3H, OCH_3], 3.41 [2s, 3H, NCH_3 isomers], 1.39 [s, 6H, Aib β-CH_3].

$C_9H_{17}AuBr_2N_2O_3S_2$ (PM.620.13) Elemental analysis %: (calculated) found C (17.43) 17.94, H (2.44) 1.99, N (4.52) 4.44, S (10.34) 10.30. Color: orange.

2.3.2 Gold(III)-tert-butyl-ester-containing-dipeptides derivatives

[Au^{III}(dtc-Sar-Gly-O*t*Bu)Br_2] (AuD_6)

This complexe was prepared by a similar method to that of the glycyl-methyl-ester-containing derivative. Anhydrous K[$AuBr_4$] (0.15 g, 0.27 mmol) reacted with a solution of HCl·Sar-Gly-O*t*Bu (0.13 g, 0.54 mmol), CS_2 (0.03 ml, 0.54 mmol) and NaOH (0.02 g, 0.54 mmol).

Yield: 77 %.

M.p.: decomposes at 152.6 °C.

IR (KBr): 3352, 1736, 1673, 1568, 1228,1161, 1006, 556, 387, 252, 227 cm^{-1}.

^{1}H NMR (acetone-D_6, 300.13 MHz), δ/ppm: 7.96 [m, 1H, Gly NH] , 4.75, 4.71 [2s, 2H, Sar α-CH_2 isomers], 3.96, 3.95 [2d, 2H, Gly α-CH_2 isomers], 3.57, 3.53 [2s, 3H, NCH_3 isomers], 1.41 [s, 9H, $C(CH_3)_3$].

^{13}C NMR (acetone-D_6, 75.48 MHz), δ/ppm: 200.48, 196.74 [CSS C], 169.93 [Gly carbonylic C], 165.35, 165.06 [Sar carbonylic C], 82.59 [O*t*Bu quaternary C], 58.98, 55.12 [Sar secondary C], 43.09 [Gly secondary C], 41.12, 40.13 [NCH_3 C], 28.66 [$(CH_3)_3$ C].

$C_{10}H_{17}AuBr_2N_2O_3S_2$ (MW. 634.16) Elemental analysis %: (calculated) found C (18.94) 19.20, H (2.70) 2.88, N (4.42) 4.42, S (10.11) 10.45. Color: orange.

[$Au^{III}Cl_2$(dtc-Sar-Gly-O*t*Bu)] (AuD_7)

This complexe was prepared by a similar method to that of the glycyl-methyl-ester-containing derivative. K[$AuCl_4$].xH_2O (0.15 g, 0.40 mmol) reacted with a solution of HCl·Sar-Gly-O*t*Bu (0.19 g, 0.79 mmol), CS_2 (0.05 ml, 0.79 mmol) and NaOH (0.03 g, 0.79 mmol).

Yield: 77 %.

M.p.: decomposes at 155.3 °C.

IR (KBr): 3349, 1737, 1672, 1561, 1229, 1162, 1006, 558, 384, 358, 339 cm^{-1}.

^{1}H NMR (acetone-D_6, 300.13 MHz), δ/ppm: 7.96 [m, 1H, Gly NH] , 4.75, 4.71 [2s, 2H, Sar α-CH_2 isomers], 3.96, 3.95 [m, 2H, Gly α-CH_2 isomers], 3.57, 3.53 [2s, 3H, NCH_3 isomers], 1.41 [s, 9H, $C(CH_3)_3$].

^{13}C NMR (acetone-D_6, 75.48 MHz), δ/ppm: 200.60, 195.45 [CSS C], 169.82 [Gly carbonylic C], 165.10 [Sar carbonylic C], 82.66 [O*t*Bu quaternary C], 55.64 [Sar secondary C], 43.27 [Gly secondary C], 41.10, 40.66 [NCH_3 C], 28.70 [$(CH_3)_3$ C].

$C_{10}H_{17}AuCl_2N_2O_3S_2$ (MW. 545.26) Elemental analysis %: (calculated) found C (22.03) 22.00, H (3.14) 3.23, N (5.14) 5.08, S (11.76) 11.96. Color: earthy-yellow.

[$Au^{III}Br_2$(dtc-Sar-Aib-O*t*Bu)] (AuD_8

This complexe was prepared by a similar method to that of the glycyl-methyl-ester-containing derivative. Anhydrous K[$AuBr_4$] (0.15 g, 0.27 mmol) reacted with a solution of HCl·Sar-Aib-O*t*Bu (0.14 g, 0.54 mmol), CS_2 (0.03 ml, 0.54 mmol) and NaOH (0.02 g, 0.54 mmol).

Yield: 76 %.

M.p.: decomposes at 165.9 °C.

IR (KBr): 3362, 1734, 1690, 1560, 1531, 1215, 1144, 996, 545, 383, 253, 223 cm^{-1}.

^{1}H NMR (acetone-D_6, 300.13 MHz), δ/ppm: 7.90 [s, 1H, Aib NH], 4.66, 4.62 [2s, 2H, Sar α-CH_2 isomers], 3.54, 3.51 [m, 3H, NCH_3 isomers], 1.46, 1.45 [2s, 6H, β-CH_3 isomers], 1.44 [s, 9H, $C(CH_3)_3$].

^{13}C NMR (acetone-D_6, 75.48 MHz), δ/ppm: 200.26, 196.57 [CSS C], 173.73 [Aib C carbonylic], 164.00 [Sar carbonylic C], 81.91 [O*t*Bu quaternary C], 58.35 [Aib quaternary C], 56.15, 55.26 [Sar secondary C], 41.20, 40.21 [NCH_3 C], 28.60 [$(CH_3)_3$ C], 25.61 [Aib $(CH_3)_2$ C].

$C_{12}H_{21}AuBr_2N_2O_3S_2$ (MW. 662.21) Elemental analysis %: (calculated) found C (21.76) 22.03, H (3.20) 3.33, N (4.23) 4.34, S (9.68) 8.58. Color: orange.

[$Au^{III}Cl_2$(dtc-Sar-Aib-O*t*Bu)] (AuD_9)

This complexe was prepared by a similar method to that of the glycyl-methyl-ester-containing derivative. K[$AuCl_4$].xH_2O (0.15 g, 0.40 mmol) reacted with a solution of HCl·Sar-Aib-O*t*Bu (0.21 g, 0.79 mmol), CS_2 (0.05 ml, 0.79 mmol) and NaOH (0.03 g, 0.79 mmol).

Yield: 81 %.

M.p.: decomposes at 166.6 °C.

IR (KBr): 3365, 1733, 1691, 1564, 1534, 1214, 1146, 996, 547, 383, 347 cm^{-1}.

^{1}H NMR (acetone-D_6, 300.13 MHz), δ/ppm: 7.89 [m, 1H, Aib NH], 4.66 [s, 2H, Sar α-CH_2], 3.55, 3.54 [2s, 3H, NCH_3 isomers], 1.46, 1.45 [2s, 6H, β-CH_3 isomers], 1.44 [s, 9H, $C(CH_3)_3$].

^{13}C NMR (acetone-D_6, 75.48 MHz), δ/ppm: 200.19, 196.09 [CSS C], 173.62 [Aib carbonylic C], 163.80 [Sar carbonylic C], 81.87 [O*t*Bu quaternary C], 58.20 [Aib quaternary C], 55.67 [Sar secondary C], 41.04, 40.64 [NCH_3 C], 28.50 [$(CH_3)_3$ C], 25.52 [Aib $(CH_3)_2$ C].

$C_{12}H_{21}AuCl_2N_2O_3S_2$ (MW. 573.31) Elemental analysis %: (calculated) found C (25.14) 25.11, H (3.69) 3.84, N (4.89) 4.84, S (11.19) 11.37. Color: earthy-yellow.

[$Au^{III}Br_2$(dtc-Sar-Phe-O*t*Bu)] (AuD_{10})

This complexe was prepared by a similar method to that of the glycyl-methyl-ester-containing derivative. Anhydrous K[$AuBr_4$] (0.15 g, 0.27 mmol) reacted with a solution of HCl·Sar-Phe-O*t*Bu (0.18 g, 0.54 mmol), CS_2 (0.03 ml, 0.54 mmol) and NaOH (0.02 g, 0.54 mmol).

Yield: 72 %.

M.p.: decomposes at 124.3 °C.

IR (KBr): 3431, 1731, 1683, 1558, 1543, 1214, 1155, 994, 562, 381, 252, 221 cm^{-1}.

^{1}H NMR (acetone-D_6, 300.13 MHz), δ/ppm: 7.91 [d, 1H, Phe NH], 7.25-7.33 [m, 5H, Phe phenyl], 4.74-4.67 [m, 1H, α-CH], 4.70-4.65 [m, 2H, Sar α-CH_2], 3.49, 3.45 [2s, 3H, NCH_3 isomers], 3.20-2.98 [m, 2H, β-CH_2], 1.43 [s, 9H, $C(CH_3)_3$].

^{13}C NMR (acetone-D_6, 75.48 MHz), δ/ppm: 199.61, 194.45 [CSS C], 170.93 [Phe carbonylic C], 164.10, 163.97 [Sar carbonylic C],137.73 [Phe phenylic C_1], 130.40 [Phe phenylic C_2], 129.15 [Phe phenylic C_3], 127.50 [Phe phenylic C_4], 82.33 [O*t*Bu quaternary C], 55.31 [Sar secondary C], 54.97 [Phe α-CH C], , 40.49 [NCH_3 C], 38.29 [Phe β-CH_2 C], 27.86 [$(CH_3)_3$ C].

$C_{17}H_{23}AuBr_2N_2O_3S_2$ (MW. 721.92) Elemental analysis %: (calculated) found C (28.19) 28.34, H (3.20) 3.09, N (3.87) 3.87, S (8.85) 8.63. Color: orange.

[$Au^{III}Cl_2$(dtc-Sar-Phe-O*t*Bu)] (AuD_{11})

This complexe was prepared by a similar method to that of the glycyl-methyl-ester-containing derivative. K[$AuCl_4$].xH_2O (0.15 g, 0.40 mmol) reacted with a solution of HCl·Sar-Phe-O*t*Bu (0.26 g, 0.79 mmol), CS_2 (0.05 ml, 0.79 mmol) and NaOH (0.03 g, 0.79 mmol).

Yield: 81 %.

M.p.: decomposes at 138.3 °C.

IR (KBr): 3342, 1733, 1684, 1559, 1542, 1213, 1155, 994, 563, 383, 359 cm^{-1}.

^{1}H NMR (acetone-D_6, 300.13 MHz), δ/ppm: 7.92 [d, 1H, Phe NH], 7.25-7.33 [m, 5H, Phe phenyl], 4.74-4.67 [m, 1H, α-CH], 4.70 [m, 2H, Sar α-CH_2], 3.49 [s, 3H, NCH_3], 3.20-2.98 [m, 2H, β-CH_2], 1.43 [s, 9H, $C(CH_3)_3$].

^{13}C NMR (acetone-D_6, 75.48 MHz), δ/ppm: 199.33, 196.11 [CSS C], 170.75 [Phe carbonylic C], 164.33, 164.10 [Sar carbonylic C], 137.72 [Phe phenylic C_1], 130.43 [Phe phenylic C_2], 129.41 [Phe phenylic C_3], 127.86 [Phe phenylic C_4], 82.56 [O*t*Bu quaternary C], 55.23 [Phe α-CH C], 55.56, 54,65 [Sar secondary C], 40.74-39.74 [NCH_3 C], 38.50 [Phe β-CH_2 C], 28.11 [$(CH_3)_3$ C].

$C_{17}H_{23}AuCl_2N_2O_3S_2$ (MW. 635.38) Elemental analysis %: (calculated) found C (32.14) 32.31, H (3.65) 3.54, N (4.41) 4.40, S (10.09) 9.95. Color: clearly brown.

[Au^{III}Br$_2$(dtc-Sar-Ser(*t*Bu)-O*t*Bu)] (AuD$_{16}$)

Gold(III)-dibromo[(C^{β}-O-tert-butyl)tert-butyloxyserylsarcosyldithiocarbamato]

This complexe was prepared by a similar method to that of the glycyl-methyl-ester-containing derivative. K[$AuBr_4$].2H_2O (0.15 g, 0.25 mmol) reacted with a solution of HCl·Sar-Ser(*t*Bu)-O*t*Bu (0.17 g, 0.51 mmol), CS_2 (0.03 ml, 0.51 mmol) and NaOH (0.02 g, 0.51 mmol).

Yield: 78 %.

IR (KBr): 3427, 1736, 1675, 1564, 1234, 1159 cm^{-1}.

^{1}H NMR (acetone-D_6, 300.13 MHz), δ/ppm: 8.07-7.95 [m, 1H, Ser NH isomers], 4.78-4.74 [m, 2H, Sar α-CH_2 isomers], 4.58-4.54 [m, 1H, Ser α-CH isomers], 3.85-3.58 [m, 2H, Ser β- CH_2 isomers], 3.56, 3.53 [2s, 3H, NCH_3 isomers], 1.46 [s, 9H, O*t*Bu C$(CH_3)_3$], 1.15 [s, 9H, Ser(*t*Bu) C$(CH_3)_3$]. $C_{15}H_{27}AuBr_2N_2O_4S_2$ (MW. 720.29) Elemental analysis %: (calculated) found C (25.01) 23.88, H (3.78) 3.68, N (3.89) 3.83, S (8.90) 7.42. Color: orange.

The characterization of this gold(III) derivative is still in progress.

[Au^{III}Cl$_2$(dtc-Sar-Ser(*t*Bu)-O*t*Bu)] (AuD$_{17}$)

This complexe was prepared by a similar method to that of the glycyl-methyl-ester-containing derivative. K[$AuCl_4$].xH_2O (0.15 g, 0.40 mmol) reacted with a solution of HCl·Sar-Ser(*t*Bu)-O*t*Bu (0.26 g, 0.79 mmol), CS_2 (0.05 ml, 0.79 mmol) and NaOH (0.03 g, 0.79 mmol).

Yield: 57 %.

IR (KBr): 3424, 1736, 1685, 1561, 1234, 1160 cm^{-1}.

^{1}H NMR (acetone-D_6, 300.13 MHz), δ/ppm: 8.13-8.01 [m, 1H, Ser NH isomers], 4.79-4.78 [m, 2H, Sar α-CH_2 isomers], 4.59-4.54 [m, 1H, Ser α-CH isomers], 3.86-3.58 [m, 2H, Ser β- CH_2 isomers], 3.57, 3.56 [2s, 3H, NCH_3 isomers], 1.46 [s, 9H, O*t*Bu C$(CH_3)_3$], 1.15 [s, 9H, Ser(*t*Bu) C$(CH_3)_3$].

$C_{15}H_{27}AuCl_2N_2O_4S_2$ (PM. 631.39) Elemental analysis %: (calculated) found C (28.53) 27.33, H (4.31) 4.16, N (4.44) 4.23, S (10.16) 11.41. Color: yellow-green.

The characterization of this gold(III) derivative is still in progress.

[$Au^{III}Br_2$(dtc-Pro-Aib-O*t*Bu)] (AuD_{22})

This complexe was prepared by a similar method to that of the glycyl-methyl-ester-containing derivative. $K[AuBr_4].2H_2O$ (0.15 g, 0.25 mmol) reacted with a solution of HCl·Sar-Pro-O*t*Bu (0.15 g, 0.51 mmol), CS_2 (0.03 ml, 0.51 mmol) and NaOH (0.02 g, 0.51 mmol).

The characterization of this derivative is still in progress.

2.3.3 Gold(III)-tert-butyl-ester-containing-tripeptides derivatives

[$Au^{III}Br_2$(dtc-Sar-$(Aib)_2$-O*t*Bu)] (AuD_{13})

This complexe was prepared by a similar method to that of the glycyl-methyl-ester-containing derivative. $K[AuBr_4].2H_2O$ (0.15 g, 0.25 mmol) reacted with a solution of HCl·Sar-$(Aib)_2$-O*t*Bu (0.18 g, 0.51 mmol), CS_2 (0.03 ml, 0.51 mmol) and NaOH (0.02 g, 0.51 mmol).

Yield: 67 %.

M.p.: decomposes at 119.3 °C.

IR (KBr): 3403, 1719, 1688, 1558, 1509, 1218, 1146, 543, 384, 252 cm^{-1}.

^1H NMR (acetone-D_6, 300.13 MHz), δ/ppm: 7.90 [s, 1H, Aib^1 NH], 7.83 [s, 1H, Aib^2 NH], 4.73, 4.69 [2s, 2H, Sar α-CH_2 isomers], 3.55, 3.51 [2s, 3H, NCH_3 isomers], 1.53-1.48 [m, 6H, Aib^1 β-CH_3 isomers], 1.42 [s, 9H, $C(CH_3)_3$], 1.40 [s, 6H, Aib^2 β-CH_3].

^{13}C NMR (acetone-D_6, 75.48 MHz), δ/ppm: 199.35, 195.67 [CSS C], 175.56, 173.47 [Aib^1 carbonylic C isomers], 173.79 [Aib^2 carbonylic C], 163.53, 163.30 [Sar carbonylic C isomers], 80.48 [O*t*Bu quaternary C], 57.84, 56.39 [Aib^1 quaternary C isomers], 56.74 [Aib^2 quaternary C], 55.77, 54.85 [Sar secondary C isomers], 40.37, 39.40 [NCH_3 C isomers], 27.79 [$(CH_3)_3$ C], 24.79 [Aib^1 $(CH_3)_2$ C, Aib^2 $(CH_3)_2$ C].

$C_{16}H_{28}AuBr_2N_3O_4S_2$ (MW. 747.32) Elemental analysis %: (calculated) found C (25.71) 26.12, H (3.78) 3.66, N (5.62) 5.64, S (8.58) 8.73. Color: dark orange.

[$Au^{III}Cl_2$(dtc-Sar-$(Aib)_2$-O*t*Bu)] (AuD_{14})

This complexe was prepared by a similar method to that of the glycyl-methyl-ester-containing derivative. $K[AuCl_4].xH_2O$ (0.15 g, 0.40 mmol) reacted with a solution of HCl·Sar-$(Aib)_2$-O*t*Bu (0.28 g, 0.79 mmol), CS_2 (0.05 ml, 0.79 mmol) and NaOH (0.03 g, 0.79 mmol).

Yield: 62 %.

M.p.: -

IR (KBr): 3392, 1729, 1689, 1559, 1512, 1220, 1146, 1015, 543, 383, 340, 322 cm^{-1}.

^{1}H NMR (acetone-D_6, 300.13 MHz), δ/ppm: 7.88, 7.80 [2m, 1H, Aib^{1} NH isomers], 7.41, 7.31 [s, 1H, Aib^{2} NH isomers], 4.73 [m, 2H, Sar α-CH_2 isomers], 3.55 [m, 3H, NCH_3 isomers], 1.53-1.49 [m, 6H, Aib^{1} β-CH_3 isomers], 1.42 [s, 9H, $C(CH_3)_3$], 1.41 [s, 6H, Aib^{2} β-CH_3].

^{13}C NMR (acetone-D_6, 75.48 MHz), δ/ppm: 200.06, 195.07 [CSS C], 176.28, 173.79 [Aib^{1} carbonylic C isomers], 174.48 [Aib^{2} carbonylic C], 163.99 [Sar carbonylic C isomers], 81.24 [O*t*Bu quaternary C], 58.62, 57.16 [Aib^{1} quaternary C isomers], 57.47 [Aib^{2} quaternary C], 56.07 [Sar secondary C], 41.06, 40.62 [NCH_3 C isomers], 28.52 [$(CH_3)_3$ C], 26.42 [Aib^{1} $(CH_3)_2$ C, Aib^{2} $(CH_3)_2$ C].

$C_{16}H_{28}AuCl_2N_3O_4S_2$ (MW. 658.41) Elemental analysis %: (calculated) found C (29.19) 29.17, H (4.29) 4.48, N (6.38) 6.34, S (9.74) 9.92. Color: yellow-green.

[Au^{III}Br$_2$(dtc-Pro-(Aib)$_2$-O*t*Bu)] (AuD$_{20}$)

This complexe was prepared by a similar method to that of the glycyl-methyl-ester-containing derivative. $K[AuBr_4].2H_2O$ (0.10 g, 0.17 mmol) reacted with a solution of HCl·Pro-$(Aib)_2$-O*t*Bu (0.13 g, 0.34 mmol), CS_2 (0.02 ml, 0.51 mmol) and NaOH (0.01 g, 0.51 mmol).

Yield: 94 %.

M.p.: decomposes at 122.3 °C.

IR (KBr): 3410, 1728, 1685, 1662, 1546, 1227, 1147 cm^{-1}.

$C_{18}H_{30}AuBr_2N_3O_4S_2$ (PM. 773.35) Elemental analysis %: (calculated) found C (27.96) 27.24, H (3.91) 4.01, N (5.43) 5.50, S (8.29) 10.12. Color: orange.

The characterization of this gold(III) derivative is still in progress.

[Au^{III}Cl$_2$(dtc-Pro-(Aib)$_2$-O*t*Bu)] (AuD$_{21}$)

This complexe was prepared by a similar method to that of the glycyl-methyl-ester-containing derivative. $K[AuCl_4].xH_2O$ (0.20 g, 0.53 mmol) reacted with a solution of HCl·Pro-$(Aib)_2$-O*t*Bu (0.20 g, 0.53 mmol), CS_2 (0.03 ml, 0.53 mmol) and NaOH (0.02 g, 0.53 mmol).

Yield: 80 %.

M.p.: decomposes at 124.0 °C.

IR (KBr): 3407, 1730, 1685, 1542, 1228, 1147 cm^{-1}.

$C_{18}H_{30}AuCl_2N_3O_4S_2$ (PM. 684.45) Elemental analysis %: (calculated) found C (31.59) 31.01, H (4.42) 4.56, N (6.14) 6.06, S (9.37) 8.84. Color: yellow-green.

The characterization of this gold(III) derivative is still in progress.

2.3.4 Gold(III)-tert-butyl-ester-containing-tetrapeptide derivatives

[$Au^{III}Br_2$(dtc-Sar-$(Aib)_3$-O*t*Bu)] (AuD_{18})

This complexe was prepared by a similar method to that of the glycyl-methyl-ester-containing derivative. $K[AuBr_4].2H_2O$ (0.15 g, 0.25 mmol) reacted with a solution of HCl·Sar-$(Aib)_3$-O*t*Bu (0.22 g, 0.51 mmol), CS_2 (0.03 ml, 0.51 mmol) and NaOH (0.02 g, 0.51 mmol).

Yield: 92 %.

IR (KBr): 3399, 1720, 1682, 1653, 1560, 1533, 1219, 1147 cm^{-1}.

^1H NMR (acetone-D_6, 300.13 MHz), δ/ppm: 8.70-8.51, 7.53-7.48, 7.23-7.16 [3m, 1H, Aib^1 NH isomers; 1H, Aib^2 NH isomers; 1H, Aib^3 NH isomers], 4.90-4.82 [m, 2H, Sar α-CH_2 isomers], 3.59, 3.55 [2s, 3H, NCH_3 isomers], 1.46-1.39 [m, 6H, Aib^1 β-CH_3; 6H, Aib^2 β-CH_3; 6H, Aib^3 β-CH_3; 9H, $C(CH_3)_3$].

$C_{20}H_{35}AuBr_2N_4O_5S_2$ (MW. 832.42) Elemental analysis %: (calculated) found C (28.86) 28.66, H (4.24) 4.46, N (6.73) 6.60, S (7.70) 9.53. Color: orange.

The characterization of this gold(III) derivative is still in progress.

[$Au^{III}Cl_2$(dtc-Sar-$(Aib)_3$-O*t*Bu)] (AuD_{19})

This complexe was prepared by a similar method to that of the glycyl-methyl-ester-containing derivative. $K[AuCl_4].xH_2O$ (0.15 g, 0.40 mmol) reacted with a solution of HCl·Sar-$(Aib)_3$-O*t*Bu (0.35 g, 0.79 mmol), CS_2 (0.05 ml, 0.79 mmol) and NaOH (0.03 g, 0.79 mmol).

Yield: 84 %.

M.p.: decomposes at 145.3 °C.

IR (KBr): 3371, 1722, 1681, 1560, 1533, 1218, 1147 cm^{-1}.

^1H NMR (acetone-D_6, 300.13 MHz), δ/ppm: 8.61-8.38, 7.45-7.39, 7.23-7.16 [3m, 1H, Aib^1 NH isomers; 1H, Aib^2 NH isomers; 1H, Aib^3 NH isomers], 5.16-4.82 [m, 2H, Sar α-CH_2 isomers], 3.59 [m, 3H, NCH_3 isomers], 1.46-1.40 [m, 6H, Aib^1 β-CH_3; 6H, Aib^2 β-CH_3; 6H, Aib^3 β-CH_3; 9H, $C(CH_3)_3$].

$C_{20}H_{35}AuCl_2N_4O_5S_2$ (MW. 743.45) Elemental analysis %: (calculated) found C (32.31) 31.91, H (4.74) 5.17, N (7.54) 7.27, S (8.63) 8.20. Color: yellow-green.

The characterization of this gold(III) derivative is still in progress.

2.3.5 Gold(III)-ethyl-ester-containing-pentapeptide derivatives

[$Au^{III}Br_2$(dtc-Sar-$(Aib)_3$-Gly-OEt)] (AuD_{12})

This complexe was prepared by a similar method to that of the glycyl-methyl-ester-containing derivative. $K[AuBr_4].2H_2O$ (0.15 g, 0.25 mmol) reacted with a solution of HCl·Sar-$(Aib)_3$-Gly-OEt (0.22 g, 0.51 mmol), CS_2 (0.03 ml, 0.51 mmol) and NaOH (0.02 g, 0.51 mmol).

Yield: 82 %.

M.p.: decomposes at 106.2 °C

IR (KBr): 3343, 1728, 1661, 1553, 1216, 1099, 1028, 560, 383, 252, 227 cm^{-1}.

^{1}H NMR (acetone-D_6, 300.13 MHz), δ/ppm: 8.57, 8.46 [2s, 1H, Aib^1 NH isomers], 7.98, 7.94 [2s, 1H, Aib^2 NH isomers], 7.68 [m, 1H, Gly NH isomers], 7.20, 7.17[2s, 1H, Aib^3 NH isomers], 4.89, 4.84 [2s, 2H, Sar α-CH_2 isomers], 4.10 [q, 2H, Et CH_2], 3.87, 3.86 [2d, 2H, Gly α-CH_2 isomers], 3.59 3,54 [2s, 3H, NCH_3 isomers], 1.52 [s, 6H, Aib^3 β-CH_3], 1.43 [m, 6H, Aib^1 β-CH_3], 1.38 [m, 6H, Aib^2 β-CH_3], 1.22 [t, 3H, Et CH_3].

^{13}C NMR (DMSO, 75.48 MHz), δ/ppm: 200.32, 197.11 [CSS C], 176.39 [Aib^3 carbonylic C], 175.68 [Aib^1 carbonylic C], 174.42 [Aib^2 carbonylic C], 171.22 [Gly carbonylic C], 166.23, 165.84 [Sar carbonylic C isomers], 61.54 [OEt secondary C], 58.54 [Aib^3 quaternary C], 57.91 [Aib^2 quaternary C], 58.11 [Aib^1 quaternary C], 56.73, 55.66 [Sar secondary C isomers], 42.50, 42.17 [Gly secondary C isomers], 41.43, 40.37 [NCH_3 C], 26.66 [Aib^3 $(CH_3)_2$ C], 26.06 [Aib^2 $(CH_3)_2$ C], 25.45 [Aib^1 $(CH_3)_2$ C], 14.97 [OEt primary C] .

$C_{20}H_{34}AuBr_2N_5O_6S_2$ (MW. 861.42) Elemental analysis %: (calculated) found C (27.89) 23.55, H (3.98) 3.54, N (8.13) 6.86, S (7.44) 9.66 . Color: orange.

[$Au^{III}Cl_2$(dtc-Sar-$(Aib)_3$-Gly-OEt)] (AuD_{15})

This complexe was prepared by a similar method to that of the glycyl-methyl-ester-containing derivative. $K[AuCl_4].xH_2O$ (0.15 g, 0.40 mmol) reacted with a solution of HCl·Sar-$(Aib)_3$-Gly-OEt (0.34 g, 0.79 mmol), CS_2 (0.05 ml, 0.79 mmol) and NaOH (0.03 g, 0.79 mmol).

Yield: 67 %.

M.p.: decomposes at 126.9 °C

IR (KBr): 3340, 1728, 1657, 1557, 1216, 1101, 1028, 562, 382, 338, 322 cm^{-1}.

^{1}H NMR (acetone-D_6, 300.13 MHz), δ/ppm: 8.45 [m, 1H, Aib^1 NH isomers], 7.87 [m, 1H, Aib^2 NH isomers], 7.67 [m, 1H, Gly NH isomers], 7.19[m, 1H, Aib^3 NH isomers], 4.85 [m, 2H, Sar α-CH_2 isomers], 4.10 [m, 2H, Et CH_2], 3.86 [2d, 2H, Gly α-CH_2 isomers], 3.59 [m, 3H, NCH_3

isomers], 1.51 [m, 6H, Aib^3 β-CH_3], 1.48 [m, 6H, Aib^1 β-CH_3], 1.37 [m, 6H, Aib^2 β-CH_3], 1.22 [m, 3H, Et CH_3].

^{13}C NMR (DMSO, 75.48 MHz), δ/ppm: 200.35, 195.70 [CSS C], 176.37 [Aib^3 carbonylic C], 175.60 [Aib^1 carbonylic C], 174.42 [Aib^2 carbonylic C], 170.90 [Gly carbonylic C], 165.67 [Sar carbonylic C], 61.52 [OEt secondary C], 58.56 [Aib^1 quaternary C], 58.24 [Aib^2 quaternary C], 57.94 [Aib^3 quaternary C], 55.94 [Sar secondary C], 42.34 [Gly secondary C], 40.88 [NCH_3 C], 26.55 [Aib^3 $(CH_3)_2$ C], 26.04 [Aib^2 $(CH_3)_2$ C], 25.48 [Aib^1 $(CH_3)_2$ C], 14.92 [OEt primary C] .

$C_{20}H_{34}AuCl_2N_5O_6S_2$ (MW. 772.52) Elemental analysis %: (calculated) found C (31.10) 30.71, H (4.44) 4.52, N (9.07) 8.94, S (8.30) 7.24. Color. Yellow-green.

CHAPTER III. RESULTS AND DISCUSSION

3.1 PEPTIDE SYNTHESIS AND CONFORMATIONAL STUDIES

3.1.1 Peptide design

Given the synthetic target previously outlined (see chapter 1.), to achieve the goal some prerequisites were necessary in the synthesis design:

- ✓ Identify the convenient amino acid residues and esters for the preparation of sequential peptides that could favour membrane permeability and influence the biological response through their conformational behaviour.
- ✓ Devise efficient strategies for the peptide synthesis, in particular concerning the choice of the reaction phase, of suitable protecting groups and activation protocols.

Since the decisions taken about each point were conditioning the subsequent steps, in the next sections one point at a time will be addressed.

3.1.1.1 Choice of the amino acids and esters

The identification of the amino acids and esters was done gradually moving from di- to pentapeptides. We chose to keep a sarcosine (Sar) residue (**Scheme 3.1**) at position 1, where the dithiocarbamate group has to be linked, as this amino acid is present in the very active, antitumor Au(III)-dithiocarbamate-Sar complex, discovered by Fregona and coworkers.[167]

For the dipeptides of general formula HCl·Sar-Xxx-OR, we chose as Xxx Gly, Aib, Phe and Ser (**Scheme 3.1**). Gly is the simplest, achiral, protein amino acid that could favour the flexibility, if required by the final Au(III) complex. On the contrary, the also achiral C^{α}-tetrasubstitued amino acid Aib, natural but non-coded, confers conformational rigidity to the final molecule. Thus, Gly and Aib allow for an evaluation of the influence of flexibility and rigidity on the bioactivity. The chiral amino acids Phe and Ser were instead chosen to evaluate the hydrophilicity/hydrophobicity importance.

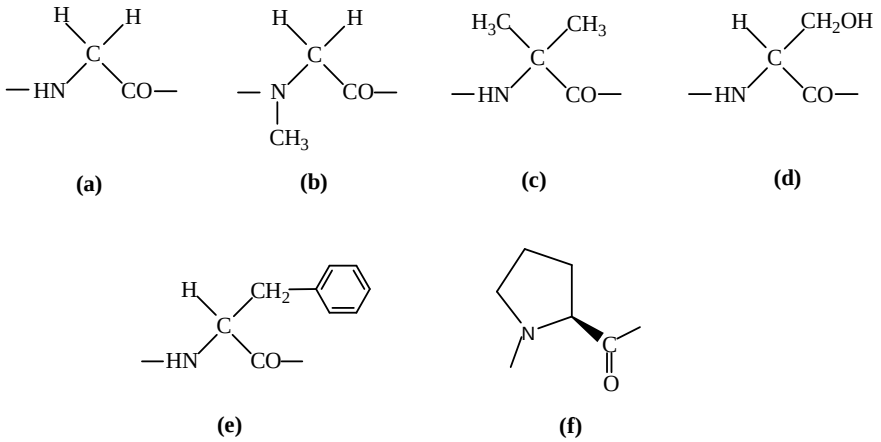

Scheme 3.1 Chemical structures of the amino acids Gly **(a)**, Sar **(b)**, Aib **(c)**, Ser **(d)**, Phe **(e)** and Pro **(f)**.

The methyl, ethyl and *tert*-butyl esters (**Scheme 3.2**) were chosen as C-protecting groups (*i.e.* COOR) to assess the eventual influence of this part of the molecule on the anticancer activity: the methyl has least steric hindrance and favours water solubility, whereas the bulky *tert*-butyl group has opposite features. It is important to mask the carboxylic function, since it has been previously shown the COOH-containing derivatives are not active.[155] To avoid possible reactions between the hydroxyl group of the Ser side chain and the dithiocarbamate moiety in the subsequent reaction, the *t*Bu ether was chosen as O-protecting group in the HCl·Sar-Ser(*t*Bu)-O*t*Bu dipeptide. This choice turned out to be useful to verify whether a very hydrophobic ligand (two *t*Bu groups) would be beneficial to the biological behaviour of the Au(III) complexe. Indeed, we subsequently discovered that the -O*t*Bu ester is much better than the –OMe ester in terms of antitumor activity.

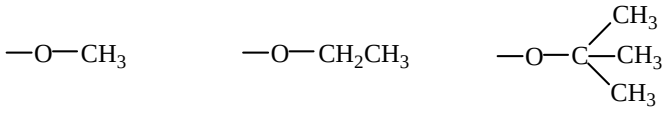

Scheme 3.2 Chemical structure of C-protecting groups used: methyl **(a)**, ethyl **(b)** and *tert*-butyl **(c)** esters.

The tri- and tetrapeptides were designed as HCl·Sar-$(Aib)_n$-O*t*Bu (n= 2, 3) to see if, knowing the Aib antimicrobial and conformational properties, the presence of more residues could increase the anticancer activity.

In the pentapeptide HCl·Sar-$(Aib)_3$-Gly-OEt, the Gly residue and ethyl ester were chosen to reduce the hydrophobicity of the molecule, while maintaining the properties of a longer peptides and avoiding the introduction of chirality in the molecule.

Finally, as proline (Pro) is the only protein *N*,*N*-disubtituted residue, as Sar, but in addition it is chiral, we decided to synthesize also the peptides HCl·Pro-$(Aib)_n$-O*t*Bu (n= 2, 3) to compare the bioactivity of the corresponding Au(III)-dithiocarbamato derivatives to that of the Sar-containing analogues.

Concerning the configuration of the chiral amino acids, the L- residues were used as they are those of the protein pool.

3.1.1.2 Synthetic strategy

For the peptides herein described, the solution phase synthesis seemed the most appropriate: indeed, the reduced reactivity of the hindered amino acids generally makes couplings on solid phase sluggish. Normally, the solution phase synthesis of a peptide is done by stages (*step by step*), *i.e.* adding the amino acids one by one, starting from the C-terminal residue conveniently protected at the carboxylic function. This strategy allows to minimize the risks of racemisation, as the amino acid added to the peptide N-terminus are protected with an uretanic function, known to impart resistance to racemisation. However, this synthetic approach needs long times to complete the synthesis of polypeptides, unless relatively short ones (as our di-, tri- and tetrapeptides) have to be prepared.

An effective alternative is the *segment condensation* strategy. This approach generally allows to obtain larger quantities of final products, while speeding up the synthesis, and it can be used for parallel synthesis. In addition, the products can be easily isolated since they significantly differ from reagents by means of their molecular weight, and consequently by their physico-chemical properties.

The synthetic strategy adopted to obtain the pentapeptide is a compromise between the sequential approach and the *segment condensation*.

3.1.1.3 Choice of suitable protecting groups

Generally speaking, the functions that require protection in peptide synthesis are the N-terminal amino and C-terminal carboxyl group, as well as functional groups at the side chains. The ideal conditions are satisfied when *orthogonal* protecting groups are employed:[226] two protecting groups are fully orthogonal if either group can be removed under conditions which do not compromise the stability of the other; partial orthogonality refers to the case that only one can be removed without causing removal of the other.

Consequently, for the synthesis of methyl ester containing dipeptides, the *tert*-butyloxycarbonyl (Boc)[220] was used as α-amino protecting group, since this C-protecting group is base-labile. The Boc group is removed in acidic conditions.

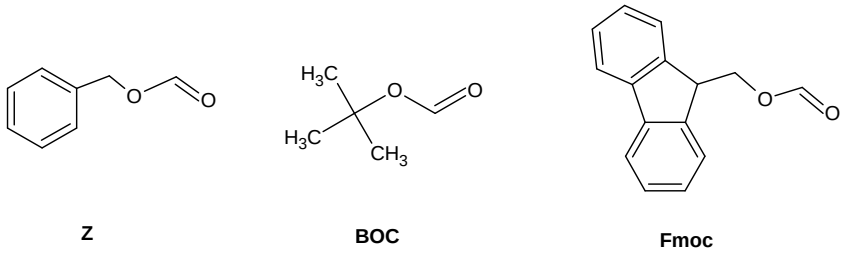

Z **BOC** **Fmoc**

Scheme 3.3 α-amino protecting groups Z, left; Boc, middle; Fmoc, right.

For the protection of the *tert*-butyl ester containing peptides, the benzyloxycarbonyl (Z) protecting group was used for the α-amino moiety. The three main advantages of the use of this group are: (i) the good physical and chemical stability of Z-protected peptides, (ii) the ease of deprotection by catalytic hydrogenolysis, forming volatile co-products, which are smoothly eliminated by evaporation and (iii) the increased tendency to precipitation and even to crystallization of pure protected peptides.

As the hydroxy group of the Ser side chain could also react with acylating agents used for the synthesis, it was necessary to protect it. For the synthesis of the methyl ester Ser-containing dipeptide, the commercially available Z-Ser(*t*Bu)-OH (*tert*-butyl ether protecting group) and Boc-Ser(Bzl)-OH (benzyl ether protecting group) were used. The benzyl group was removed simultaneously with the Z group presented in the dipeptide by catalytic hydrogenolysis. The *tert*-butyl was cleaved simultaneously with the Boc group by a 1:1 CH_2Cl_2/TFA mixture. For the synthesis of *tert*-butyl ester Ser-containing dipeptide, the Fmoc (9-fluorenylmethoxycarbonyl) protection was required, as this α-amino protecting group is orthogonal to both the Bzl and *tert*-butyl ester groups. Thus, the commercially available Fmoc-Ser(Bzl)-OH was used. The Fmoc group was cleaved with a 30% DEA/CH_2Cl_2 solution.

3.1.2 Peptides synthesis

3.1.2.1 Coupling methods

Several coupling methods were used for the peptides synthesis. For the introduction of the differently protected Sar or the Z-protected Pro in the di- and tripeptides, the isochloroformiate method, which proceed *via* mixed anhydrides (**Scheme 3.4**)[224] was used.

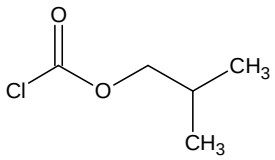

Scheme 3.4 Isochlorofomate structure.

Three decades of research on C^{α}-tetrasubstituted amino acid containing peptides have provided our laboratory with a strong know-how about the activation of hindered, C^{α}-tetrasubstituted residues.[221] The two most common and powerful activation methods are the *in situ* formation of active esters (*via* EDC/HOAt[227], **Scheme 3.5**, left and middle) and the use of preformed symmetric anhydrides (**Scheme 3.5**, right).

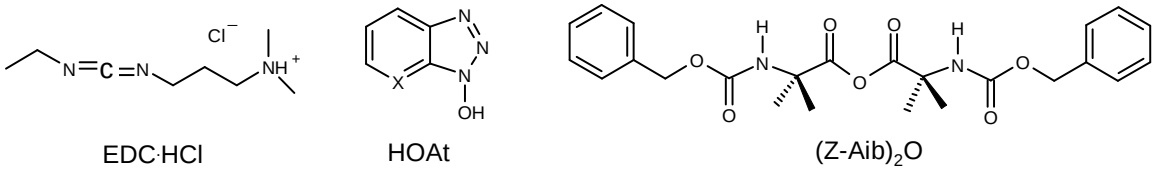

Scheme 3.5 *Coupling reagents* (EDC·HCl, left; HOAt, X=N, HOBt, X=CH, middle) for the formation of active esters and symmetric anhydride derived from Z-Aib-OH (right).

The use of HOAt efficiently suppresses racemisation due to carbodiimide overactivation,[227] and the side products deriving from the coupling reagents can be eliminated by acidic or basic washing. However, the unreacted active ester is not completely hydrolyzed or eliminated by washing and often chromatographic purification is necessary. The HOAt catalytic effect is due to the assistance that the nitrogen atoms at position 2 and 7 of its structure give to the amino group.

On the contrary, couplings *via* symmetric anhydride form a smaller number of side products, resulting in a simpler work-up, but they require more steps (anhydride synthesis and purification, coupling, sometimes N-protected amino acid recovery). Indeed, 2 equivalent of N-protected amino acid are required in order to generate 1 equivalent of acylating agent, and 1 equivalent of amino acid salt is formed after the coupling, thus making the amino acid recovery necessary when working with large amounts or valuable compounds.

The active ester coupling method was therefore used for the activation of Sar in the tetra- and pentapeptide synthesis, but the less expensive HOBt[228] (**Scheme 3.5**, middle) was used instead of HOAt. The activation as symmetric anhydride was often employed for Aib in the Aib homopeptides synthesis.

In the pentapeptide synthesis, the *segment condensation* was obtained through the C-terminal carboxylic function activation as 5(4*H*)-oxazolone(**Scheme 3.6**). This heterocycle is a

mild acylating agent. Nevertheless, by extending the reaction time at the solvent (THF) boiling point, we obtained a good yield, greater than 80%.[229-231]

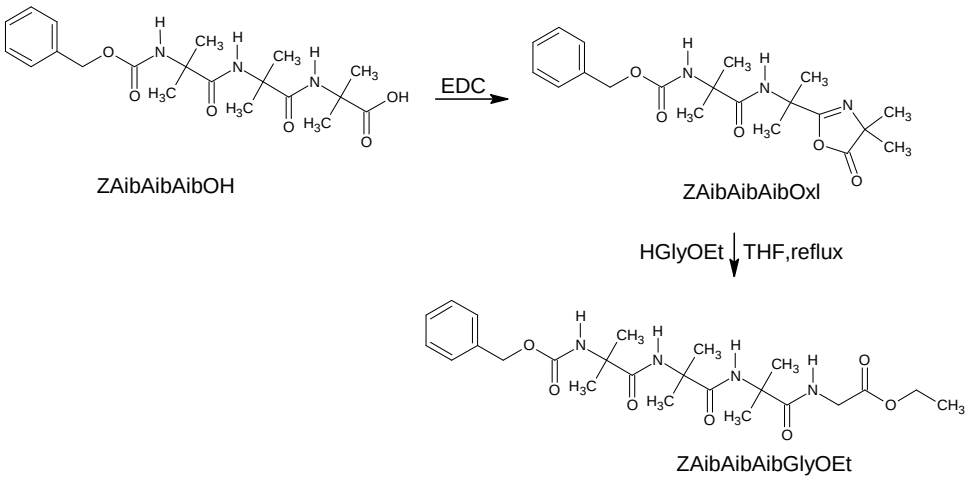

Scheme 3.6 Coupling via 5(*4H*)-oxazolone.

3.1.2.2 Synthesis of methyl and *tert*-butyl ester containing dipeptides

The methyl ester containing dipeptides were synthesized using the synthetic strategy illustrated in the **Scheme 3.7**.

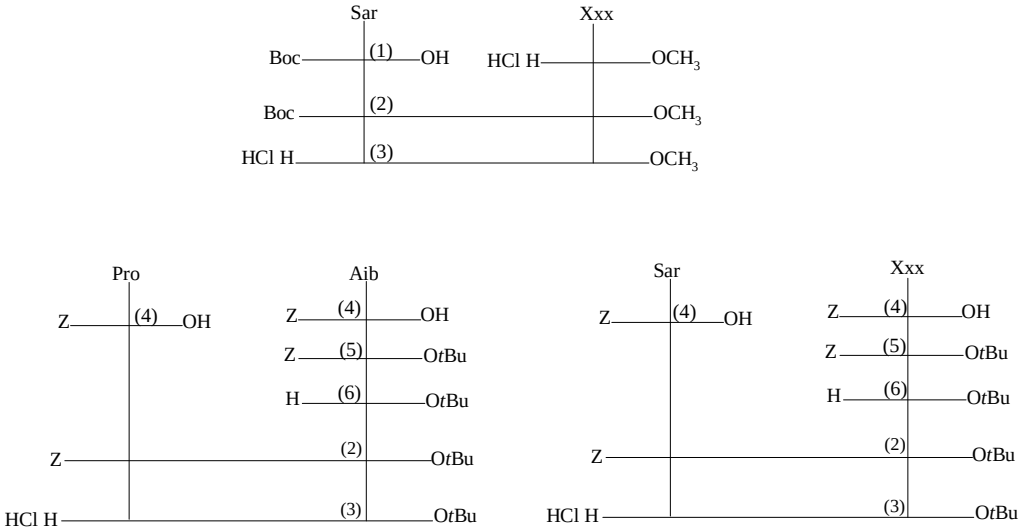

Scheme 3.7 Synthetic strategy of methyl and *tert*-butyl esters containing peptides: HCl·H-Sar-Xxx-OMe (top), HCl·H-Pro-Aib-O*t*Bu (left); and HCl·H-Sar-Xxx-O*t*Bu (right) (Xxx= Gly, Aib, Phe). (1) 1N NaOH, Boc_2O, dioxane, H_2O; (2) NMM, $ClCOOCH_2CH(CH_3)_2$, THF, $CHCl_3$; (3) HCl/Et_2O, (4) ZOSu, TEA, CH_3CN e H_2O; (5) $(CH_3)_2C=CH_2$ in CH_2Cl_2, H_2SO_4 cat.; (6) Pd/C 10%, H_2, MeOH.

The synthesis of the *tert*-butyl ester dipeptides series was more complex than that of the methyl ester. In fact, to prepare H-Xxx-O*t*Bu (Xxx = Gly, Aib, Phe), to be coupled with Z-Sar-OH or Z-Pro-OH, it was necessary to: (i) protect the amine function with the Z group, (ii) form the *tert*-butyl ester through an acid-catalyzed reaction with isobutene (**Scheme 3.8**) and (iii) remove the Z group.

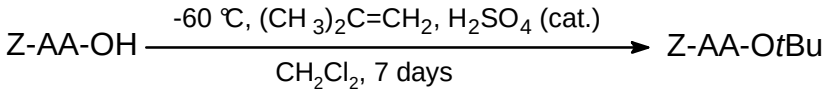

Scheme 3.8 The acid-catalyzed reaction of Z-AA-OH (AA= Aib, Phe) with isobutene.

The dipeptides Z-Sar-Xxx-O*t*Bu (Xxx = Gly, Aib, Phe) were obtained by the condensation of Z-Sar-OH, with H-Xxx-O*t*Bu (obtained by the catalytic hydrogenation of the related Z-protected derivative). Z-Pro-Aib-O*t*Bu was obtained in a similar way. Finally, the catalytic hydrogenation with Pd on charcoal led to H-Sar-Xxx-O*t*Bu that was successively transformed to its hydrochloride through a cautious addition of one HCl equivalent (in diluted diethyl ether solution). This procedure allowed us to avoid *tert*-butyl ester acidolysis. In general, with the *tert*-butyl esters the yields were greater than with the methyl ester analogues and there were less impurities.

3.1.2.3 Synthesis of serine containing dipeptides

Scheme 3.9 illustrates the synthetic strategy of the serine containing dipeptides herein discussed.

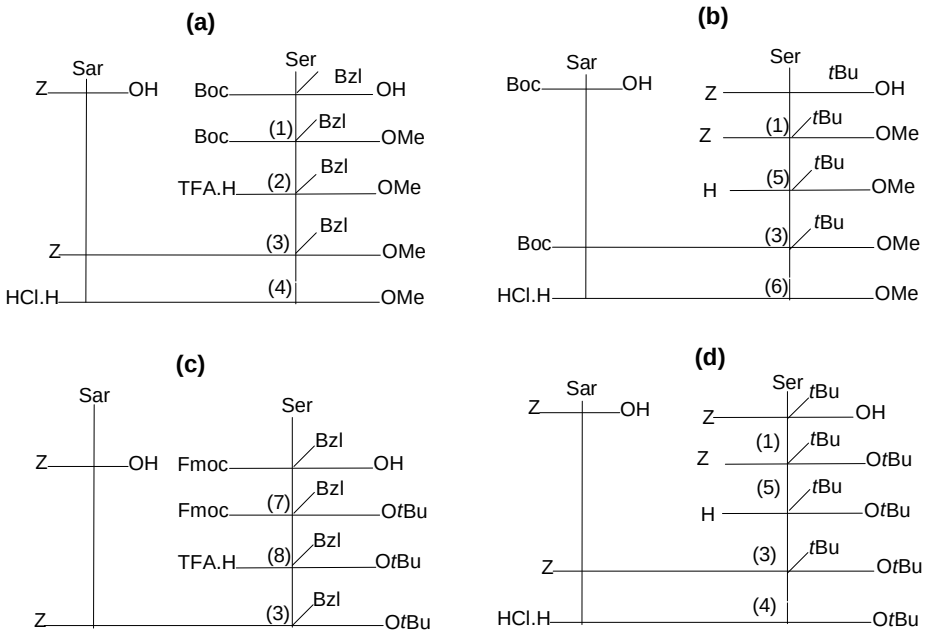

Scheme 3.9 Synthetic strategies followed for the syntheses of HCl·H-Sar-Ser-OMe (a) and (b), HCl·H-Sar-Ser-O*t*Bu (c) and HCl·H-Sar-Ser(*t*Bu)-O*t*Bu (d). (1): CH_2Cl_2, 0 °C, DMAP, ROH (R= Me, *t*Bu), EDC; (2): CH_2Cl_2/TFA; (3): NMM, $ClCOOCH_2CH(CH_3)_2$, THF e $CHCl_3$; (4): Pd/C 10%, H_2, MeOH, HCl/Et_2O; (5): Pd/C 10%, H_2,CH_2Cl_2; (6): CH_2Cl_2/TFA , HCl/Et_2O; (7): $(CH_3)_2C=CH_2$, CH_2Cl_2, H_2SO_4; (8): DEA/CH_2Cl_2 30 %.

The synthesis of HCl·H-Sar-Ser-OMe was done with two different synthetic methods. In the first method, to synthesize H-Ser(*t*Bu)-OMe, subsequently coupled to Boc-Sar-OH, the Z-Ser(tBu)-OH methyl ester was initially formed, by reaction with MeOH in the presence of DMAP and EDC· HCl, followed by the hydrogenolysis of the Z-group. In the second method, it was required to synthesize TFA·H-Ser(Bzl)-OMe to be coupled with Z-Sar-OH. Thus, Boc-Ser(Bzl)-OH methyl ester was initially formed as previously described for Z-Ser(tBu)-OH, followed by the acidolysis of the Boc group using TFA. The peptides Boc-Sar-Ser(*t*Bu)-OMe and Z-Sar-Ser(Bzl)-OMe were obtained by the condensation of Boc-Sar-OH with H-Ser(*t*Bu)-OMe and Z-Sar-OH with TFA·H-Ser(Bzl)-OMe, respectively, mediated by isobutylchloroformate. The catalytic hydrogenolysis of Z-Sar-Ser(Bzl)-OMe was followed by the salification of the resulting H-Sar-Ser(Bzl)-OMe derivative with a saturated solution of HCl in diethylether. The reaction of Boc-Sar-Ser(*t*Bu)-OMe with TFA (diluited in CH_2Cl_2) led to TFA·H-Sar-Ser-OMe, that was treated with the saturated solution of HCl in diethylether to form the hydrochloride. This second method resulted to be more efficient because of the reduced number of steps, the greater yields and the reduced number of impurities.

H-Ser(*t*Bu)-O*t*Bu to be coupled with Z-Sar-OH in the syntesis of Z-Sar-Ser(*t*Bu)-O*t*Bu in a similar manner as described for H-Ser(*t*Bu)-OMe, but the yield of the esterification was lower, probably due to the sterical hindrance of the *tert*-butyl group.

Concerning the synthesis of Z-Sar-Ser(Bzl)-OtBu, Fmoc-Ser(Bzl)-O*t*Bu was first prepared from the commercially available Fmoc-Ser(Bzl)-OH. Then, the Fmoc group was removed with a 30 % solution of DEA in CH_2Cl_2, purified by *flash* chromatography, and coupled to Z-Sar-OH by the isobutylchloroformate method. The cleavage of the benzyl group on the side chain resulted to be very difficult, whereas the Z group was removed in 45 min.

3.1.2.4 Synthesis of the Sar and Pro tripeptides

As already mentioned, the C^{α}-tetrasubstituted α-amino acids are little reactive in peptide bond formation because of their steric hindrance at the C^{α}. This negative influence is of greater intensity on the amino group as compared to the carboxylic group. Thus, for the synthesis of Z-$(Aib)_2$-O*t*Bu the condensation via an efficient acylating agent as the symmetric anhydride $(Z\text{-}Aib)_2O$ was chosen (**Scheme 3.10**).

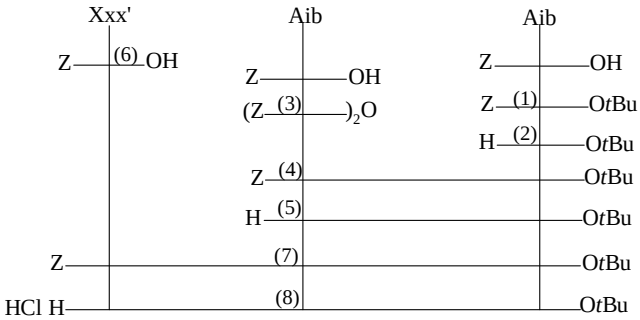

Scheme 3.10 Synthetic strategy followed for the preparation of the tripeptides HCl·H-Xxx-Aib-Aib-O*t*Bu (Xxx= Sar, Pro). (1): $(CH_3)_2C{=}CH_2$ in CH_2Cl_2, H_2SO_4 cat.; (2) H_2, Pd/C in CH_2Cl_2; (3): ½ equiv. EDC; (4): NMM; (5): H_2, Pd/C in MeOH; (6): ZOSu, TEA, Xxx'= Sar; (7): NMM, $ClC(O)OCH_2CH(CH_3)_2$; (8) H_2, Pd/C, HCl/Et_2O, Xxx= Sar; (8'): H_2,Pd/C, HCl/MeOH, Xxx= Pro.

The synthesis of the tripeptides HCl·H-Xxx'-Aib_2-O*t*Bu (Xxx'= Sar, Pro) was done by condensing Z-Sar-OH and Z-Pro-OH with H-Aib_2-O*t*Bu by means of the isobutylchloroformate method, as discussed for the HCl·Sar-Xxx-O*t*Bu dipeptides (Xxx= Gly, Aib, Phe). The yields were moderate as compared to those of the dipeptides.

3.1.2.5 Synthesis of the Sar-containing tetra- and pentapeptide

The synthetic strategy of the tetra- and pentapeptide herein discussed are reported on **Scheme 3.11**.

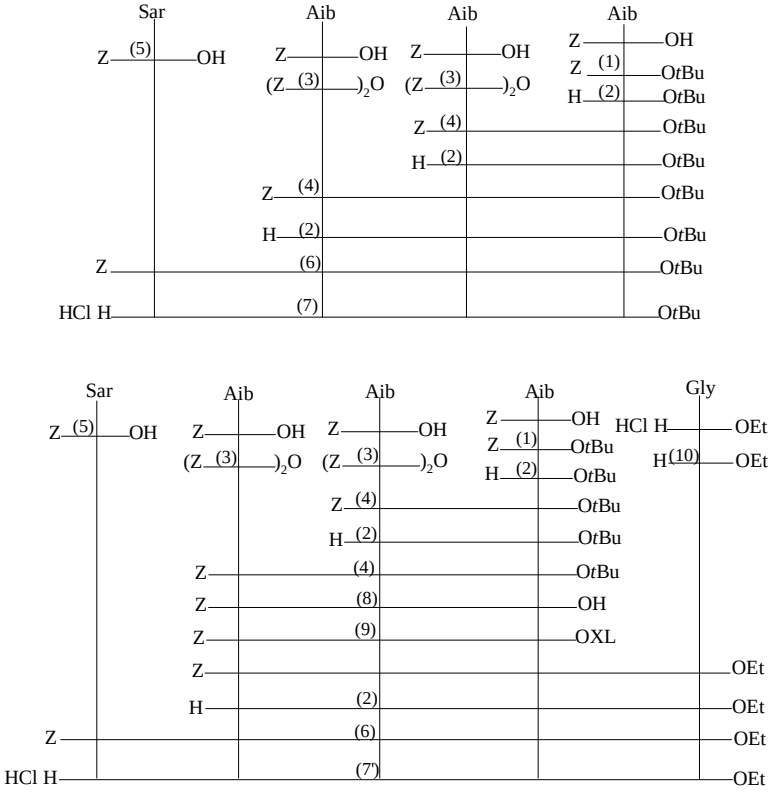

Scheme 3.11 Synthetic strategy of HCl·H-Sar-Aib$_3$-O*t*Bu up and HCl·H-Sar-Aib$_3$-Gly-OEt down. (1): $(CH_3)_2C{=}CH_2$ in CH_2Cl_2, H_2SO_4 cat.; (2): H_2, Pd/C; (3): ½ equiv. EDC; (4): NMM; (5): ZOSu, TEA, Xxx= Sar; (6): HOBt, EDC, NMM; (7): H_2, Pd/C in MeOH, HCl/Et_2O; (7'): H_2, Pd/C in EtOH, HCl/Et_2O; (8): TFA; (9): EDC; (10): $NaHCO_3$.

The Z-(Aib)$_3$-Gly-OEt tetrapeptide was obtained by activating Z-(Aib)$_3$-OH as 5(4*H*)-oxazolone and refluxing it in acetonitrile in the presence of H-Gly-OEt. The reaction yield was good, greater than 80%.[229-231]

For the preparation of Z-Sar-Aib$_3$-O*t*Bu and Z-Sar-Aib$_3$-Gly-OEt, Z-Sar-OH was introduced with reasonable yields on the C-terminal tri- and tetrapeptide segments by activation *via* EDC/HOBt. The catalytic hydrogenolysis of Z-Aib$_3$-Gly-OEt and Z-Sar-Aib$_3$-Gly-OEt was carried out in EtOH, rather than in the commonly used MeOH, to avoid any risk of transesterification.

3.1.3 Infrared absorption spectroscopy

The Aib-containing tri-, tetra- and pentapeptides are long enough to adopt secondary structures. Therefore, an IR absorption study was performed in deuterochloroform, a low-polarity solvent often employed for conformational studies on peptides. The two frequency intervals richest in conformational information are:[232]

(i) 3550-3200 cm^{-1} (*Amide A band*), related to the stretching vibrations of the N-H bonds belonging to the urethane and amide groups;

(ii) 1800-1600 cm^{-1} (*Amide I band*), related to the stretching vibrations of the C=O bonds of the ester, urethane and amide groups.

The presence of an H-bond between a donor (*e.g.* the amide N-H) and an acceptor (*e.g.* the amide C=O group) modifies the bond strength constant of both groups involved, causing an alteration of their *bending* and *stretching* vibration frequencies. Under the harmonic approximation for the oscillators, vibration frequencies are given by the Hooke's law:

$$\nu_{vibr} = \frac{1}{2\pi c} \cdot \sqrt{\frac{k}{\mu}}$$

where : ν_{vibr} = vibration frequency

c = speed of light

k = bond strength constant

μ = reduced mass $[(m_1 \cdot m_2)/(m_1+m_2)]$

More precisely, a general displacement to lower vibration frequencies (*red shift*) is observed, with formation of more intense and broader bands, when an H-bond is present. From the experimental observation of this phenomenon it is possible to obtain information on the presence of NH groups engaged in hydrogen bonds or exposed to the solvent (the so-called 'free NHs').

Indeed, it is generally assumed that in deuterochloroform solvated NH groups resonate at wavenumbers higher than 3400 cm^{-1}, whereas H-bonded NHs resonate at lower wavelengths.[233,234]

Moreover, it is possible to discriminate between *intra*- and *inter*-molecular hydrogen bonds through the analysis of the variation of the relative intensity of the bands of the bonded and 'free' NHs as the concentration is changed, since *intra*molecular H-bonds are insensitive to dilution, whereas *inter*molecular H-bonds are favoured at higher concentrations. In turn, the discrimination between *inter*- and *intra*molecular hydrogen bonds gives hints about the conformation of the peptide in solution.

The discrimination between solvated and hydrogen-bonded NH groups is possible only in solvents of low polarity, such as chloroform, which do not alter the position of the bands of the solvent exposed NHs. On the contrary, more polar solvents can form hydrogen bonds with the amide NHs and shift their absorption bands close to the region where the bands of the NHs bound to the peptide CO groups are found. Therefore, in high polarity solvents, it is very difficult to discriminate between solvated and bonded NH groups. Consequently, because the peptide hydrochlorides were not soluble in deuterochloroform, their conformational analysis was not possible with this technique.

The amide A region of the IR absorption spectra of Z-Sar-Aib$_n$-O*t*Bu (n= 1, 2, 3) and Z-Sar-Aib$_3$-Gly-OEt at the concentration 1x10^{-3} M is shown in **Fig. 3.1**. The related absorption maxima frequencies are summarized in **Tab. 3.1**.

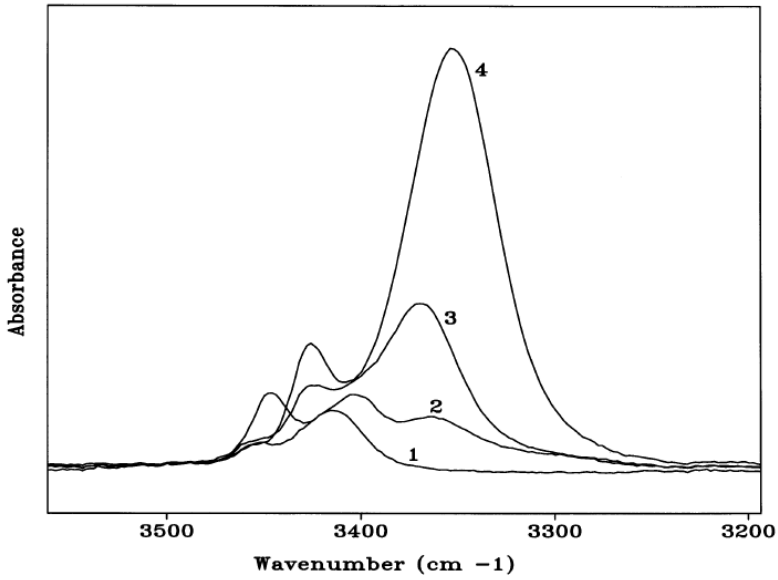

Figure 3.1 Amide A region of the IR absorption spectra of (1) Z-Sar-Aib-O*t*Bu, (2) Z-Sar-Aib$_2$O*t*Bu, (3) Z-Sar-Aib$_3$-O*t*Bu and (4) Z-Sar-Aib$_3$-Gly-OEt in $CDCl_3$ at 1x10^{-3} M concentration.

Peptide	3600-3200 cm^{-1}	1800-1600 cm^{-1}
Z-Sar-Aib-O*t*Bu	3448, 3414[b]	1728, 1712[a], 1672, 1660, 1642, 1624
Z-Sar-Aib$_2$-O*t*Bu	3456, 3426, 3402, 3362	1728[a], 1712, 1688, 1662, 1626[b]
Z-Sar-Aib$_3$-O*t*Bu	3458, 3428, 3402, 3368	1726, 1688, 1662, 1624[b]
Z-Sar-Aib$_3$-Gly-OEt	3458, 3428, 3402, 3352[b]	1746, 1728[a], 1714, 1682[b], 1654[a], 1618[a]

Notes: [a] shoulder, [b] broad band; underlined values refer to weak (. .) or strong (__) bands; values not underlined are referred to bands of intermediate intensity.

Table 3.1 IR absorption frequencies (cm^{-1}) of the previous peptides in $CDCl_3$ at 1x10^{-3} M concentration.

To ascertain whether the observed bands of bound NHs in the spectra were due to *inter*molecular or *intra*molecular interactions, three measurements were done at different concentrations on Z-Sar-Aib$_3$-Gly-OEt, as, being the longest peptide, is the one which has the highest probability to self-aggregate. Its IR absorption spectra at three different concentrations ($1\cdot10^{-2}$, $1\cdot10^{-3}$, $1\cdot10^{-4}$ M) in the 3400-3200 cm^{-1} region are reported in **Fig. 3.2**. These spectra are normalized, since tenfold dilutions are compensated by tenfold increases of cell path length (0.1, 1.0 and 10mm for $1\cdot10^{-2}$, $1\cdot10^{-3}$ and $1\cdot10^{-4}$ M concentrations respectively).

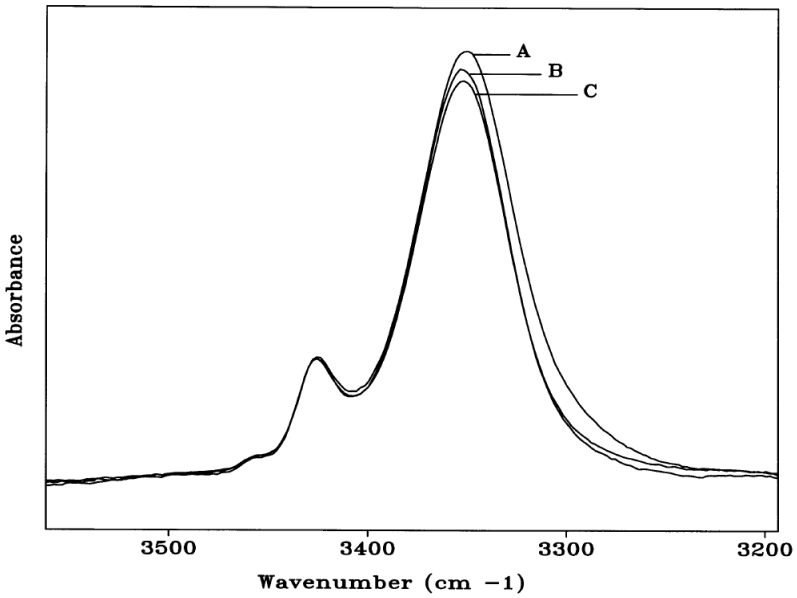

Figure 3.2 Amide A region of the IR absorption spectra of Z-Sar-Aib$_3$-Gly-OEt in $CDCl_3$ at concentrations 1x10^{-2} M (A), 1x10^{-3} M (B) e 1x10^{-4} M (C).

In **Fig. 3.1** and **Tab. 3.1** it can be observed that the band due to bound NHs appears only from the tripeptide spectrum (at 3362 cm^{-1}). In the pentapeptide spectrum, this band is at 3352 cm^{-1} and results to be very strong. This behaviour is typical of a peptide with an helical structure, that begins to fold in a β-turn at the level of the tripeptide. The presence of three Aib residues in the pentapeptide Z-Sar-Aib$_3$-Gly-OEt induces us to believe that it forms a 3_{10}-helix, stabilized by three intramolecular H-bonds. Dilution effects are unnoticeable for this peptide, in particular going from $1\cdot10^{-3}$ to $1\cdot10^{-4}$ M. Therefore *inter*molecular H-bonds are negligible, while the intense band centred at 3352 cm^{-1} can be assigned to *intra*molecular. The same conclusions can be extended to the tri- and tetrapeptide, since shorter peptides of a same series, in general, have a smaller propensity to self-associate.

In the 1730-1710 cm^{-1} region (**Tab. 3.1**), the bands related to the stretching of the uretanic and esters (tert-butylic) carbonyl group appear. The absorption of the peptide carbonyl group (amide I band) falls in the range 1690-1610 cm^{-1}.[234,235] In the Z-Sar-Aib_3-Gly-OEt spectrum, the absorption maximum of the amide I band is localized at around 1682 cm^{-1}. This maximum is closed to the amide I band position in type III β-turn structures, as expected for an Aib-rich peptide,[236] and it seems to confirm that these three peptides tend to have an helical structure.

3.1.4 NMR spectrometry

NMR conformational investigation was performed on the longest peptide, Z-Sar-Aib_3-Gly-OEt, to compare its outcome with the results obtained by means of IR absorption. The presence of three Aib residues suggests that this pentapeptide is likewise folded in a 3_{10}-helical structure. It is not yet clear if a well-defined secondary structure in a peptide ligand would be beneficial for the antitumor activity of a Au(III) complex. An answer will soon come from the biological tests currently under way.

The conformational analysis by ^{1}H-NMR spectrometry was performed in $CDCl_3$, the same solvent used for the IR characterization.

Working in $CDCl_3$ solution allows one to obtain useful information on the H-bonding stabilization of peptide amide NHs, which is easily related to the peptide conformation. This can be done by adding increasing amounts of the good H-bond acceptor dimethylsulfoxide (DMSO)[237] to a peptide in $CDCl_3$ solution. Indeed, the amide protons which are exposed to the solvent are stabilized by H-bond formation with DMSO molecules. This, in turn, causes a downfield shift of their signals. On the other side, amide protons already engaged in stable H-bonds are solvent-shielded and their chemical shift is little affected by the variation in the solvent composition. Consequently, it is expected that NH protons whose NMR signals do not change significantly by DMSO addition are stabilized by *intra*molecular H-bonds, unless there are reasons to believe that very strong intermolecular interactions are present.

If the NH signals in the monodimensional ^{1}H-NMR spectrum have been identified and assigned, it is therefore possible, by using the method described above, to know which NH groups are involved in *intra*molecular H-bonds. This is an advantage compared to the analysis by IR spectroscopy, which allows an estimation of the fraction of *intra*molecularly H-bonded NHs, but not their identification (see Section 3.1.2).

The assignment of 1D ^{1}H-NMR spectra of small peptides can be tentatively performed by inspection and comparison with already assigned spectra of similar compounds. For a complete

and correct assignment, however, the best way is to rely on the information obtained by two-dimensional (2D) spectra.

Two kinds of 2D NMR experiments have been performed on Z-Sar-Aib$_3$-Gly-OEt , each offering different and complementary information: TOCSY experiments,[238] that allow the identification of spin systems (i.e. groups of nuclei connected by scalar coupling relations) and ROESY experiments,[239] that are instead sensitive to the spatial proximity of the nuclei.

In general, the backbone and the alkyl chain portion of the side-chain of each amino acid residue form a spin system, whose signals can be related by TOCSY experiments. ROESY experiments can then connect residues which are next to each other along the backbone, allowing the complete assignment. In folded peptides made of protein residues a specific process, called *sequential assignment,*[240] is well established. It employs the through-space connectivity along the backbone of the kind $C^{\alpha}H(i)\rightarrow NH(i+3)$ and $NH(i)\rightarrow NH(i+1)$, derived from ROESY experiments, in order to obtain the sequence of the residues forming a peptide, whose signals have been connected by TOCSY experiments.

Once the attribution has been completed, the information about spatial proximity obtained by ROESY experiments can be usefully employed. In particular, when nuclei which are many bonds apart appear to be next to each other, additional data on the peptide conformation are obtained. This can be used also for gaining insight in the side-chain conformation, on which it is more difficult to gather information by other techniques.

Firstly, the 1D NMR spectrum of Z-Sar-Aib$_3$-Gly-OEt was completely assigned by performing 2D TOCSY and ROESY experiments.

Fig. 3.3 presents the variation of the chemical shifts of the NH protons of the three peptides by addition of increasing amounts of DMSO-d_6. Indeed, the signals the NH of Aib^2 is shifted downfields as the DMSO concentration increases, whereas Aib^3, Aib^4 and Gly^5 NHs are almost insensitive to DMSO addition. Therefore the latter protons are involved in intramolecular H-bonds. This observation is compatible with the hypothesis proposed by studying the IR absorption spectra *i.e.*, this peptide has a folded helical structure, mot probably of the 3_{10}-type.

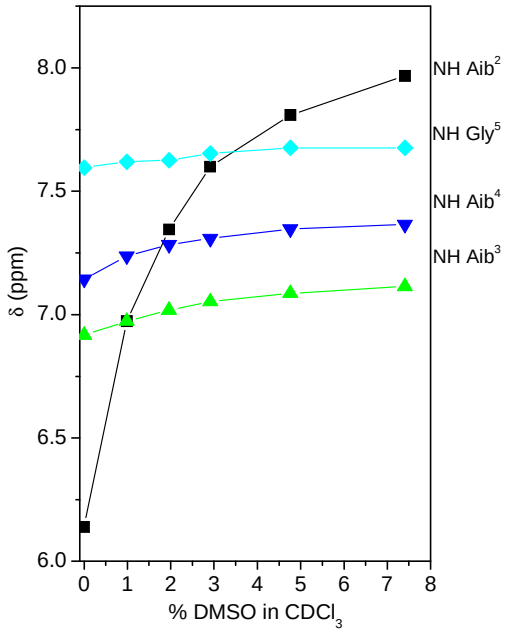

Figure 3.3 Variation of the chemical shift of the NH protons of Z-Sar-Aib$_3$-Gly-OEt in $CDCl_3$ solution at $1 \cdot 10^{-3}$ M concentration by addition of increasing amounts of d_6-DMSO.

Subsequently, the study was extended to the ROESY experiment which additionally substantiated such considerations. A portion of the ROESY spectrum of Z-Sar-Aib$_3$-Gly-OEt is shown in **Fig. 3.4**.

It is interesting to note the presence of four NH(*i*)→NH(*i*+1) consecutive cross-peaks (from Aib^2 to Gly^5) and of the $C^{\alpha}H(i) \rightarrow NH(i+1)$ cross-peaks of Sar^1, all of which are diagnostic of the assumption of a folded conformation.[240] Sar does not have a proton amide. However, a cross peak between its N-methyl and the amide NH of Aib^2, also pointing to an helical structure, is present (**Fig. 3.4**, right spectrum).

The cross-peaks between αNCH_3 and the αNH of Aib^4, similar to a NH(*i*)→NH(*i*+3) is compatible with both α and 3_{10} folded conformations,[241] but does not allow to discriminate between the two helical structures. Again, this findings are in agreement with the information obtained from other experiments and from the IR absorption analysis.

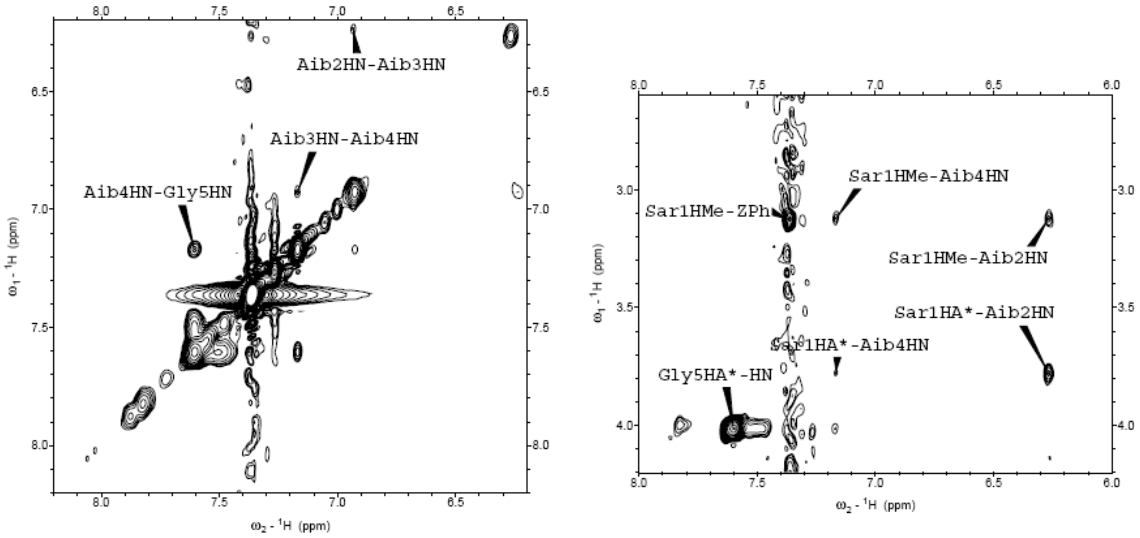

Figure 3.4 Portions of the ROESY spectrum of Z-Sar-Aib_3-Gly-OEt $1 \cdot 10^{-3}$ M in $CDCl_3$. Diagnostic cross-peaks for the adoption of folded stuctures are labelled.

3.2 GOLD(III)-DITHIOCARBAMATO COMPLEXES

3.2.1 Synthesis

The main synthetic route to dithiocarbamate is based on the nucleophilic attack of an amino group to the carbon disulphide in the presence of a strong base[242] This process can even take place without a strong base, but it was shown that, in this case, the yield in dithiocarbamate is much lower.[243]

The peptides used for this work were synthesized as hydrochlorides with the methods described in section 2.2. Then, they were added to carbon disulphide in basic aqueous medium. As we were unable to isolate these dithiocarbamate ligands without causing their degradation during the separation/purification steps, the complexes were obtained by a template reaction involving two phases, as illustrated in **Scheme 3.12** for the Sar-containing derivatives.

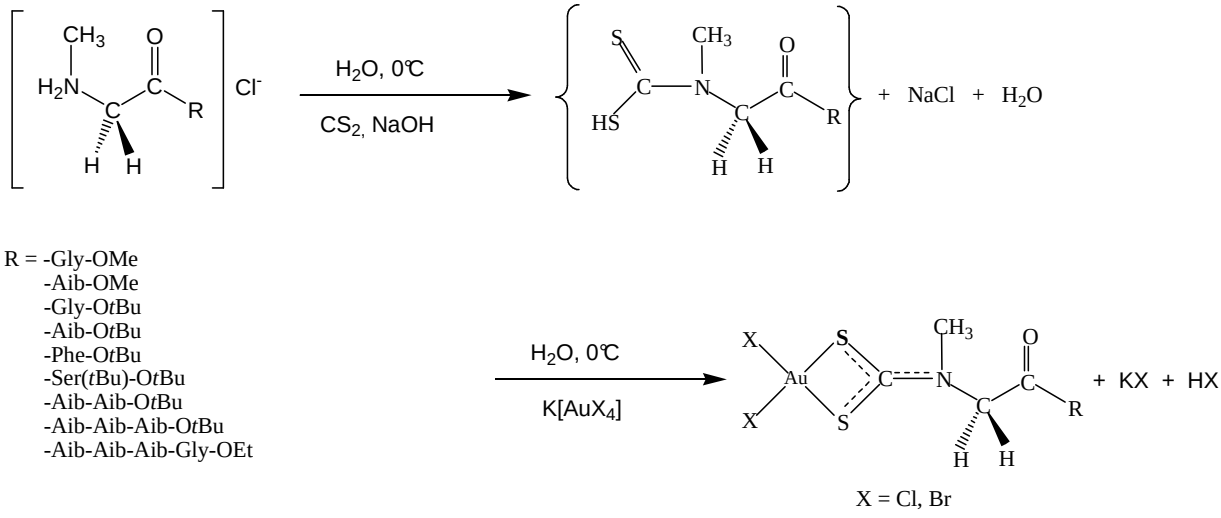

Scheme 3.12 Template reaction leading to the synthesis of Sar-containing gold(III)-dthiocarbamato complexes.

During the first step, the dithiocarbamic acids were generated in solution through the reaction in water at 0 °C between a peptide, carbon disulphide and sodium hydroxide in equimolar ratios.[244] The pH value turned from 10 to 6 in a time span varying with the length of the peptide ligand. Since the reaction proceeds through a nucleophilic attack of the peptide free

amine, the bulkiness of the longer peptides could have slowed down the formation of the corresponding dithiocarbamic acid.

The solutions thus obtained were reacted with 0.5 equivalent of $KAuX_4$ (X= Br, Cl) in water at 0 °C, leading to the immediate precipitation of the complexes $[AuX_2(pdtc)]$ (X= Br, Cl; pdtc= di- to pentapeptidodithiocarbamato).

In the past we have studied, by means of NMR spectroscopy, why an Au(III)/peptide ligand 1:2 stoichiometric ratio leads to complexes with a 1:1 metal-to-dithiocarbamate ratio.[155] The first step of the reaction, *i.e.* the formation of the ethylsarcosinedithiocarbamic acid (for the synthesis of a similar complex Au(III)/dtc-Sar-OEt), is accompanied by two side products, deriving from the hydrolysis of the ester moiety. Any modification of the experimental conditions (temperature, amount of base) did not affect the yield of ethylsarcosinedithiocarbamic acid (which did not exceed 40 %), but only that of the hydrolysis products. In fact, the addition of a double amount of base promoted a more efficient hydrolysis and, in turn, the reaction between the hydrolysis product and unreacted CS_2, thus leading to the formation of Sar-dithiocarbamic acid as additional product. On the basis of these studies, in this thesis work an Au(III)/peptide ligand 1:2 ratio was used to overcome the problem of low yields and to minimize the loss of gold(III) precursor.

In the case of gold(III)-methyl-ester-containing derivatives, the cyclization of the dipeptide to diketopiperazine, together with the hydrolysis occurring in the first step of the reaction, could be responsible for the low yields observed. Indeed, with the *tert*-butyl ester, less sensible to basic hydrolysis, good yields were obtained. We also noticed that the bulkiness of the peptide was detrimental for the yield, whereas addition of an excess of carbon disulphide turned out to increase the final yield.

Finally, it is worth mentioning that the water-solubility of some complexes made the product isolation very troublesome.

The structure of the Sar-containing gold(III)-pedtidodithiocarbamato complexes are illustrated in **Scheme 3.13**.

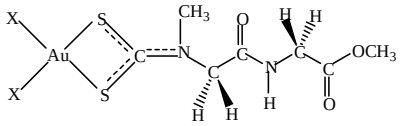

X= Br, [$AuBr_2$(MeO-Gly-Sar-dtc)] (AuD_2)

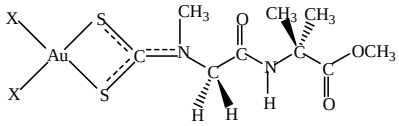

X= Br, [$AuBr_2$(MeO-Aib-Sar-dtc)] (AuD_3)

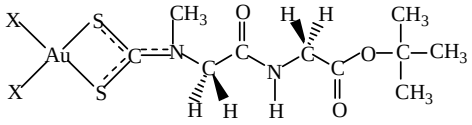

X= Br, [$AuBr_2$(*t*BuO-Gly-Sar-dtc)] (AuD_6)
X= Cl, [$AuCl_2$(*t*BuO-Gly-Sar-dtc)] (AuD_7)

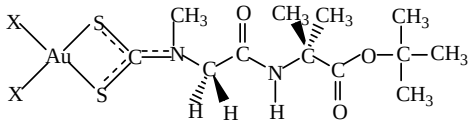

X= Br, [$AuBr_2$(*t*BuO-Aib-Sar-dtc)] (AuD_8)
X= Cl, [$AuCl_2$(*t*BuO-Aib-Sar-dtc)] (AuD_9)

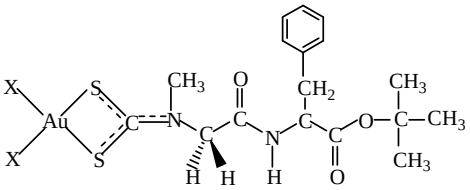

X= Br, [$AuBr_2$(*t*BuO-Phe-Sar-dtc)] (AuD_{10})
X= Cl, [$AuCl_2$(*t*BuO-Phe-Sar-dtc)] (AuD_{11})

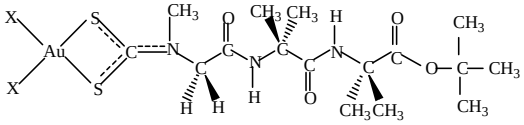

X= Br, [$AuBr_2$(*t*BuO-Aib-Aib-Sar-dtc)] (AuD_{13})
X= Cl, [$AuCl_2$(*t*BuO-Aib-Aib-Sar-dtc)] (AuD_{14})

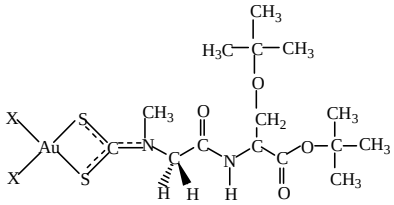

X= Br, [$AuBr_2$(*t*BuO-Ser(*t*Bu)-Sar-dtc)] (AuD_{16})
X= Cl, [$AuCl_2$(*t*BuO-Ser(*t*Bu)-Sar-dtc)] (AuD_{17})

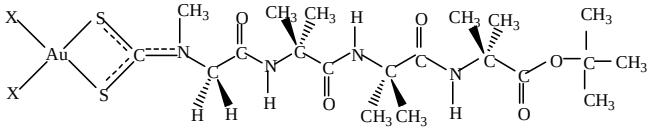

X= Br, [$AuBr_2$(*t*BuO-Aib-Aib-Aib-Sar-dtc)] (AuD_{18})
X= Cl, [$AuCl_2$(*t*BuO-Aib-Aib-Aib-Sar-dtc)] (AuD_{19})

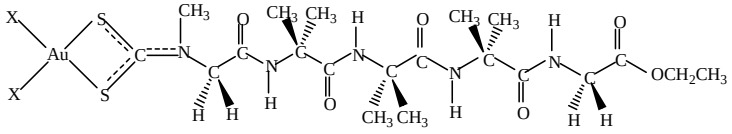

X= Br, [$AuBr_2$(EtO-Gly-Aib-Aib-Aib-Sar-dtc)] (AuD_{12})
X= Cl, [$AuCl_2$(EtO-Gly-Aib-Aib-Aib-Sar-dtc)] (AuD_{15})

Scheme 3.13. structure of the Sar-containing derivatives

3.2.2 Complexes characterization

3.2.2.1 FT-IR spectroscopy

The main significant bands recorded in the FT-IR spectra of the peptides and the corresponding gold(III)-dithiocarbamato complexes are summarised in **Tab.3.2** and **Tab.3 3**.

Compound		**A**	**AuD$_1$**	**B**	**AuD$_3$**	**C**	**AuD$_6$**	**AuD$_7$**	**D**	**AuD$_8$**	**AuD$_9$**
ν(N-H)		3419	3409	3314	3423	3307	3352	3349	3192	3362	3365
ν(NH_2^+)		3231	-	3200	-	2777/2709	-	-	2744/2683	-	-
ν(C=O)		-	1744	1740	1739	1732	1736	1737	1735	1734	1733
ν(NHC=O)		1684	1669	1679	1685	1669	1673	1672	1689	1690	1691
ν(CN- H)+ ν(SSCN)		1558	1558	1555	1559	1576	1568	1561	1563	1560/1531	1564/1534
ν(C-OMe)		1217	1209	-	-	-	-	-	-	-	-
ν(C-OEt)		-	-	-	-	-	-	-	-	-	-
ν(C-O*t*Bu)		-	-	-	-	1241	1228	1229	1259	1215	1214
ν(*t*Bu-O)		-	-	-	-	1167	1161	1162	1152	1144	1146
ν(Et-O)		-	-	-	-	-	-	-	-	-	-
ν(S-C-S)	asym.	-	-	-	-	-	1006	1006	-	996	996
	sym.	-	-	-	-	-	556	558	-	545	547
ν(S-Au-S)	asym.	-	-	-	-	-	387	384	-	383	383
	sym.	-	-	-	-						
ν(Br-Au-Br)	asym.	-	-	-	-	-	252	-	-	252	-
	sym.	-	-	-	-	-	227	-	-	223	-
ν(Cl-Au-Cl)	asym.	-	-	-	-	-	-	358	-	-	347
	sym.	-	-	-	-	-	-	339	-	-	

Table 3.2 Selected IR frequencies [cm^{-1}] of the peptides: HCl·Sar-Gly-OMe **A**, HCl·Sar-Aib-OMe **B**, HCl·Sar-Gly-O*t*Bu **C**, HCl·Sar-Aib-O*t*Bu **D** and their corresponding gold(III)-dithiocarbamato complexes.

Compound		E	AuD_{10}	AuD_{11}	F	AuD_{12}	AuD_{15}	G	AuD_{13}	AuD_{14}
ν(N-H)		3330	3431	3342	3351/3311	3343	3340	3421/3276	3403	3392
ν(NH_2^+)		2775/2706	-	-	2751/2711	-	-	2762/2692	-	-
ν(C=O)		1736	1731	1733	1739	1728	1728	1727	1719	1729
ν(NHC=O)		1665	1683	1684	1694/1657	1661	1657	1688/1647	1688	1689/1612
ν(CN- H)+ ν(SSCN)		1543	1558	1559	1543/1727	1553	1557	1545/1518	1558/1509	1559/1512
ν(C-OMe)		-	-	-	-	-	-	-	-	-
ν(C-OEt)		-	-	-	1221	1216	1216	-	-	-
ν(C-O*t*Bu)		1220	1214	1213	-	-	-	1226	1218	1220
ν(*t*Bu-O)		1163	1155	1155	-	-	-	1158	1146	1146
ν(Et-O)		-	-	-	1037	1099	1101	-	-	-
ν(S-C-S)	asym.	-	994	994	-	1028	1028	-	-	1015
	sym.	-	562	563	-	560	562	-	543	543
ν(S-Au-S)	asym.	-	381	383	-	383	383	-	384	383
	sym.	-			-			-		
ν(Br-Au-Br)	asym.	-	252	-	-	252	-	-	252	-
	sym.	-	221	-	-	227	-	-	-	-
ν(Cl-Au-Cl)	asym.	-	-	359	-	-	338	-	-	340
	sym.	-	-		-	-	322	-	-	322

Table 3.3 Selected IR frequencies [cm^{-1}] of the peptides: HCl·Sar-Phe-O*t*Bu **E**, HCl·Sar-Aib_2-O*t*Bu **F**, HCl·Sar-Aib_3-Gly-OEt **G** and their corresponding gold(III)-dithiocarbamato complexes.

The interpretation of FT-IR spectra of dithiocarbamato complexes of transition metals has arisen interest both diagnostically to determine the mode of coordination and as a meaning of assessing the nature of bounding in the complexes. As concerns the dithiocarbamate moiety, the three main regions of the IR are of interest. Firstly, the (1580-1450) cm^{-1} region which is primarily associated with the "thioureide" band due to the ν(N-CSS) vibration; secondly, the (1060-940) cm^{-1} region which is associated to ν(C-S) vibrations, and, thirdly, the (420-250) cm^{-1} region associated with ν(M-S) vibrations.[245]

Dithiocarbamato compounds exhibit a characteristic band at around 1500 cm^{-1} assignable to the ν(N-CSS);[246-248] this band defines a carbon-nitrogen bond order between a single bond (1350-1250 cm^{-1}) and a double bond (1690-1640 cm^{-1}).[249] The appearance of a band in that region indicates that of the three possible resonance structures reported by Chatt et al,[250] (characterized by a strong delocalization of electrons in the dithiocarbamate moiety (**Scheme 3.14**), in our case, we are dealing with a considerable contribution of structure **III**.

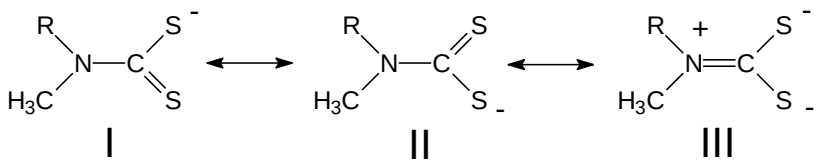

Scheme 3.14 Resonance forms of the dithiocarbamic –$NCSS^-$ moiety.

To discern the bonding type of the dithiocarbamato ligands in the complexes, the Bonati-Ugo method[251] is, by far, the most popular one. It consists of tracing the (1060-940) cm^{-1} spectral region, where the ν(C-S) modes are thought to appear. In fact, the band due to –CSS moiety are usually coupled to other vibrations and are very sensitive to the environment around this group, but they are also useful to distinguish between monodentate and bidentate coordination.[252] The presence of only one band in the investigated region, commonly attributed to ν_a(C-S) mode, is assumed to indicate a completely symmetrically bonding of the dithiocarbamate ligand, acting in a bidentate mode (**Scheme 3.15 a**), and this is the case of all these gold(III)-peptidodithiocarbamato derivatives. Conversely, a split band indicates an asymmetrically-bonded bidentate ligand ($\Delta\nu < 20$ cm^{-1}, **Scheme 3.15 b**) or a monodentate bound ligand ($\Delta\nu > 20$ cm^{-1}, **Scheme 3.15 c**).

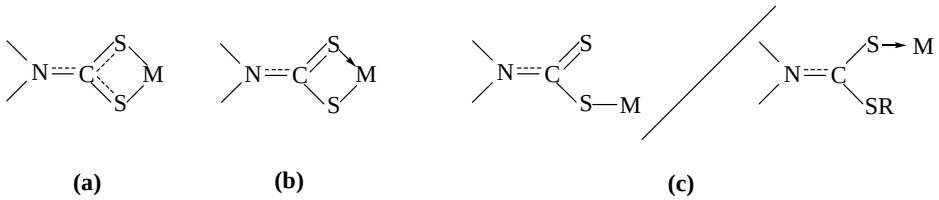

(a) **(b)** **(c)**

Scheme 3.15 Different ways of metal-sulfur binding in dithiocarbamate complexes: symmetrical bidentate (**a**), asymmetrical bidentate (**b**) and monodentate (**c**).

New bands absent in the spectra of the starting materials, are observed in the (420-250) cm^{-1} range and they can be assigned to metal-sulphur modes according to the normal coordinate analysis of the dithiocarbamate complexes and previous works on gold derivatives.[253,254]

In the same range, other informative bands are detected, attributed to the ν(Au-X) (X = Cl, Br) modes. These bands are ascribed to the Au-X stretching frequencies for terminal halides.[254-256] It is worth observing that in the far FT-IR spectra of all chloro-derivatives, the bands assignable to the ν(Au-Cl) vibrations are broad or even doubled because of the isotopic splitting ν(Au-$^{35/37}$Cl). Isotopic are clearer for compounds containing one Au-Cl bond than those containing more than one chlorine atom bound to the same gold center; the fact there is only one stable isotope ^{197}Au helps to make Au-Cl isotopic splitting more easily observable than in the case of chlorides of elements consisting of a mixture of stable isotopes.[256]

3.2.2.2 NMR spectroscopy

Some features of ^{1}H-NMR spectra of HCl·Sar-Gly-OMe, HCl·Sar-Aib-OMe, HCl·Sar- Gly-O*t*Bu, HCl·Sar-Aib-O*t*Bu, HCl·Sar-Phe-O*t*Bu, HCl·Sar-Aib_2-O*t*Bu, HCl·Sar-Aib_3-Gly-OEt and

their corresponding gold(III)-dithiocarbamato complexes are reported on **Table 3.4**. A shift towards δ larger values is observed from a peptide to the corresponding gold derivatives, in particular for the sarcosine *N*-methyl and C^{α}-methylene protons. This is probably due to the bonding of the sarcosine nitrogen atom to the dithiocarbamate moeity. It is worth noting that this conversion is associated to the disappearance of the NH_2^+ signal. Moving away from the dithiocarbamato group, this influence diminishes until be insignificant, as there is no relevant difference between the chemical shifts of the ester moiety, moving from the peptide to the corresponding complexes.

Compound	NH_2^+ Sar	NH	αCH_2 Sar	N-CH_3 Sar
A[(a)]	8.83	8.94	3.75	2.54
AuD$_2$[(a)]	-	8.89	4.56	-
B[(a)]	8.81	8.91	3.68	2.5
AuD$_3$[(a)]	-	8.82	4.48	3.41
C[(a)]	8.99	8.91	3.72	2.53
AuD$_6$[(b)]	-	7.96	4.71/4.75[(c)]	3.53/3.57[(c)]
AuD$_7$[(b)]	-	7.92	4.75	3.56/3.57[(c)]
D[(a)]	9.05	8.84	3.64	2.52
AuD$_8$[(b)]	-	7.90	4.62/4.66	3.51/3.54[(c)]
AuD$_9$[(b)]	-	7.89	4.66	3.54/3.55[(c)]
E[(a)]	8.92	8.80	3.62	2.44
AuD$_{10}$[(b)]	-	7.91	4.65/4.70[(c)]	3.49
AuD$_{11}$[(b)]	-	7.92	4.70	3.49
F[(a)]	8.96	8.88[1], 8.04[2], 7.90[g], 7.26[3]	3.72	2.57
AuD$_{12}$[(b)]	-	(8.57/8.46)[1, (c)], (7.98/7.94)[2, (c)], 7.68[g], (7.20/7.17)[3, (c)]	4.89/4.84[(c)]	3.59/3.54[(c)]
AuD$_{15}$[(b)]	-	8.45[1], 7.87[2] 7.67[g], 7.19[3]	4.85	3.59
G[(a)]	8.95	8.49[1], 7.64[2]	3.68	2.51
AuD$_{13}$[(b)]	-	7.90[1], 7.83[2]	4.73/4.69[(c)]	3.55/3.51[(c)]
AuD$_{14}$[(b)]	-	(7.88/7.80)[1, (c)], (7.41/7.31)[1, (c)]	4.73	3.55

[(a)] performed in $(CD_3)_2SO$, [(b)] performed in $(CD_3)_2CO$, [(c)] isomers. [1] Aib_1, [2] Aib_2, [3] Aib_3, [g] Gly.

Table 3.4 ^{1}H NMR spectral data [ppm] of HCl·Sar-Gly-OMe **A**, HCl·Sar-Aib-OMe **B**, HCl·Sar-Gly-O*t*Bu **C**, HCl·Sar-Aib-O*t*Bu **D**, HCl·Sar-Phe-O*t*Bu **E**, HCl·Sar-Aib_2-O*t*Bu **F**, HCl·Sar-Aib_3-Gly-OEt **G** and their corresponding gold(III)-dithiocarbamato complexes.

This behaviour is remarkable, when considering the ^{13}C values (**Tab. 3.5**). In addition, other important signals are observable, ascribed to dithiocarbamic carbon atoms (NCSS).

The δ(N^{13}CSS) values are found in the range (190-215) ppm, and it is generally assumed that they are strongly dependent on both the type of dithiocarbamate-metal bond and the oxidation state of the metal center.[257] For high oxidation state transition metal dithiocarbamates derivatived, such as gol(III) ones, the δ(N^{13}CSS) values are usually found in the range(202-206) ppm.[258] In the other hand, dithiocarbamato complexes of transition metal owing a d^{10} electronic configuration, the δ(N^{13}CSS) values are shifted to lower fields in the range of (202-206) ppm.[259] There is a strong empirical correlation between δ(N^{13}CSS) values and the carbon-nitrogen stretching vibrations in the infra-red spectra: higher ν(N-CSS) values indicates carbon-nitrogen double bond character, which well correlates with lower δ(N^{13}CSS) values because of a greater electron density on the –NCSS moiety. In a semi-empirical way, δ(N^{13}CSS) could be expressed as a linear function of the sum of CN, CS1, CS2 π-bond orders, and ν(N-CSS) of the CN π-bond order.[257] The sum of the π-bond order is derived to be maximal for equal π bonds and to decrease with increasing inequality of the three π bonds. Therefore, the compounds with high ν(N-CSS) values have low CS and low total π-bond orders, thus leading to low δ(N^{13}CSS) values, and *vice versa*. All these considerations are compatible with the reported data in literature on gold(III)-dithiocarbamato complexes.[253,260,261]

Compound	CSS	αCH_2 Sar	N-CH_3 Sar
A	n.d.	n.d	n.d
AuD_2	n.d.	n.d.	n.d.
B	n.d.	n.d.	n.d.
AuD_3	n.d.	n.d.	n.d.
C[(a)]	-	48.59	32.38
AuD_6[(b)]	196.74/200.48	55.12/58.98	40.13/41.12
AuD_7[(b)]	195.45/200.60	55.64	40.66/41.10
D[(a)]	-	48.61	32.41
AuD_8[(b)]	196.57/200.26	55.26/56.15	40.21/41.20
AuD_9[(b)]	195.09/200.19	55.67	40.64/41.09
E[(a)]	-	49.20	32.80
AuD_{10}[(b)]	196.11/199.33	54.65/55.56	39.74/40.74
AuD_{11}[(b)]	194.45/199.61	55.31	40.49
F[(a)]	-	48.87	32.41
AuD_{12}[(b)]	197.11/ 200.32	55.66/ 56.73	40.37/41.43
AuD_{15}[(b)]	195.70/200.35	55.94	40.88
G[(a)]	-	49.75	32.95
AuD_{13}[(b)]	195.67/199.35	54.85/ 55.77	39.40/40.37
AuD_{14}[(b)]	195.07/200.06	56.07	40.62/41.06

[(a)] performed in $(CD_3)_2SO$, [(b)] performed in $(CD_3)_2CO$.

Table 3.5 ^{13}C NMR spectral data [ppm] of HCl·Sar-Gly-OMe **A**, HCl·Sar-Aib-OMe **B**, HCl·Sar-Gly-O*t*Bu **C**, HCl·Sar-Aib-O*t*Bu **D**, HCl·Sar-Phe-O*t*Bu **E**, HCl·Sar-Aib_2-O*t*Bu **F**, HCl·Sar-Aib_3-Gly-OEt **G** and their corresponding gold(III)-dithiocarbamato complexes.

^{1}H-NMR spectra of the Au(III)-peptidodithiocarbamato derivatives in $(CD_3)_2CO$ at different times were performed to clarify their solution chemistry. As example, in **Fig. 3.5** the ^{1}H-NMR spectra of AuD_6 [$Au^{III}Br_2$(*t*BuO-Gly-Sar-dtc)] are reported. It is worth observing that, after 17 hours, the amide proton is not detectable, leading to the consequently simplification of the glycine methylenic protons signal. This could be explained taking in consideration the interchange of this proton with the acetone-d_6 deuterium, since it does not happen in DMSO-d_6 (**Fig.3.6**). The interchange between amide proton and deuterium, in presence of deuterated solvents, as D_2O or CD_3OD is a well-known phenomenon, but is not reported for organic aprotic deuterated solvents.

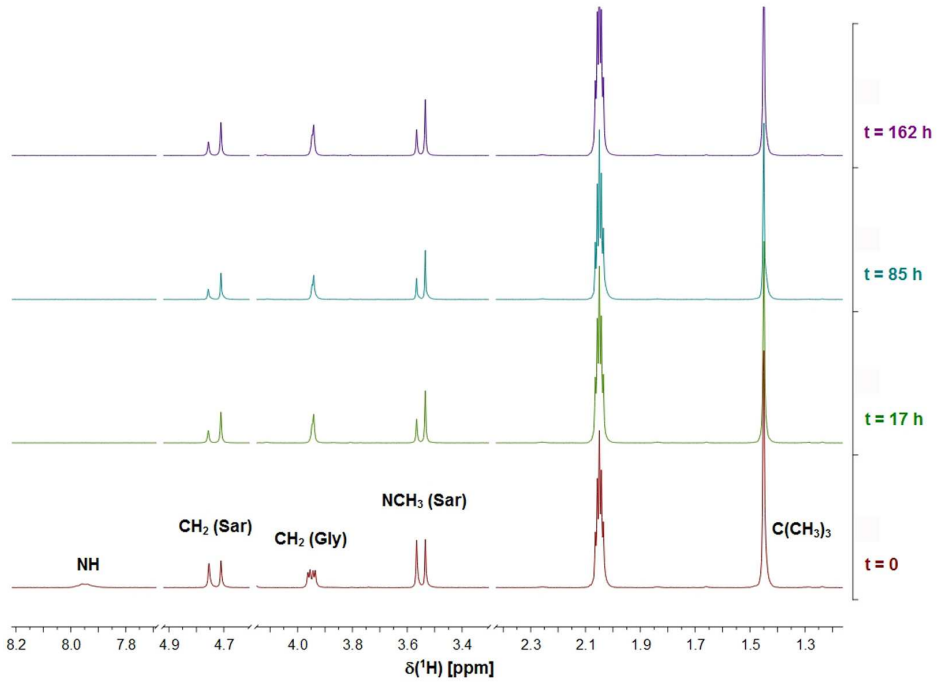

Figure 3.5 ^{1}H NMR spectra of AuD_6 in $(CD_3)_2CO$ performed at different times.

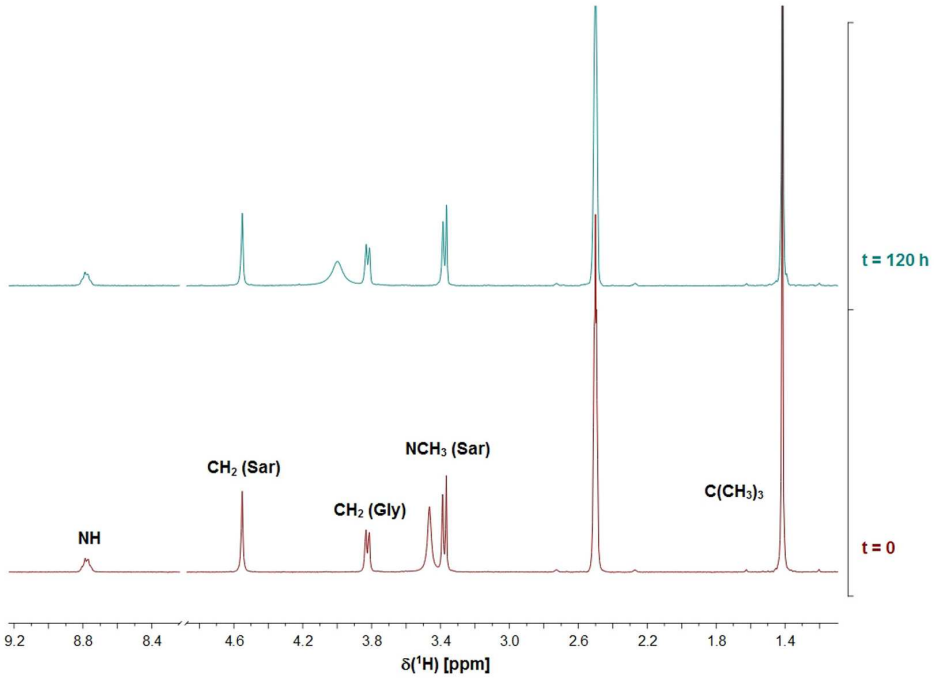

Figure 3.6 ^{1}H NMR spectra of AuD_6 in $(CD_3)_2SO$ performed at different times.

Moreover, it was observed that all the studied complexes give rise to isomerization in solution, in particular, as concerns the $–CH_2N(CH_3)CSS$ group. In **Fig 3.5**, soon after dissolution, the *N*-methyl and *N*-methylene protons have, each, two signals (singlets) in 1:1 ratio, as the glycine methylene protons show a doublet of doublets in 1:1 ratio; over time, the lower field peaks, referred to one of the isomers, progressively decrease in intensity in favour of the higher field isomers reaching a 1:2 ratio.

The presence of two isomers is easily put in evidence on the [^{1}H, ^{13}C] HMBC NMR (**Fig. 3.7**), where two distinct signals are recorded for each of sarcosine methyl and methylene carbon atoms, and the correlations between them. In addition, two signals for –CSS carbon atom are also illustrated on the same figure and each dithiocarbamic carbon gives rise to a long range coupling with the sarcosine *N*-methyl and *N*-methylene protons.

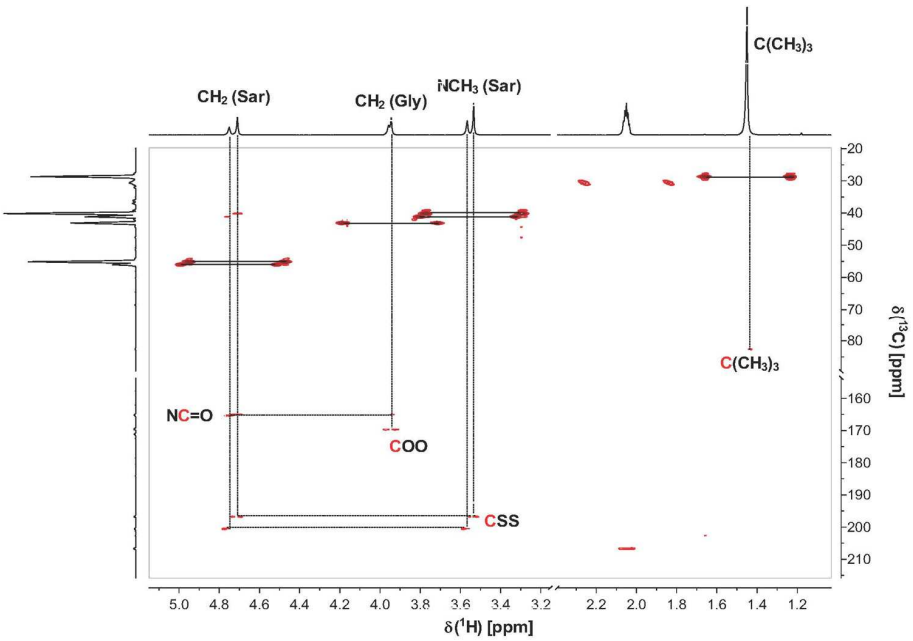

Figure 3.7 $^{1}H^{13}C$-HMBC spectrum of AuD_6 in $(CD_3)_2CO$ (detail).

This behaviour, also, seems to be solvent-dependent. In fact, the AuD_6 spectra in DMSO-d_6 do not change with time and the two isomers are in the same ratio even after 120 hours. A similar observation was previously made for gold(III) ethylsarcosinedithiocarbamate complexe $[Au^{III}Br_2(ESDT)]$, of which a crystal structure was obtained through X-rays.[166] Unfortunately, it contained only one crystalline form (excluding the little disorder of the ethyl ester moiety). The herein studied complexes do not have stereocenters able to generate two different isomers, at least as concern the dithiocabamate moiety. Their elucidation is not yet achieved and studies are still going one to clarify it.

3.2.2.3 Thermal studies

The thermal behaviour of the synthesized complexes have been studied by thermogravimetric (TG) and differential scanning calorimetry (DSC) techniques in a dynamic atmosphere of air, in order to establish the different decomposition processes and to confirm the proposed stoichiometry. The experimental data agree to a good extent with the ones obtained by the other spectroscopic techniques, and the results of such analysis summarized in **Tab. 3.6**, indicate a good correlation between calculated (to metallic gold) and found weight loss values for all the investigated compounds.

Compound	Weight loss [%]		DSC
	Found	Calculated	Peak temperature[°C] (process(*))
AuD_2	-66.70	-66.73	198.8 endo / 507.3 exo
AuD_3	-66.57	-68.23	167.0, 316.6, 1070.4 endo
AuD_6	-66.62	-68.94	152.6, 1065.4, 1074.9, 1079.1 endo/ 481.3 exo
AuD_7	-61.72	-63.88	155.3, 1063.8 endo/ 526.0 exo
AuD_8	-69.22	-70.26	165.9, 1064.4, 1070.8 endo/ 472.3 exo
AuD_9	-63.40	-65.64	166.6, 205.3, 1061.8 endo/ 516.0 exo
AuD_{10}	-72.94	-72.72	113.4, 124.3, 1066.8, 1069.4, 1074.2 endo/ 519.0 exo
AuD_{11}	-69.07	-69.01	118.0, 138.3,192.6, 1065.6, 1065.9 endo/ 518.4 exo
AuD_{12}	-74.03	-77.13	106.0, 152.2, 178.6 endo/ 433.7, 507.4, 1084.1 exo
AuD_{15}	-72.75	-74.50	126.9, 185.5, 1065.7 endo/ 121.3, 158.3, 443.1, 583.0, 1072.1 exo
AuD_{13}	-72.91	-73.64	119.3, 1064.4 endo/ 180.6, 499.4, 1072.1 exo
AuD_{14}	-65.96	-70.08	487.0, 1079.7 exo
AuD_{18}	-76.17	-76.34	1074.1 endo/ 335.9, 440.1, 534.7 exo
AuD_{19}	-71.96	-73.51	145.3, 1070.4 endo/ 514.4, 554.0 exo

(*) endo/exo = endothermic/exothermic process.

Table 3.6 Thermogravimetric (TG) and differential scanning calorimetric (DSC) data.

The thermal degradation of all the complexes may occur in two major steps, the first TG step corresponding to the pyrolysis, the decarboxylation and reduction elimination Au(III) → Au(I), thus leading to [Au(SCN)] as the residue, a commonly discovered intermediate in the thermal decomposition of metal dithiocarbamates.[262,263] The removal of the remaining ligand atoms at higher temperature is followed by complete degradation leading to metallic gold.[253,264,265] This ultimate event is confirmed by the presence of an endothermic DSC peak at around 1070 °C due to the metallic gold melting.

3.2.2.4 Circular Dichroism

Circular dichroism is an analytical technique based on the differential absorption of circularly polarized light by chromophores set in an asymmetric environment. The spectral region most commonly investigated for the conformational analysis of peptides lies in the far UV region (λ= 190-260 nm). The amide chromophore of peptides displays two bands in this interval, corresponding to the $\pi \rightarrow \pi^*$ and $n \rightarrow \pi^*$ transitions. The amide group is planar and therefore its transitions are optically inactive, but the presence of chiral elements (such as the C^α atoms of chiral amino acids) next to the cromophore, as well as its incorporation in helical secondary

structures, which are intrinsically dissymmetric, make it optically active, therefore liable to CD analysis.

The interactions among consecutive amide chromophores along the backbone modulate their optical transitions in a way that depends on their relative orientation, induced by the peptide secondary structure. The global outcome is that the spectral features depend on the peptide secondary structure, so that useful information can be obtained both from the shape and from the intensity of the dichroic bands of peptides[266,267] The *molar ellipticity* $[\Theta]_T$ ($deg \cdot cm^2 \cdot dmol^{-1}$) is the parameter used for comparing the intensity of the CD signal (Θ) by normalization with regard to concentration (c, mol/L) and optical path (l, cm), using the relation $[\Theta]_T = \Theta/(c \cdot l)$.

The peptide ligands used in this Thesis work are very short peptides. Therefore, with the exception of the tetra- and pentapeptide, they are not long enough to display a well defined secondary structure, to be readily studied by CD. In addition, most of them, including the tetra- and pentapeptide, are not chiral. However, we decided anyway to undertake a CD analysis of a representative set of compounds with chiral peptides, mainly to see if the chiral peptide ligand is able to induce asymmetry in the transitions of the metal complex. In particular, we recorded the CD spectra in MeOH of HCl·Pro-$(Aib)_2$-OtBu, AuD_{20} and AuD_{21}. As the peptide ligand does not have absorptions above 240 nm, **Fig.3.8** shows only the spectra of AuD_{20} and AuD_{21} in the 200-500 region.

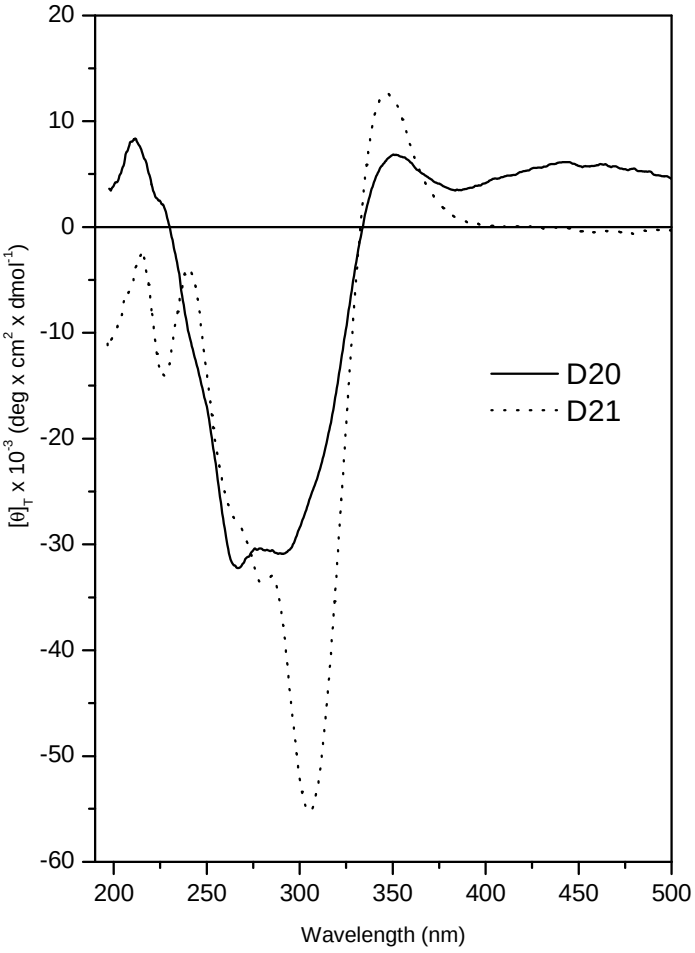

Figure 3.8 CD spectra of AuD_{20} and AuD_{21} in MeOH at ~10-4 M concentration, in the $200 \leq \lambda \leq 500$ nm.

It is interesting to note that the coordination of the peptide to gold is able to induce asymmetry on gold(III) transitions, thus making them optically active. There are relevant intensity differences in the near UV/Vis region among the AuD_{20} and AuD_{21} spectra (**Fig.3.9**). This finding is somewhat surprising as the two complexes differ only for the alogen type (Cl and Br, respectively) . The two spectra are rich of information as several bands are observed. In particular, it is worth mentioning the bands (i) at about 265 nm and 310 nm, probably due to the $\pi \rightarrow \pi^*$ transitions of the –NCS and–CSS moiety, (ii) at about 340 nm, arising from the $n \rightarrow \pi^*$ transition where *n* is the in-plane non-bonding sulphur orbital,[268] and (iii) at about 440 nm, assignable to the d→d metal orbital transitions.

At this moment, it is difficult to interpret these dichroic signals, as little or no literature is available on this subject. However, we believe that this type of measurements could display its usefulness in the future, when more Au(III) complexes with chiral peptide ligands will be available.

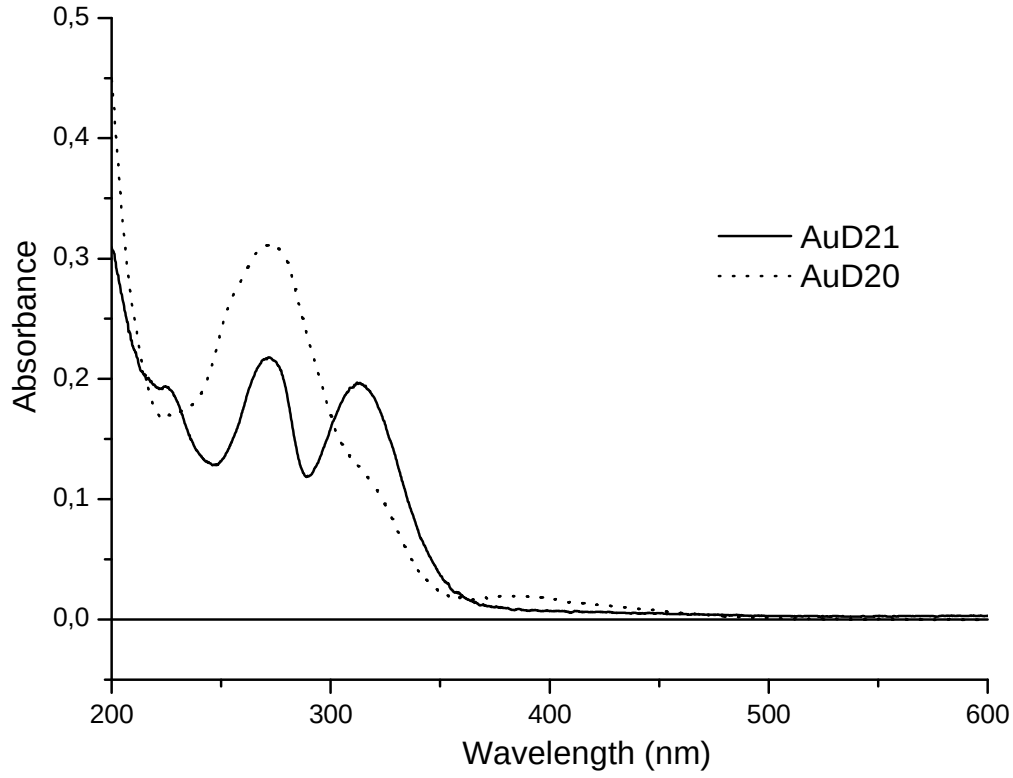

Figure 3.9 UV-Visible spectra of AuD_{20} and AuD_{21} in MeOH at ~10-4 M concentration, in the $200 \leq \lambda \leq 500$ nm.

3.2.3 Stability in the presence of the reductive agent L-NAC

Au(III) complexes tend to easily reduce to Au(I) and successively to Au(0) in physiological environment. This poor stability have limited its use as therapeutic agent. Nevertheless, the coordination of Au(III) to dithiocarbamic ligands lead to a high stabilization of the metal center in the +3 oxidation state.

Glutathione (γ-Glu-Cys-Gly) is one of the reductive agents present in physiological environment in high quantities. It tends to oxidize to a disulphide compound **(Scheme 3.16).**

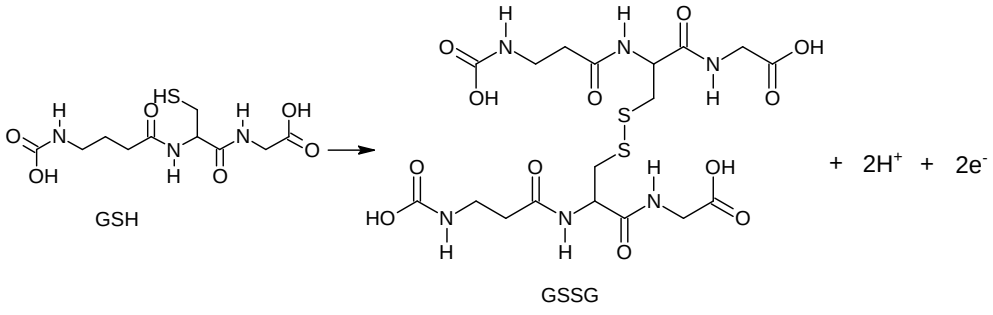

Scheme 3.16 Reduction of glutathione(GSH) to a disulphide compound (GSSG).[269]

The reduction of Au(III) complexes to Au(I) could be a determinant factor for the activation or deactivation of their potential pharmacological properties. Therefore, the stability of the studied complexes in the presence of L-NAC reagent was evaluated though the registration of a series of ^{1}H-NMR at different times. As the L-NAC can be a mimetic of glutathione, it was used in place of glutathione in order to simplify the spectra. These studies were done on AuD_6 [$Au^{III}Br_2$(dtc-Sar-Gly-O*t*Bu)]. The kinetic profile of the reaction of AuD_6 with L-NAC in 1:2 molar ratio in DMSO-d_6 is reported in **Fig. 3.10**.

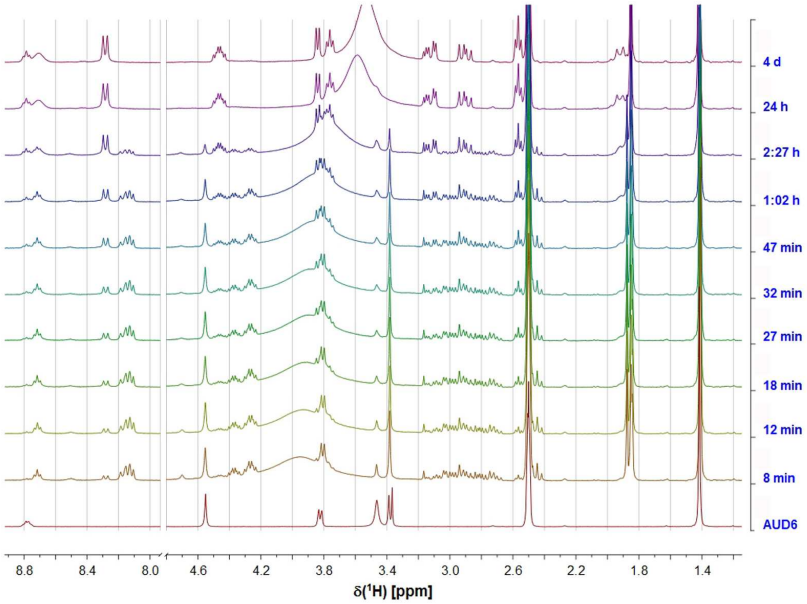

Figure 3.10 ^{1}H-NMR spectra of the reaction of AuD_6 with L-NAC performed in DMSO-d_6, at different times.

It is worth noting that the reagents reacted immediately leading to a number of intermediates not yet exactly identified. After 24 hours the system resulted to be stabilized, and the solution colour had changed from the initially orange to perfectly colourless.

A comparison was made between the ^{1}H-NMR spectra in DMSO-d_6 of the strarting reagents (AuD_6 and L-NAC), the L-NAC oxidation product *i. e.* L-NACy (N-acetyl-cystine), the analogue HBr·Sar-Gly-O*t*Bu (obtained by direct reaction of HCl·Sar-Gly-O*t*Bu with 2 equivalents of HBr), and the previously discussed ^{1}H-NMR spectrum obtained after 24 hours. The AuD_6/L-NAC 1:2 spectrum after 24 hours resulted to be surprisingly 'clean' compared to the ones of intermediate times(**Fig. 3.11**)

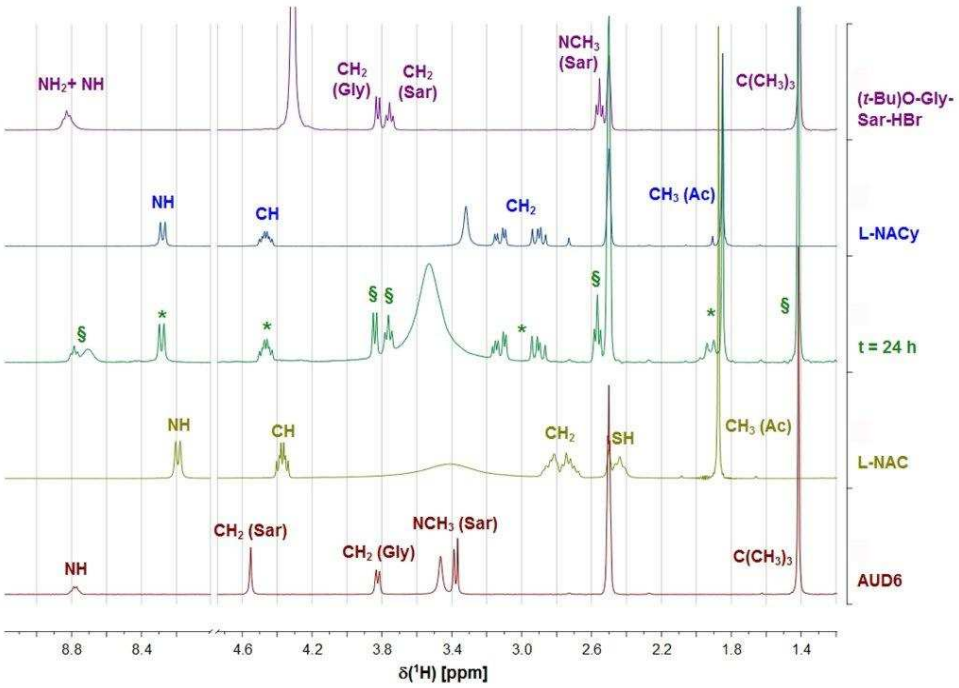

Figure 3.11 Comparison between the ^{1}H-NMR spectra of AuD_6, L-NAC, AuD_6 + L-NAC after 24 hours, L-NACy and HBr·Sar-Gly-O*t*Bu.

On this spectrum, no signal related to the initial AuD_6 or L-NAC was detected, while only two different species were identificated: L-NACy and HBr·Sar-Gly-O*t*Bu. Since the L-NAC was completely oxidized to L-NACy, it was hypothesised a reaction mechanism reported in **Scheme 3.17.**

In the first step, a bromide is substituted by one thiol-containing molecule leading to the release of HBr. Successively, a second L-NAC molecule could be coordinated to the metal center Au(III) causing the cleavage of the Au-S bond and consequently generate a monodentate coordination structure through the C=S group (2).

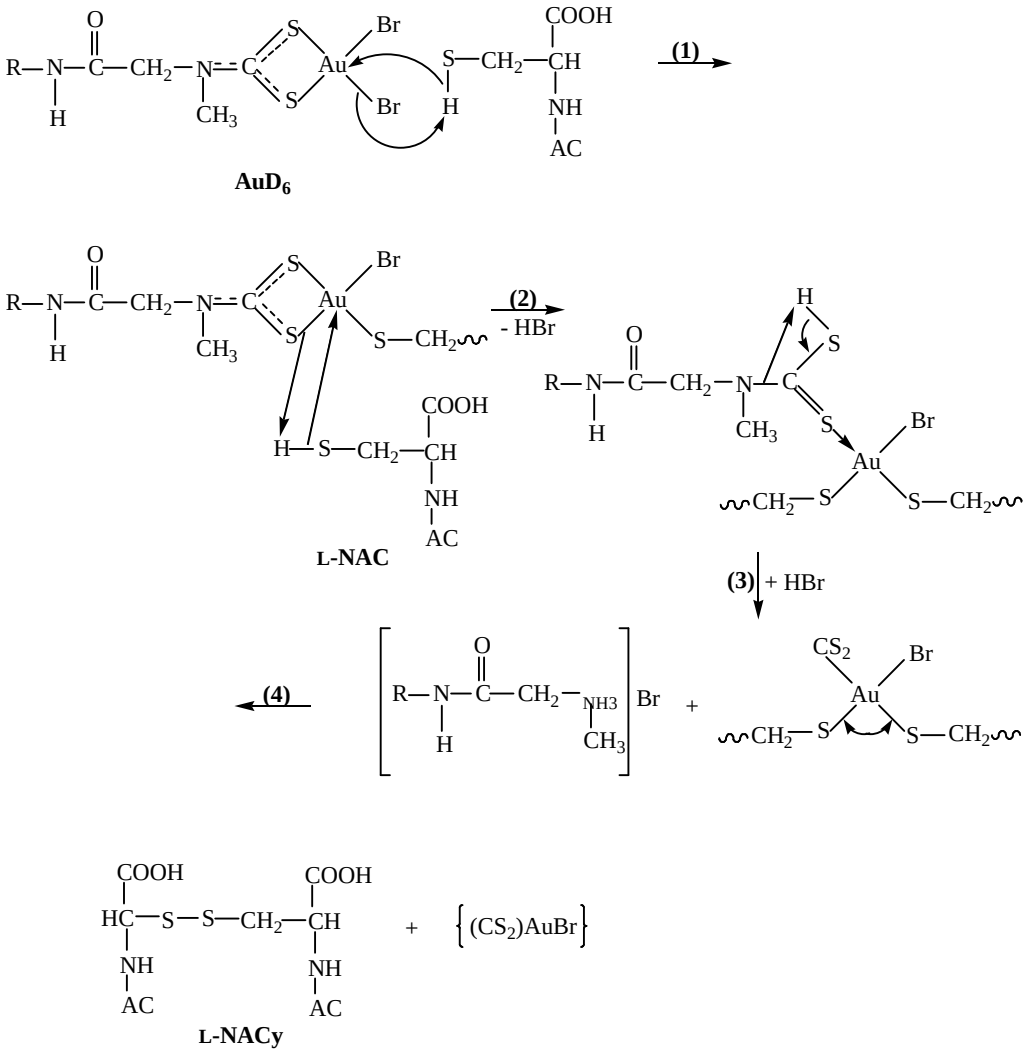

Scheme 3.17. Hypothetical reaction mechanism for the reduction of AuD_6 by L-NAC.

Dithiocarbamic acids are unstable and have the propensity to decompose into reagents hypothetically used for their synthesis, the amino- substrate and the CS_2. Therefore, the decomposition of the dithiocarbamic ligand gives HBr·Sar-Gly-O*t*Bu (3). Finally, the presence of two molecules of L-NAC coordinated at *cis* position could favour the effective redox reaction leading to a Au(I) derivative $\{(CS_2)Au^{I}Br\}$. This hypothesis agree with the few literature data, [270] but could explain the transition between the complexity of the spectra at different times (**Fig. 3.10**) and the final spectrum with easily identifiable signals.

The shortcoming of this mechanism is the confirmation of obtainment of the $\{(CS_2)Au^{I}Br\}$ derivative, which have not been clearly proved, even though our studies are consistent with this hypothesis. For this, There are ongoing experiments to ascertain its existence, as well as studies of possible consequences of the interaction of the studied Au(III) complexes and L-NAC (thus with glutathione) in a biological point of view.

3.3 BIOLOGICAL STUDIES

3.3.1 In vitro cytotoxicity studies

3.3.1.1 In vitro cytotoxic activity assays

Some gold(III) complexes have been examined for their *in vitro* cytotoxic activity. A first set of experiments was performed on a panel of three human tumour cell lines. This panel includes: PC3 (androgen-independent prostate carcinoma), Du145 (human prostate cancer) and L540 (Hodgkin's lymphoma) cell lines. For comparison purpose, the cytotoxicity of cisplatin was also evaluated under the same experimental conditions. The results are summarized in terms of IC_{50} values (**Tab. 3.7**).

IC_{50}	Compound											
	AUD_2	AUD_3	AUD_6	AUD_7	AUD_8	AUD_9	AUD_{10}	AUD_{11}	AUD_{13}	AUD_{14}	AUD_{15}	cisplatin
PC3	6.6	1.8	0.85	1.0	0.55	0.75	16.08	16.5	5.8	5.8	20	2.6
DU145	3	2.1	2.0	2.5	0.25	1.4	13	15	4.5	7.3	20	3
L540	ND	ND	2.1	3.4	1.5	1.7	11.8	7.5	4	4.2	20	1.25

Table 3.7 Evaluation of in vitro cytotoxic activity of some of the investigated gold(III) complexes toward some human tumour cell lines after 72 hours. IC_{50} [μM].

Exposure of PC3 to increasing concentrations of AuD gold resulted in a remarkable dose-dependent growth inhibition with IC_{50} (the concentration of drug required to cause 50 % growth inhibition), 5-fold lower for the more active AuD_8 compound, than that of the reference drug cisplatin. As referred to **Tab.3.7**, a similar activity of gold compounds was also observed in the DU145 cell lines. On the contrary, all tested compounds were less active than cisplatin against the Hodgkin's lymphoma L540.

It is apparent that the trend in cytotoxicity seemed to be related to the peptide length and the presence of the *tert*-butyl ester seemed to promote a higher activity.

A second experiment was performed on AuD_6 and AuD_8 in order to evaluate their cell growth inhibitory properties on the highly metastatic oestrogen receptor α-negative human breast carcinoma MDA-MB-231 cells after 22 hours. As reported in **Fig. 3.12**, AuD_6 and AuD_8 have similar concentration-dependent inhibitory patterns, the latter showing slightly higher activity. Moreover, these results suggest that both compounds are similarly potent in inhibiting human breast cancer MDA-MB-231 cells growth as the previously investigated Au(III)-dithiocarbamato analogues.[271]

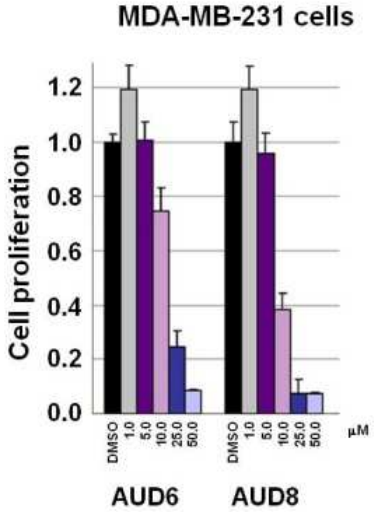

Figure 3.12 Proliferation-inhibitory effect of AuD_6 and AuD_8 on oestrogen receptor α-negative human breast carcinoma MDA-MB-231 cells.

3.3.1.2 Ability to induce apoptosis

Apoptosis derived from an ancient Greek word that suggest 'leaves falling from a tree'.[272-274] In the contrast to the swelling of the cell and its organelles that defines necrosis, the principal morphologic feature of apoptosis is the shrinkage of the cell and its nucleus. The distinction between necrosis and apoptosis is due in part to differences in how the plasma membrane participates in these processes. In necrosis, early loss of integrity of the membrane allows an influx of extracellular ions and fluid, with resultant swelling of the cell and its organelles.[275-280] In apoptosis, plasma-membrane integrity persists until late in the process. A key feature of apoptosis is cleavage of cytoskeletal proteins by aspartate-specific proteases, which thereby collapses subcellular components.[273,281-283] Other characteristic features are chromatin condensation and the formation of plasma-membrane blebs.

On the earlier features of apoptosis, the translocation of the membrane phospholipid phosphatidylserine (PS) from the internal layer to the external layer of the cell membrane. In the presence of calcium ions, Annexin V has a high specificity and a high affinity for PS (**Fig. 3.13**, top). Thus, the binding of Annexin V to cells with exposed PS provides a very sensitive method for detecting cellular apoptosis.

A population of apoptotic cells may contain necrotic cells that also bind Annexin V due to their damaged plasma membrane. To distinguish between apoptotic and necrotic cells, the fluorescent dye propydium iodide is used as it can only enter necrotic cells across a damaged plasma membrane. Staining with fluorescein isothiocyanate (FITC)-conjugated Annexin V and propydium iodide (PI) to identify subpopulations of cells with membrane changes and the associated loss of membrane integrity (**Fig. 3.13**, bottom).

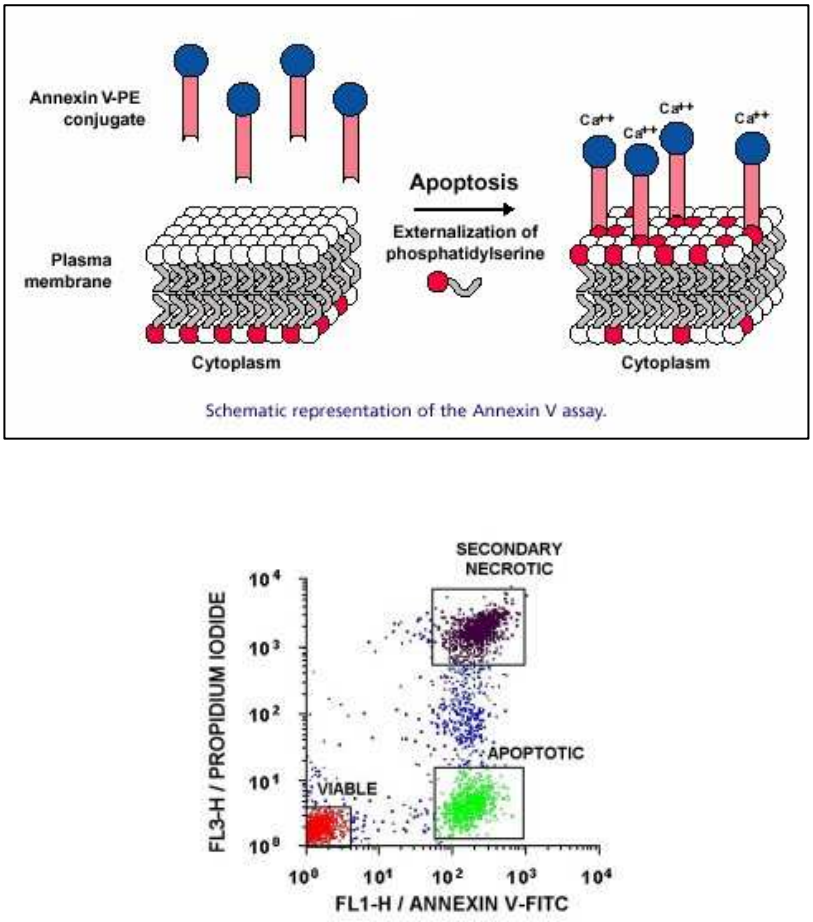

Figure 3.13. Annexin-propydium iodide apoptosis detection.

Consequently, Annexin V-Propydium iodide was used to evaluate the ability of the investigated complexes to induce apoptosis in PC3, DU145 and L540 cells.

As clearly shown in **Fig. 3.14**, AuD_6, AuD_7, AuD_8 and AuD_9 are able to induce apotosis in PC3 cells, inducing a significant increase of Annexin binding/propidium staining. For AuD_8 and AuD_9, the induction of apoptosis is greater than that of necrosis. On the contrary, AuD_6 and AuD_7 induce more necrosis.

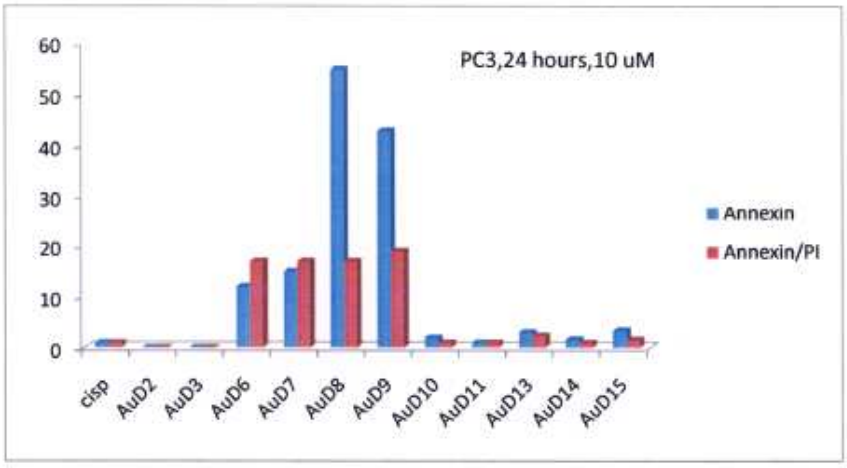

Figure 3.14 Apoptosis induction in the PC3 prostate carcinoma in 24 hours, at 10μM.

Concerning the Du145 cells, it can be observed that AuD_2, AuD_3 and cisplatin have a similar apoptosis induction profile, while AuD_6, AuD_7, AuD_8 and AuD_9 are more active in inducing early apoptosis or necrosis (**Fig. 3.15**).

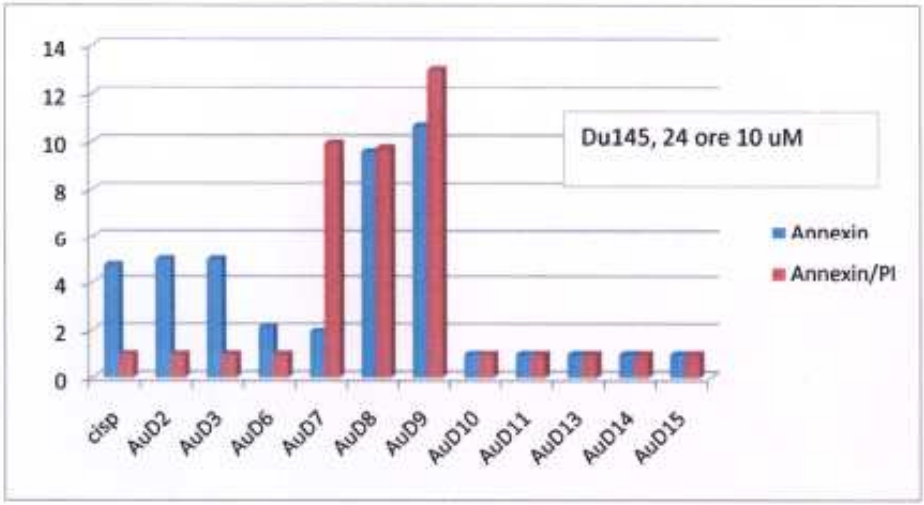

Figure 3.15 Apoptosis induction in the DU145 prostate carcinoma in 24 hours, at 10μM.

In the case of L540 cells line (**Fig. 3.16**), it is worth noting that AuD_7, AuD_8 and AuD_9 are more active to induce necrosis than apoptosis.

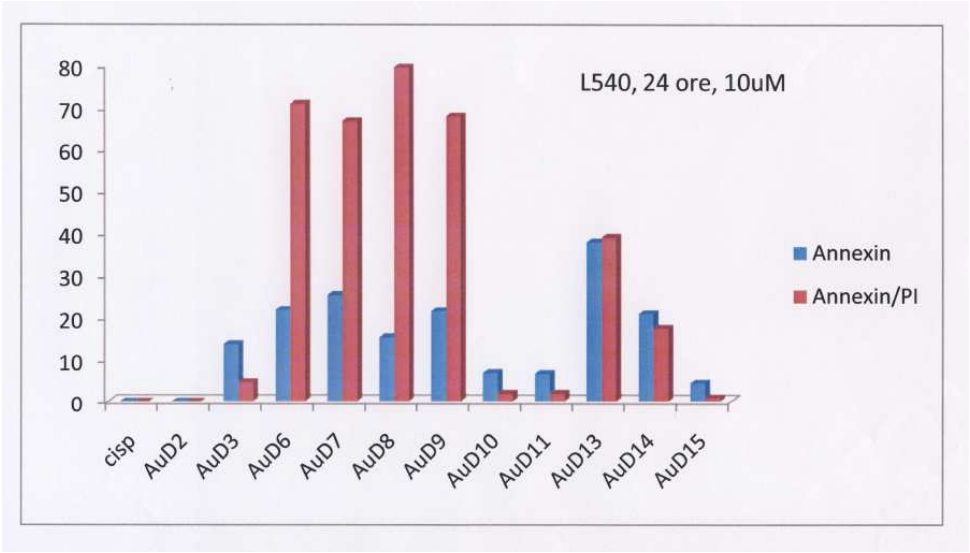

Figure 3.16 Apoptosis induction in the L540 Hodgkin's lymphoma in 24 hours, at 10μM.

3.3.1.3 Inhibition of proteasomal chymotrypsin-like activity

To investigate if AuD compounds could also have the proteasome as a biological target, the inhibition of proteasomal chymotrypsin-like activity by AuD_6 and AuD_8, in a purified 20S rabbit proteasome and MDA-MB-231 whole cell extract was studied. After 2 hours all the Au(III) complexes were proved to inhibit the proteasomal chymotrypsin-like activity of both purified rabbit 20S proteasome (**Fig. 3.17 A**) and MDA-MB-231 whole cell extract (**Fig. 3.17 B**) in a concentration-dependent way, resulting again, two-fold more potent than the previously investigated Au(III)-dithiocarbamato analogues.[271]

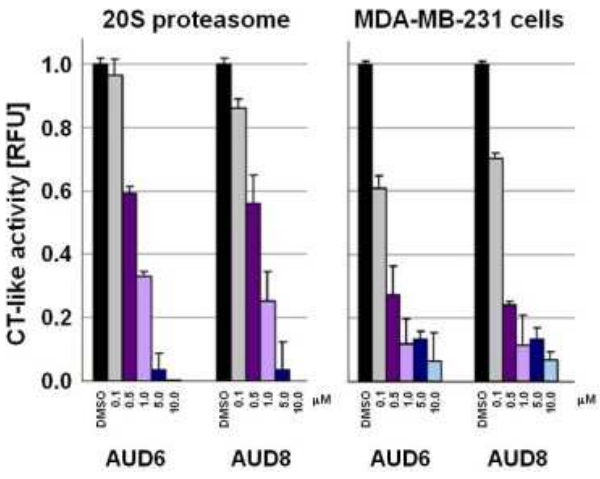

(A) (B)

Figure 3.17 Inhibition of proteasomal chymotrypsin-like activity induced by AuD_6 and AuD_8, in a purified 20S rabbit proteasome (A) and MDA-MB-231 whole cell extract (B).

Further studies (still in progress), have been preliminary showed that both investigated Au(III) complexes induce accumulation of proteasome target proteins such as Bax and p27, indicating that proteasome inhibition (associated with cell death) by AuD_6 and AuD_8 is functional and that the proteasome is the major target.

3.3.2 *In vivo* experiments

The capability of both AuD_6 and AuD_8 complexes to inhibit the growth of human breast cancer MDA-MB-231 xenografts *in vivo* was investigated. With reference to **Fig. 3.18**, significant tumour growth inhibition was observed after 13 days in tumour-bearing mice treated with AuD_8. Control grew to an average size of 453 mm^3, whereas AuD_8-treated tumours grew to a much smaller average size, corresponding to > 90 % inhibition. Analogous treatment with AuD_6 led to a moderate inhibition of tumour growth (~ 33 %). These result consistent with the previously discussed *in vitro* studies, in which AuD_8 was shown to be more potent than AuD_6 in inhibiting MDA-MB-231 cells proliferation. In addition, no toxicity, weight loss, decreased activity or anorexia were observed in mice during the 13-day treatment (1 $mg \cdot kg^{-1}$ per day), implying a possible selectivity for cancer cells respect to healthy ones. These are preliminary results and more accurate experiments are still being carried out.

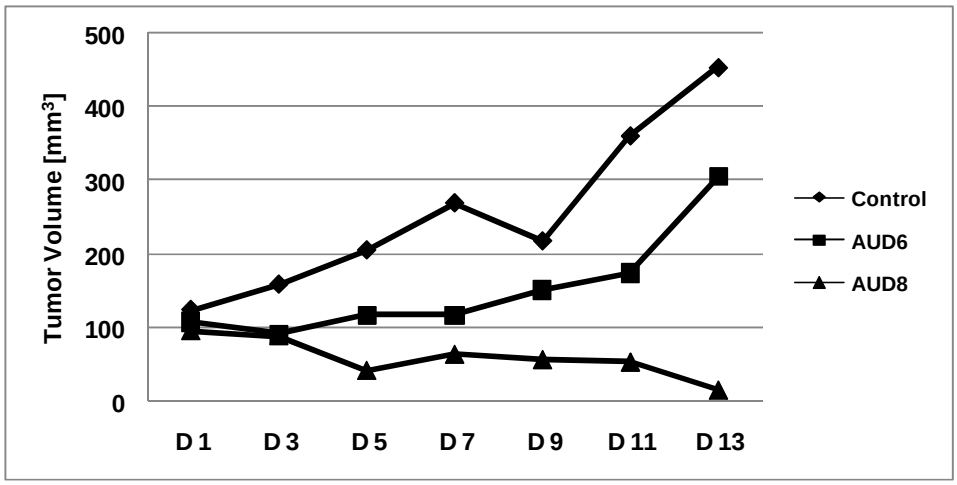

Figure 3.18 In vivo inhibitory effect of AuD_6 and AuD_8 on human breast cancer xenografts.

4. CONCLUSIONS

This project work was aimed at synthesizing and characterizing a series of Au(III)-dithiocarbamato complexes, covalently bound to oligopeptides showing different features, in terms of amino acids sequence, length, hydrophilicity/hydrophobicity, chirality and nature of the C-terminal protecting/blocking group, and evaluating the influence of all these factors on the anticancer activity. In addition, it intended to possibly increase the bioavailability of the synthesized compounds compared to cisplatin through their membrane proteins internalisation.

A panel of oligopeptides, from di- to pentapeptides were synthesized and characterised. The conformation of Aib containing compounds was studied by IR and NMR spectroscopy in $CDCl_3$. A propensity to autoassociation, parallel with the increase of peptide lengh was observed, and it was demonstrated that the pentapeptide, the longest among all, had a fold structure.

The corresponding Au(III)-dithiocarbamato complexes were synthesized by a template reaction and characterised by means of IR, mono- and bidimensional NMR spectroscopy, and thermogravimetric analysis. All the studied Au(III)-peptidodithiocarbamato complexes resulted to assumed a square-planar geometry in which the dithicarbamate ligand is chelated in a symmetrical bidentate mode.

The conformation of two chiral Aib containing complexes was studied through CD, but it was not possible to reach conclusions from the spectra because of lack published data.

The reaction with L-NAC was used to mimic the possible reduction reaction of the studied complexes by the biological active molecule glutathione, responsible for the resistance to cisplatin. A mechanism was proposed for the redox reactions occurred and the existence of two of the reaction products was assessed by ^{1}H NMR spectroscopy.

The investigated Au(III)-peptidodithiocarbamato complexes proved to be more potent *in vitro* and *in vivo* than the clinically used chemotherapeutic agent, cisplatin, and even than the previously synthesised Au(III) analogues towards some human cell lines. The cytotoxicity seemed to be related to the amino acidic composition of the oligopeptide and the chain length. In fact, Au(III)-tri- and pentapeptide derivatives resulted to be less active. However, as these experiments are preliminary, and as the biological behaviour of all the compounds has not yet been extensively studied, an overview of the influence of the previously discussed factors on the antitumour activity of Au(III)-peptidodithiocarbamato complexes is as yet risky. Nevertheless, in the in vivo experiments, the studied compounds showed to be somehow selective, since there was neither toxicity, weight loss, decreased activity nor anorexia observed in mice during the 13-day treatment.

In the future, we intend to pursue the full characterization of the remaining Au(III)-peptidodithiocarbamato derivatives, extend the biological studies, and deepen the sudy of interaction with biological active molecules and the proteins.

REFERENCES

1. Thompson C. B., *Science*, **1995**, *267*, 1456.
2. Ferlay J., Bray F., Pisani P., *et al*, GLOBOCAN 2002, IARC Cancer Base N° 5, *IARC press*, Lyon, France.
3. Soldi S., *Chim. Ind.*, **1995**, *77*, 989.
4. Peyrone M., *Ann. Chem. Pharm.*, **1845**, *51*, 1.
5. Reyset J., *Compt. Rend.*, **1844**, *18*, 1103.
6. Werner A., *Z. Anorg. Chem.*, **1893**, *3*, 267.
7. Rosenberg B., Van Camp L., Krigas T., *Nature*, **1965**, *205*, 698.
8. Rosenberg B., Renshaw E., Van Camp L., Hartwick J., Drobnik J., *J. Bacteriol.*, **1967**, *93*, 716.
9. Rosenberg B., Van Camp L., Grimley E. B., Thompson A. j., *J. Biol. Chem.*, **1967**, *242*, 1347.
10. Rosenberg B., Van Camp L., Trosko J. E., Mansour V. H., *Nature*, **1969**, *222*, 385.
11. Higby D. J., Wallace Jr. H. J., Albert D. J., Holland J. F., *Cancer*, **1974**, *33*, 1219.
12. Hambley T. W., *Dalton Trans.*, **2007**, *43*, 4929.
13. Kelland L., *Nat. Rev. Cancer*, **2007**, *7*, 573.
14. Dresser M. J., Leabman M. K., Giacomini K. M., *J. Pharm. Sci.*, **2001**, *90*, 397.
15. Muller J., Lips K. S., Metzner L., Neubert R. H., Koepsell H., Brandsch M., *Biochem. Pharmacol.*, **2005**, *70*, 1851.
16. Zhang S., Lovejov K. S., Shima J. E., Lagpacan L. L., Shu Y., Lapuk A., Chen Y., Komori T., Gray J. W., Chen X., Lippard S. J., Giacomini K. M., *Cancer Res.*, **2008**, *66*, 8847.
17. Lovejoy K. S., Todd R. C., Zhang S., McCormick M. S., D'Aquino J. A., Reardon J. T., Sancar A., Giacomini K. M., Lippard S. J., *Proc. Natl. Acad. Sci. U.S.A.*, **2008**, *105*, 8902.
18. Safei R., Howell S. B., *Crit. Rev. Oncol. Hematol.*, **2005**, *53*, 13.
19. Safei R., *Cancer Lett.*, **2006**, *234*, 34.
20. Ishida S., Lee J., Thiele D. J., Herskowitz I., *Proc. Natl. Acad. Sci. U.S.A.*, **2002**, *99*, 14298.
21. Katz A. I., *Kidney Int.*, **1986**, *29*, 21.
22. Andrews P. A., Velury S. , Mann S. C., Howell S. B., *Cancer Res.*, **1988**, *48*, 68.
23. Smith E., Brock A. P., *Br. J. Cancer*, **1989**, *59*, 873.
24. Andrews P. A., Mann S. C., Huynh H. H., Albright K. D., *Cancer Res.*, **1991**, *51*,3677.
25. Kasahara K., Fujimura M., Bando T., Shibita K., Shirasaki H., Matsuda T., *Br. J. Cancer*, **1996**, *74*, 1553.
26. Cheng P.W., Liu S. H., Hsu C. J., Lin-Shiau S. Y., *Hear. Res.*, **2005**, *205*, 102.

27. Davies M. S., Berners-Price S. J., Hambley T. W., *J. Inorg. Biochem.*, **2000**, *79*, 167.
28. Lim M. C., Martin R. B., *J. Inorg. Nucl. Chem.*, **1976**, *38*, 1911.
29. Pil P., Lippard S. J., in: Bertino J. R. (Ed.), *Encyclopedia of Cancer*, Vol. 1, Academic Press, San Diego, **1997**, p. 392.
30. Frit P., Calsou P., Conitrat Y., Muller C., Salles B., *Anticancer Drugs*, **1996**, *7*, 101.
31. Cohen G. L., Ledner, Bauer W. R., Ushay R. M., Carovana C., Lippard S. J., *J. Am. Chem. Soc.*, **1980**, *102*, 2497.
32. Tullius T. D., Lippard S. J., *J. Am. Chem. Soc.*, **1981**, *103*, 4620.
33. Rayer Pokora B., Gordon L. K., Haseltine W. A., *Nucleic Acids Res.*, **1981**, *9*, 4595.
34. Pinto A. L., Lippard S. J., *Proc. Natl. Acad. Sci. U.S.A.*, **1986**, *82*, 4616.
35. Fichtinger Schepman A. M. J., Lohman P. H. M., Reedijk J., *Nucleic Acids Res.*, **1982**, *10*, 5345.
36. Fichtinger Schepman A. M. J., van der Veer J. L., den Hartog J. H. J., Lohman P. H. M., Reedijk J., *Biochem.*, **1985**, *24*, 707.
37. Eastman A., *Biochem.*, **1986**, 25, 3912.
38. Plooy A. C. M., Fichtinger Schepman A. M. J., Schutte H. H., van Dijk M., Lohman P. H. M., *Carcinogenesis*, **1985**, *6*, 561.
39. Pinto A. L., Lippard S. J., in: Spiro T. G. (Ed.), *Metal Ions in Biology 1*, John Wiley & sons, **1980**, p.31.
40. Eastman A., in: Lippert B. (Ed.), *Cisplatin: Chemistry and Biochemistry of a Leading Anticancer drug*, Wiley-VCH, Zurich, **1999**, p. 111.
41. Berners Price S. J., Barnham, Frey U., Sadler P. J., *Chem. Eur. J.*, **1996**, *2*, 1283.
42. Reeder F., Guo Z., Murdoch P. S., Hambley T. W., Berners Price S. J., Sadler P. J., *Eur. J. Biochem.*, **1997**, *249*, 370.
43. Reeder F., Gonnet F., Kozelka J., Chottard J.C., *Chem. Eur. J.*, **1996**, *2*, 1068.
44. Eastman A., *Biochem.*, **1985**, *24*, 5027.
45. Eastman A., *Chem.-Biol. Interact.*, **1987**, *61*, 241.
46. Lippard S. J., *Pure Appl. Chem.*, **1987**, *59*, 731.
47. Macquet J. P., Buntour J. L., *Biochimie*, **1978**, *60*, 901.
48. Cohen G. L., Bauer W. R., Barton J. K., Lippard S. J., *Science*, **1979**, *203*, 1014.
49. Huang H., Zhu L., Reid B. R., Drobny G. P., Hopkins, *Science*, **1995**, *270*, 1842.
50. Marzilli L. G., Saad J. S., Kuklenyik Z., Keating K. A., Xu Y., *J. Am. Chem. Soc.*, **2001**, *123*, 4661.
51. Desoize B., Madoulet C., *Crit. Rev. Oncol./ Hematol.*, **2002**, *42*, *317*.

[52.] Zamble D. B., Lippard S. J., in Lippert B. (Ed.), *Cisplatin: Chemistry and Biochemistry of a Leading Anticancer drug*, Wiley-VCH, Zurich, **1999**, p. 73.

[53.] Wang D., Hara R., Singh G., Sancar A., Lippard S. J., *Biochemistry*, **2003**, *42*, 6747.

[54.] Cheung P., Allis C. D., Sassone-Corsi P., *Cell*, **2000**, *103*, 263.

[55.] Kwon J., Morshead K. B., Guyon J. R., Kingston R. E., Oettinger M. A., *Mol. Cell.*, **2000**, *6*, 1037.

[56.] Bustin M., Reeves R., *Prog. Nucl. Acids Res. Mol. Biol.*, **1996**, *54*, 35.

[57.] Turchi J. J., Henkels K. M., Hermanson I. L., Patrick S. M., *J. Inorg. Biochem.*, **1999**, *77*, 83.

[58.] Kartalou M., Essigmann J. M., *Mutat. Res.-DNA Repair*, **2001**, *478*, 1.

[59.] Ohndorf U. M., A Rould M., He Q., Pabo C. O., Lippard S. J., *Nature*, **1999**, *399*, 708.

[60.] Hickman J. A., *Cancer Metat. Rev.*, **1992**, *11*, 121.

[61.] Dive C., Willie A. H., in: Hickman J. A. and Tritton T. R. (Eds.)., *Frontiers In Pharmacology*, Blackwell Scientific press, Oxford, **1993**, p.21.

[62.] Fisher D.E., *Cell*, **1994**, *78*,539.

[63.] Eliopoulos A. G., Kerr D. J., Herod J., Hodgkins L., KrajewsKi S., Reed J. C., Youg L. S., *Oncogene*, **1995**, *11*, 1217.

[64.] Alnemri E. S., *J. Cell Biochem.*, **1997**, *64*, 33.

[65.] Jamieson E. R., Lippard S. J., *Chem. Rev.*, **1999**, *99*, 2467.

[66.] Gonzalez V. M., Fuertes M. A, Alonso C., Perez J. M., *Mol. Pharmacol.*, **2001**, *59*, 657.

[67.] Hoffmann K., Bucher P., Tschoop J., *Trends Biochem. Sci.*, **1997**, *22*, 155.

[68.] Enary M., Talanian R. V., Wong W. W., Nagata S., *Nature*, **1996**, *380*, 723.

[69.] Muzio M., Stockwell B. R., Stennicke H. R., Salresen G. S., Dixit V. M., *J. Biol. Chem.*, **1998**, *273*, 2926.

[70.] Fulda S., los M., Friesen C., Debatin K. M., *Br. J. Cancer*, **1998**, *67*, 1171.

[71.] Li P., Nijhawan D., Budihardjo I., Srinivasula S. M., Ahmad M., Alnemri E. S., Wang X, *Cell*, **1997**, *91*,479.

[72.] Srinivasula S. M., Ahmad M., Fernandes-Alnemri T., Alnemri E. S., *Mol. Cell.*, **1998**, *1*, 949.

[73.] Kojima H., Endo K., Moriyama H., Tanaka K., Alnemri E. S., Slapak C. A., Teicher B., Kufe D., Datta R., *J. Biol. Chem.*, **1998**, *273*, 16647.

[74.] Seki K., Yoshikawa H., Shiiki K., Hamada Y., Akamatsu N., Tasaka K., *Cancer Chemother. Pharmacol.*, **2000**, *45*, 199.

[75.] Henkels K. M., , Turchi J. J., *Cancer Res.*, **1999**, *59*, 3077.

[76.] Liu X., Li P., Widlak P., Zou H., Luo X., Garrad W. T., Wang X., *Proc. Natl. Acad. Sci. U.S.A.*, **1998**, *95*, 8461.

77. Reed E., in: Pinedo H. M., Longo D. L., Chabner B. A. (Eds.), *Cancer Chemotherapy and Biological Response Modifiers*, Elsevier Science BV, Amsterdam, **1999**, p. 144.

78. Zamble D. B., Jacks T., Lippard S. J., *Proc. Natl. Acad. Sci. U.S.A.*, **1998**, *95*, 6163.

79. Arky R., *Physician Desk Reference*, 50th Ed., Medical Economics Company, Montvale, **1996**.

80. Wood W. R., *Cancer Res.*, **1987**, *47*, 6549.

81. Borch R. F., Pleasants M. E., *Proc. Natl. Acad. Sci., U.S.A.*, **1979**, *76*, 6611.

82. Dorr R. T., in: Pinedo H. M., Schornagel J. H. (Eds.), *Platinum and Other Metal Coordination Compounds in Cancer Therapy 2*, Plenum press, New York, **1996**, p. 131.

83. Raymond E., *Rév. Med. Interne*, **1996**, *17*, 936.

84. Appleton T. G., Connor J. W., Hall J. R., Prenzler P. D., *Inorg. Chem.*, **1989**, *28*, 2030.

85. Freeman M. L., Meredith M. J., *Proc. Amer. Assoc. Cancer Res.*, **1989**, *30*, 460.

86. Andrews P. A., Howell S. B., *Cancer cells*, **1990**, *2*, 35.

87. Dedon P. C., Borch R. F., *Biochem. Pharmacol.*, **1987**, *36*, 1955.

88. Zunino F., Protesi G., Micheloni A., *Chem-Biol. Interact.*, **1989**, *70*, 89.

89. Homers F. P. T., Brakkee J. H., Cavalleti E., *Cancer Res.*, **1993**, *53*, 544.

90. Young, *J. Natl cancer Inst.*, **1992**, *34*, 264.

91. Stewart D. J., Verma S., Maroun J. A., *Am. J. Clin. Oncol.*, **1987**, *10*, 517.

92. Lerza R., Bogliolo G., muzzulini C., Pannacciulli I., *Life Sci. Rev.*, **1986**, *38*, 1795.

93. Dorr R. T., Lagel K., *J. Cancer Res. Clin. Oncol.*, **1989**, *115*, 604.

94. Goel R., Cleary S. M., Horton C., *J. Natl cancer Inst.*, **1989**, *81*, 1552.

95. Homers F. P. T., Pette C., Brovenloer B., *Cancer Chemother. Pharmacol.*, **1993**, *32*, 162.

96. Bodenner D. L., Dedon P. C., Keng P. C., Borch R. F., *Cancer Res.*, **1986**, *46*, 2745.

97. Borch R. F., Dedon P. C., Gringeri A., Montine T. J., in: Nicolini M. (Ed.), *Platinum and Other Metal Complexes in cancer Chemotherapy*, Martinus Nijoff Publishing, Boston, **1988**, p. 216 and references therein.

98. Tinkler J., Gott D., Bootman J., *Food Chem. Toxicol.*, 1998, 36, 849.

99. Gately D. P., Howell S. B., *Br. J. Cancer*, **1993**, *67*, 1171.

100. Katano K., Kondo A., Safaei R., Holzer A. K., Samimi G., Mishima M., Kuo Y., Rochdi M., Howell S. B., *Cancer Res.*, **2002**, *62*, 6559.

101. Holzer A. K., Howell S. B., *Mol. Pharmacol.*, **2006**, *66*, 10944.

102. Larson C. A., Blair B. G., Safaei R., Howell S. B., *Mol. Pharmacol.*, **2009**, *75*, 324.

103. Safaei R., Holzer A. K., Katano K., Samimi G., Howell S. B., *J. Inorg. Chem.*, **2004**, *98*, 607.

104. Mistry P., Kelland L. R., Abel G., Sidhar S., Harrap K. R., *Br. J. cancer*, **1991**, *64*, 215.

105. Ishikawa T., *Trends Biochem. Sci.*, **1992**, *17*, 463.

[106.] Ferry K. V., Hamilton T: C:, Johnson S. W., *Biochem. Pharmacol.*, **2000**, *60*,1305.

[107.] Chang I.-Y., Kim M.-H., Kim H. B., Lee D. Y., Kim S.-H., Kim H.-Y., You H. J., *Biophys. Res. Commun.*, **2005**, *327*, 2005.

[108.] Dabholkar M., Bostick-Bruton F., Weber C., Bohr V. A., Egwagu C., Reed E., *J. Natl. Cancer Inst.*, **1992**, *84*, 1512.

[109.] Fink D., Nebel S., Aebi S., Zheng H., Cenni B., Nehmé A., Christen R. D., Howell S. B., *Cancer Res.*, **1996**, *56*, 4881.

[110.] Zdraveski Z. Z., Mello J. A., Farinelli C. K., Essigmann J. M., Marius M. G., *J. Biol. Chem.*, **2002**, *277*, 1255.

[111.] Gifford G., Paul J., Vasey P. A., Kaye S. B., Brown R., *Clin. Cancer Res.*, **2004**, *10*, 4420.

[112.] Helleman J., van Staveren I. L., Dinjens W. N. M., van Kuijk P. F., Ritstier K., Ewing P., van der Burg M. E. L., Stoter G., Berns E. M. J. J., *B. M. C. Cancer*, **2006**, *6*, 201.

[113.] Bassett E., Vaisman A., Tropea K. A., McCall C. M., Masutani F., Hanaoka F., Chaney S. G., *DNA repair*, **2002**, *1*, 1003.

[114.] Albertella M. R., Green C. M., Lehmann A. R., O'Connor M. J., *Cancer Res.*, **2005**, *65*, 9799.

[115.] Gadducci A., Cosio S., Muraca S., Genazzani A. R., *Gynecol. Oncol.*, **2002**, *23*, 390.

[116.] Gordon A. N., *et al.*, *Gynecol. Oncol.*, **2004**, *95*, 1.

[117.] Gradishar W. J., *et al.*, *J. Clin. Oncol.*, **2005**, *23*, 7794.

[118.] Hanahan D., Wienberg R. A., *Cell*, **2000**, *100*, 57.

[119.] Harrap K. R., *Cancer Treat. Res.*, **1985**, *12*, 21.

[120.] Knox R. P., Friedlos F., Lydall D. A., Roberts J. J., *Cancer Res.*, **1986**, *46*, 1972.

[121.] Aabo K., *et al.*, *Br. J. Cancer*, **1998**, *78*, 1479.

[122.] Kidani Y., Inagaki K., Ligo M., Hoshi A., Kuretani K., *J. Med. Chem.*, **1978**, *21*, 390.

[123.] Rixe O., *et al.*, *Biochem. Pharmacol.*, **1996**, *52*, 1855.

[124.] Holzer A. K., Howell S. B., *Molec. Pharmacol.*, **2006**, *70*, 1390.

[125.] Springler B., Whittington D. A., Lippard S. J., *Inorg. Chem.*, **2001**, *40*, 5596.

[126.] Raymond E., Faivre S., Chaney S., Woynarowski J., Cvitkovic E., *Mol. Cancer Ther.*, **2002**, *1*, 227.

[127.] Sasaki Y., Tamura T., Eguchi K., *et al.*, *Cancer Chemother. Pharmacol.*, **1989**, *23*, 243.

[128.] Pendyala L., Creaven P. J., *Cancer Res.*, **1993**, *53*, 5970.

[129.] Sasaki Y., Amano T., Morita M., *et al.*, *Cancer Res.*,**1991**, *51*, 1472.

[130.] Kelland L. R., et al., *Cancer Res.*, **1993**, *53*, 2581.

[131.] McKeage M. J., et al., *Cancer Res.*, **1994**, *54*, 4118.

[132.] Sharp S. Y., Rogers P. M., Kelland L. R., *Clin. Cancer Res.*, **1995**, *1*, 981.

[133.] Kelland L. R., *Exp. Opin. Invest. Drugs*, **2000**, *9*, 1373.

[134.] Samimi G., Howell S. B., *Cancer Chemother. Pharmacol.*, **2006**, *57*, 781.

[135.] Silverman A. P., Bu W., Cohen S. M., Lippard S. J., *J. Biol. Chem.*, **2002**, *277*, 49743.

[136.] Reardon J. T., Vaisman A., Chaney S. G., Sancar A., *Cancer Res.*, **1999**, *59*, 3968.

[137.] Kostova I, *Recent Pat. Anti-cancer Drug Discovery*, **2006**, *1*, 1.

[138.] Jakupec M. A., Galanski M., Arion V. B., Hartinger C. G., Keppler B. K., *Dalton Trans.*, **2008**, 183; Wang X., Guo Z., *Dalton Trans.*, **2008**, 1521.

[139.] Fricker S. P., *Gold Bull.*, **1996**, *29*, 53.

[140.] Huanzi Z., Yuantao N., *Gold Bull.*, **2001**, *34*, 24.

[141.] Orvig C., Abrams M. J., *Chem. Rev.*, **1999**, *99*, 2201.

[142.] Gottlieb N. L., *J. Rheumatol. Suppl.*, **1982**, *8*, 99.

[143.] Tiekink E. R. T., *Bioinorg. Chem. Appl.*, **2003**, *53*, 1.

[144.] Ward J. R., *Am. J. Med.*, **1988**, *85*, 39.

[145.] Simon T. M., Kunishima D. H., vibert G. J., Lorber A., *J. Rheumatol. Suppl.*, **1971**, *5*, 91.

[146.] Ni Dhubhghail O. M., Sadler P. J., in: *Metal in Cancer Chemotherapy* , VHC, Weinheim, **1993**.

[147.] Okada T., Patterson B. K., Ye S. Q., Gurney M. E., *Virology*, **1993**, *192*, 631.

[148.] Yamaguchi K., Ushijima H., Hisano M., Inoue Y., Shimamura T., HiranoT., Müller W. E., *Microbiol. Immunol.*, **2001**, *45*, 549.

[149.] Navarro M., Perez H., Sánchez-Delgado R. A., *J. Med., Chem.*, **1997**, *40*, 1937.

[150.] Navarro M., Cisneros-Fajardo E. J., Lehmann T., Sánchez-Delgado R. A., Atencio R., Silva P., Lira R., Urbina J. A., *Inorg. Chem.*, **2001**, *40*, 6879.

[151.] Mc Keage M. J., Maharaj L., Berners-Price S. J., *Coord. Chem.*, **2002**, *232*, 127.

[152.] Sadler P. J., Sue R. E., *Met. Based Drugs*, **1994**, *1*, 107.

[153.] Kostova I., *Anticancer Agents Med. Chem.*, **2006**, *6*, 19.

[154.] Fricker S. P., *Met. Based Drugs*, **1999**, *6*, 291.

[155.] Ronconi L., Giovagnini L., Marzano C., Bettio F., Graziani R., Pilloni G., Fregona D., *Inorg. Chem.*, **2005**, *44*, 1867.

[156.] Shaw III C. F., *Chem. Rev.*, **1999**, *99*, 2589.

[157.] Parish R. V., Howe B. P., Wight J. P., Mack J., Pritchard R. G., Buckley R. G., Elsome A. M., Fricker S. P., *Inorg. Chem.*, **1996**, *35*, 1659.

[158.] Buckley R. G., Elsome A. M., Fricker S. P., Henderson G. R., Theobald B. R., Parish R. V., Howe B. P., Kelland L. R., *J. Med. Chem.*, **1996**, *39*, 1426.

[159.] Wienken M., Lippert B., Zangrando E., Randaccio L., *Inorg. Chem.*, **1992**, *31*, 1983.

[160.] Carotti S., Marcon M., Marussich M., Mazzei T., Messori L., Mini E., Orioli P., *Chem. Biol. Interact.*, **2000**, *125*, 29.

[161.] Ronconi L., Fregona D., *Dalton Trans.*, **2009**, 10670.

[162.] (a) Ronconi L., Marzano C., Fregona D., *It. Pat.*, 0001347835, **2003**; (b) Marzano C., Ronconi L., Trevisan A., Fregona D., unpublished work.

[163.] Casini A., Ketler G., Gabbiani C., Cinellu M. A., Minghetti G., Fregona D., Fiebig H.-H., Messori L., *J. Biol. Inorg. Chem.*, **2009**, DOI: 10.1007/s00775-009-0558-9.

[164.] Ronconi L., Marzano C., Zanello P. *et al.*, *J. Med. Chem.*, **2006**, *49*, 1648.

[165.] Bindoli A., Rigobello M. P., Scutari G., Gabbiani C., Casini A., Messori L., *Coord. Chem. Rev.*, **2009**, *253*, 1692.

[166.] Saggioro D., Rigobello M. P., Paloschi L., Folda A., Moggach S. A., Parsone S., Ronconi L., Fregona D., Bindoli A., *Chem. Biol.*, **2007**, *14*, 1128.

[167.] Ronconi L., Fregona D., *Dalton Trans.*, **2009**, 10670.

[168.] Milacic V., Fregona D., Dou Q. P., *Histol. Histopatol.*, **2008**, *23*, 101.

[169.] Milacic V., Dou Q. P., *Coord. Chem. Rev.*, **2009**, *253*, 1649.

[170.] Lopes U. G., Erhard P., Yooend R., Cooper G. M., *J. Biol. Chem.*, **1997**, *272*, 12893.

[171.] Zhang C., Frezza M., Milacic V., Ronconi L., Fan Y., Bi C., Fregona D., Dou Q. P., *J. Cellular Biochem.*, submitted.

[172.] Perez-Galan P., Roue G., Villamar N., Monserrat E., Campo E., Colomer D., *Blood*, **2006**, *107*, 257.

[173.] Rubio-Aliaga I., Daniel H., *Trends Pharmacol. Sci.*, **2002**, *23*, 434.

[174.] Powers J.-P. S., Hancock R. E. W., *Peptides*, **2003**, *24*, 1681.

[175.] Papo N., Shai Y., *Peptides*, **2003**, *24*, 1693.

[176.] Brogden K. A., Ackermann M., McCray P. B., Tack B. F. Jr., *Int. J. Antimicrob. Agents*, **2003**, *22*, 465.

[177.] Baker M. A., Maloy W. L., Zasloff M., Jacob L. S., *Cancer Res.*, **1993**, *53*, 3052.

[178.] Gallo R. L., Ono M., Povsic T., Page C., Eriksson E., Klagsbrun M., Bernfield M., *Proc. Natl. Acad. Sci. U.S.A.*, **1994**, *91*, 11035.

[179.] Johnstone S. A., Gelmon K., Mayer L. D., Hancock R. E. W., Bally M. B., *Anticancer Drug Des.*, **2000**, *15*, 151.

[180.] Morimoto M., Mori H., Otake T., Ueba N., Kunita N., Niwa M., Murakami T., Iwanaga S., *Chemotherapy*, **1991**, *37*, 206.

[181.] Murakami T., Niwa M., Tokunaga F., Miyata T., Iwanaga S., *Chemotherapy*, **1991**, *37*, 327.

[182.] Brown K. L., Hancock R. E. W., *Curr. Opin. Imunol.*, **2006**, *18*, 24.

[183.] (a) Benedetti E., Bavoso A., Di Blasio B., Pavone V., Pedone C., Toniolo C., Bonora, G.M., *Proc. Natl. Acad. Sci. USA*, **1982**, *79*, 7951. (b) Brückner H., Graf H., *Experientia*, **1983**, *39*, 528. (c) Toniolo C., Brückner H., Eds., *Peptaibiotics*, Wiley, 2009.

[184.] (a) Yamaguchi H., Komada H., Osada S., Kato F., Jelokhani-Niaraki M., Kondo M., *Biosci. Biotechnol. Biochem.*, **2003**, *67*, 2269. (b) De Zotti M., Biondi B., Formaggio F., Toniolo C., Stella L., Park Y., Hahm K., *J. Pept. Sci.*, **2009**, *15*, 615.

[185.] IUPAC-IUB Commission on Biochemical nomenclature, *Biochemistry*, **1970**, *9*, 3471.

[186.] Toniolo C., Benedetti E., *Trends Biochem. Sci.*, **1991**, *16*, 350.

[187.] Ramanchandran G. N., Sasisekharan V., *Adv. Protein Chem.*, **1968**, *23*, 283.

[188.] Pavone V., Di Blasio B., Pedone C., Santini A., Benedetti E., Formaggio F., Crisma M., Toniolo C., *Gazz. Chim. Ital.*, **1991**, *121*, 21.

[189.] Donohue J., *Proc. Natl. Acad. Sci. U.S.A.*, **1953**, *39*, 470.

[190.] Ramanchandran G. N., Venkatachalam C. M., Krimm S., *Biophys. J.*, **1966**, *6*, 849.

[191.] Baker E. N., Hubbard E., *Prog. Biophys. Mol. Biol.*, **1984**, *44*, 97.

[192.] Robbins A. H., Stout C. D., *Protein Struct. Funct. Genet.*, **1989**, *5*, 289.

[193.] Pathak D., Ollis D., *J. Mol. Biol.*, **1990**, *214*, 497.

[194.] Kostrikis L. G., Liu D. J., Day L. A., *Biochemistry*, **1994**, *33*.

[195.] Venkatachalam C. M., *Biopolymers*, **1968**, *6*, 1425.

[196.] (a) Ramanchandran G. N., Chandrasekharan R., *Indian J. Biochem. Biophys.*, **1972**, *9*, 1; (b) Burgess A. W., Leach S. J., *Biopolymers*, **1973**, *12*, 2599.

[197.] (a) Marshall G. R., in: Karasch N. (Ed.), *Intra-Science Chemistry Reports*, Gordon and Breach, New York (N.Y., U.S.A.), **1971**, *5*, pp 305-316; (b) Venkatachalam Prasad C. M., Sasisekharan V., *Macromolecules*, **1979**, *12*, 1107.

[198.] (a) Paterson Y., Rumsey S. M., Benedetti E., Némethy G., Scheraga H. A., *J. Am. Chem. Soc.*, **1981**, *103*, 2947; (b) Improta R., Rega N., Aleman C., Barone V., *Macromolecules*, **2001**, *34*, 7550.

[199.] Improta R., Barone V., kudin K. N., Scuseria G. E., *J. Am. Chem. Soc.*, **2002**, *123*, 3311.

[200.] (a) Gangamani B. P., Kumar V. A., Ganesh K. N., *Tetrahedron*, **1996**, *52*, 15017; (b) D'Costa M., Kumar V. A., Ganesh K. N., *Org. Lett.*, **2001**, *3*, 1281; (c) Vilaivan T., Srisuwannaket C., *Org. Lett.*, **2006**, *8*, 1897.

[201.] Benedetti E., Bavoso A., Di Blasio B., Pavone V., Pedone C., Crisma M., Bonora G. M., Toniolo C., *J. Am. Chem. Soc.*, **1982**, *104*, 2437.

[202.] Toniolo C., Valle G., Bonora G. M., Crisma M., Formaggio F., Bavoso A., Benedetti E., Di Blasio B., Pavone V., Pedone C., *Biopolymers*, **1986**, *25*, 2237.

[203.] Valle G., Crisma M., Toniolo C., Beißwenger R., Rieker A., Jung G., *Liebigs Ann. Chem.*, **1989**, 337.

[204.] Valle G., Crisma M., Toniolo C., *Zeit. Kristallogr.*, **1989**, *188*, 261.

[205.] Souhassou M., Smith G. D., Leplawy M. T., Marshall G. R., *Acta Crystallogr.*, **1990**, *A46*, suppl. C-140, PS-04.01.16.

[206.] Di Blasio B., Santini A., Pavone V., Pedone C., Benedetti E., Moretto V., Crisma M., Toniolo C., *Struct. Chem.*, **1991**, *2*, 523.

[207.] Bavoso A., Benedetti E., Di Blasio B., Pavone V., Pedone C., Toniolo C., Bonora G. M., *Proc. Natl. Acad. Sci. U.S.A.*, **1986**, *83*, 1988.

[208.] Pavone V., Di Blasio B., Santini A., Benedetti E., Pedone C., Toniolo C., Crisma M., *J. Mol. Biol.*, **1990**, *214*, 633.

[209.] Toniolo C., Crisma M., Bonora G. M., Benedetti E., Di Blasio B., Pavone V., Pedone C., Santini A., *Biopolymers*, **1991**, *31*, 129.

[210.] Geßmann R., Brückner H., Kokkinidis M., *Acta Crystallogr.*, **1998**, *B54*, 300.

[211.] Geßmann R., Brückner H., Petratos K., *J. Pept. Sci.*, **2003**, *9*, 753.

[212.] (a) Paterson Y., Stimson E. R., Evans D. J., Leach, S. J., Scheraga H. A., *Int. J. Pept. Protein Res.*, **1982**, *20*, 468; (b) Toniolo C., Bonora G. M., Barone V., Bavoso A., Benedetti E., Di Blasio B., Grimaldi P., Lelj F., Pavone V., Pedone C., *Macromolecules*, **1985**, *18*, 895.

[213.] Karle I. L., Balaram P., *Biochemistry*, **1990**, *29*, 6747.

[214.] Benedetti E., Di Blasio B., Pavone V., Pedone C., Santini A., Crisma M., Toniolo C., in: Balaram P., Ramaseshan S. (Eds.), *Molecular Conformation and Biological Interactions*, Indian Academy of Science, Bangalore (India), **1998**, 497.

[215.] Von Arx M., Faupel M., Brugger M., *J. Chromatogr.*, **1976**, *120*, 224.

[216.] Kaighn M., Nayaran K., Onhuki Y., Lechner J., Jones L., *Invest. Urol.*, **1979**, *17*, 16.

[217.] Kozlowski J. M., McEwan R., Keer H., Sensibar J., Sherwood E., Lee C., Grayhack J. T., Albini A., Martin G., in: Fidler I. J., Nicholson G. (Eds.), *Tumor Progression and Metastasis*, Alan R. Liss publishing, New York, **1988**, p 189.

[218.] Pulukuri S. M., Gondi C. S., Lakka S. S., Jutla A., Estes N., Gujrati M., Rao J. S., *J. Biol. Chem.*, **2005**, *280*, 36529.

[219.] Szabó C., Zingarelli R., O'Connor M., Salzman A. L., *Proc. Natl. Acad. Sci. U.S.A.*, **1996**, *93*, 1753.

[220.] (a) Hofmann K., Haas W., Smithers M. J., Zanetti G. D., *J. Am. Chem. Soc.*, **1965**, *87*, 631. (b) Bonora G., Toniolo C., *Biopolymers*, **1974**, *13*, 2179.

[221.] Valle G., Formaggio F., Crisma M., Bonora G. M., Toniolo C., Bavoso A., Benedetti E., Di Blasio B., Pavone V., Pedone C., *J. Chem. Soc., Perkin Trans. 2*, **1986**, 1371.

222. McGahren W. J., Goodman M., *Tetrahedron*, **1967**, *23*, 2017.

223. Dhaon M. K., Olsen R. K., Ramasamy K., *J.Org.Chem.*,**1982**, *47*, 1962.

224. Jr. Vaughan J. R., Osato R. L., *J. Am. Chem. Soc.*, **1951**, *73*, 5553.

225. Jones D. S., Kenner G. W., Preston J., Sheppard R.C., *J. Chem. Soc.*, **1965**, 6227.

226. (a) Merrifield R. B., Barany G., Cosand W. L., Engelhard M., Mojsov S., *Pept: Proc. Am. Pept. Symp., 5th*, **1977**; (b) Green T. W., Wuts P. G., *Protective groups in Organic Synthesis, 3rd edn.*, Wiley H., N.J., U.S.A., **1999**.

227. (a) Leplawy M. T., Jones D. S., Kenner G. W., Sheppard R. C., *Tetrahedron*, **1960**, *11*, 39; (b) Boissonnas R. A., Guttmann S., Jaquenoud P. -A., Waller J. -P., *Helv. Chim. Acta*, **1956**, *39***,** 1421; Corey E. J., Székely I., Shiner C. S., *Tetrahedron Lett.*, **1977**, *16***,** 3529.

228. (a-b) König W., Geiger R., *Ber. Dtsch. Chem. Ges.*, **1970**, *103*,788; 2024.

229. McGahren W. J., Goodman M., *Tetrahedron*, **1967**, *23*, 2017.

230. Jones D. S., Kenner G. W., Preston J., Sheppard R. C., *J. Chem. Soc.*, **1965**, 6227.

231. Formaggio F., Broxterman Q. B., Toniolo C., in: Goodman M., Felix A., Moroder L., Toniolo C. (Thieme Eds.), *Synthesis of peptides*, Stuttgard, Houben-Weil: Methods of Organic Chemistry, **2002**, *22b*, chap 10.3.

232. Bellamy M., in:*'The infra-Red spectra of complex molecules'*, Methuen, London, **1956**.

233. Palumbo M., Da Rin S., Bonora G. M., Toniolo C., *Makromol. Chem.*, **1976**, *177*, 1477.

234. Bonora G. M., Mapelli C., Toniolo C., Wilkening R. R., Stevens E. S., *Int. J. Biol. Macromol.*, **1984**, *6*, 179.

235. Kennedy D. F, Crisma M., Toniolo C., Chapman D., *Biochemistry*, **1991**, *30*, 654.

236. Dwivedi A. M., Krimm S., Malcom B. R., *Biopolymers*, **1984**, *23*, 2305.

237. (a) Martin R., Hauthal G., in : *Dimethyl Sulphoxide*, Van Nostrand-Reinhold, Wokingham (U. K.), **1975**; (b) Pitner T. P., Urry D. W., *J. Am. Chem. Soc*., **1972**, *94*, 1399.

238. (a) Griesinger C., Otting G., Ernst R. R., Wütrich K., *J. Am. Chem. Soc.*, **1988**, *110*, 7870; (b) Williams K. R., King R. W., *J. Chem. Ed.*, **1990**, *67*, A125.

239. (a) Braunschweiler L., Ernst R. R., *J. Magn. Reson.*, **1985**, *53*, 521; (b) Bazzo R., Boyd J., Campbell I. D., Soffe N., *J. Magn. Res.*, **1987**, *73*, 369.

240. (a) Bothner-By A. A., Stephens R. L., Lee J., Warren C. D., Jeanloz R. W., *J. Am. Chem. Soc.*, **1984**, *106*, 811; (b) Bax D., Davis D. J., *J. Magn. Reson.*, **1985**, *63*, 207.

241. Wüthrich K., in: *NMR of Proteins and Nucleic Acids*, Wiley, New York (N.Y, U.S.A.), **1986**.

242. Shkaraputa L. N., Konovos A. V., Polackov A. D., *Ukr. Chem. J.*, **1991**, *9*, 979.

243. Vasliev A. N., Polackov A. D., *Molecules*, **2000**, *5*, 1014.

244. March J., in: *Advanced Organic Chemistry: Reactions, mechanisms and structure*, John Wiley & sons, New York, **1992**, p.1184.

[245.] Brown D. A., Glass W. K., Burke M. A., *Spectrochim. Acta*, **1976**, *32A*, 137.

[246.] Nakamoto N., Fujita J., Condrote R. A., Morimoto Y., *J. Chem. Phys.*, **1963**, *39*, 42.

[247.] Durgaprasad G., Sathyanarayana D. N., Patel C. C., *Can. J. Chem.*, **1969**, *47*, 631.

[248.] Wajda S., Drabent K., *Bull. Acad. Polon., Sci. Chim.*, **1977**, *25*, 963.

[249.] Herlinger A. W., Wenhold S. N., Lang T. V., *J. Am. Chem. Soc.*, **1970**, *92*, 6474.

[250.] Chatt J., Duncanson L. A., Venanzi L. M., Suom. Komist., **1956**, *B29*, 75.

[251.] Bonati F., Ugo R., *J. Organomet. Chem.*, **1967**, *10*, 257.

[252.] Kellner R., Nikolov G. S., Trendafilova N., *Inorg. Chim. Acta*, **1984**, *84*, 233.

[253.] Criado J. J., Lopez-Arias J. A., Macias B., Fernandez-Lago L. R., Salas J. M., *Inorg. Chim.* Acta, **1992**, *193*, 229.

[254.] Forghieri F., Preti C., Tassi L., Tosi G., *Polyhedron*, **1988**, *7*, 1231.

[255.] Beurskens P. T., Blaauw H. J. A., Cras J. A., Steggerda J. J., *Inorg. Chem.*, **1968**, *7*, 805.

[256.] Coates G. E., Parkin C., *J. Chem. Soc.*, **1963**, 421.

[257.] van Gaal H. L. M., Diesveld J. W., Pijpers F. W., van der Linden J. G. M., *Inorg. Chem.*, **1979**, *18*, 3251.

[258.] Willemse J., Cras J. A., Steggerda J. J., Keyzers C. P., *Struct. Bond. (Berlin)*, **1976**, *28*, 83.

[259.] Pijpers F. W., Dix A. H., van der Linden J. G. M., *Inorg. Chem. Acta*, **1974**, *11*, 41.

[260.] Alessio E., Balducci G., Lutman A., Mestroni G., Calligaris M., Attia W. M., *Inorg. Chem. Acta*, **1993**, *203*, 205.

[261.] Ronconi L., Maccato C., Barreca D., Saini R., Zancato M., Fregona D., *Polyhedron*, **2005**, *24*, 67.

[262.] Macias B., Criado J. J., Vaquero M. V., Villa M. V., *Thermochim. Acta*, **1993**, *223*, 213.

[263.] Fernandez-Alba A., Perez-Alvarez I. J., Martinez-Vidal J. L., Gozalez-Pradas E., *Thermochim. Acta*, **1992**, *211*, 271.

[264.] Criado J. J., Fernandez I., Macias B., Salas J. M., Medarde M., *Inorg. Chem. Acta*, **1990**, *174*, 67.

[265.] Criado J. J., Carrasco A., Macias B., Salas J. M., Medarde M., Castillo M., *Inorg. Chim. Acta*, **1989**, *160*, 37.

[266.] (a) Fasman G. D., *Circular Dichroism and the Conformational Analysis of Biomolecules*, Plenum Press, New York (N. Y., U.S.A.), 1996; (b) Woody A. W., Tinoco I. jr., *J. Chem. Phys.*, **1967**, *46*, 4927.

[267.] Sudha T. S., Vijayakumar E. K. S., Balaram P., *Int. J. Pept. Prot. Res.*, **1983**, *22*, 464.

[268.] Lee A. W. M., Chan W. H., Ho M. F., *Anal. Chim. Acta*, **1991**, 443.

[269.] Schafer F. Q., Buettner G. R., *Free Radical Biol.*, **2001**, *30*, 1191.

[270.] Yangyuoru P. M., Webb J. W., Shaw C., Franck I., *J. Inorg. Biochem.*, **2008**, *102*, 584.

[271.] Milacic V., Chen D., Ronconi L., Landis-Piwowar K. R., Fregona D., Dou Q. P., *Cancer Res.*, **2006**, *66*, 10478.

[272.] Kerr J. F., Wyllie A. H., Currie A: R., *Br. J. Cancer*, **1972**, *26*, 239.

[273.] Strasser A., *Nat. Rev. Immunol.*, **2005**, *5*, 189.

[274.] Youle R. J., Strasser A., *Nat. Rev. Mol. Cell Biol.*, **2008**, *9*, 47.

[275.] Zong W. X., Thompson C. B., *Genes Dev.*, **2006**, *20*, 1.

[276.] Golstein P., Kroemer G., *Trends Biochem. Sci.*, **2007**, *32*, 37.

[277.] Festjens N., Vanden Berghe T., Vandenabeele P., *Biochim. Biophys. Acta*, **2006**, *1757*, 1371.

[278.] Luke C. J., Pak S. C., Askew Y. S., *et al.*, *Cell*, **2007**, *130*, 1108.

[279.] Nishimura Y., Lemasters J. J., *Cell Death Differ*, **2001**, *8*, 850.

[280.] Malhi H., Gores G. J., Lemasters J. J., *Hepathology*, **2006**, *43*, S31.

[281.] Adams J. M., Cory S., *Curr. Opin. Immunol.*, **2007**, *19*, 488.

[282.] Marsden V. S., Strasser A., *Annu. Rev. Immunol.*, **2003**, *21*, 71.

[283.] Green D. R., Kroemer G., *J. Clin. Invest.*, **2005**, *115*, 2610.

ACKNOWLEDGEMENTS

Je voudrais rendre grâce au Tout-puissant qui est le vrai pionier de cette œuvre ; Il m'a accompagnée pendant toutes ces terribles années

Mes remerciements et ma profonde gratitude vont au Prof. Fernando Formaggio qui a accepté la difficile responsabilité de superviser mon travail. Merçi aussi pour les enseignements, tant sur le plan de la chimie que des relations humaines.

Je remercie le Prof. Claudio Toniolo qui m'a acceptée dans son groupe de recherche.

J'adresse ma sincère gratitude à la Prof. Dolores Fregona qui a supervisé la partie inorganique de ce travail. Je lui dis merçi pour la culture de la rigueur dans le travail.

Ma gratitude va aussi à l'endroit du Dr. Marco Crisma ; à Dr. Cristina Peggion qui m'a aidé pour les spectres NMR ; à Dr. Barbara Biondi pour les spectres de masse ; au Dr. Alessandro Moretto qui s'est chargé de mon insertion dans ce laboratoire de synthèse peptidique ; au Dr. Luca Ronconi qui a enrichi ma culture en matière de chimie inorganique, chimie analytique, informatique mais qui a su, sans trop de préjugés me transmettre ses connaissances ; à Dr. Lorena Giovagnini qui m'a accompagnée dans mes débuts au laboratoires de la Prof. Fregona ; à Dr. Marta De Zotti qui s'est spécialement occupée de moi en ces derniers jours difficiles et Dr. Gemma qui pendant son séjour dans ce laboratoire ne s'est jamais refusée de m'aider.

J'exprime ma reconnaissance à tous les enseignants de l'Université de Padova, ceux de ma commission examinatrice et tous ceux qui m'ont transmis leurs connaissances.

Je dois faire un pas en arrière pour remercier le Prof Bonaventure T. Ngadjui qui m'a initiée à la recherche et a supervisé mes travaux de thèse de Maîtrise, D.E.A., et Doctorat à l'Université de Yaoundé I.

Mes remerciements vont aussi au Prof. Nkengkack, l'actuel directeur du Département de Chimie Organique de l'Université de Yaoundé I, pour ses encouragements et la disponibilité en mon égard.

J'exprime ma reconnaissance à tous les enseignants du Département de Chimie Organique de l'Université de Yaoundé I

Je remercie tous mes camarades de laboratoires ici en Italie et au Cameroun pour le temps passé ensemble dans cet univers de recherche

J’adresse un immense merçi à Glawdys, Rosette, Diane, Hervé, Valérie, Rose, Zavérie et tous ceux qui m’ont aidée de quelque manière que ce soit pendant ces années de combat.